EVALUATION OF WHITE BLOOD CELL DNA METHYLATION AS A TOOL TO PREDICT DNA METHYLATION OF THE ADRENAL AXIS IN PRENATALLY STRESSED, MATURE BRAHMAN COWS

A Dissertation

by

HALEY CLAIRE COLLINS

Submitted to the Graduate and Professional School of
Texas A&M University
in partial fulfillment of the requirements for the degree of

DOCTOR OF PHILOSOPHY

Chair of Committee,	David G. Riley
Committee Members,	Brian W. Davis
	James O. Sanders
	Thomas H. Welsh, Jr.
Head of Department,	Andy D. Herring

December 2022

Major Subject: Animal Science

ABSTRACT

This dissertation project evaluated whether methylation of DNA of peripheral white blood cells (WBC) is predictive of methylation of DNA in components of the hypothalamic-pituitary-adrenal (HPA) axis of mature Brahman cows; and if so, to what extent. This question was assessed by use of DNA extracted from the WBC, paraventricular nucleus of the hypothalamus, anterior pituitary gland, adrenal cortex, and adrenal medulla of 5-year-old Brahman cows derived from dams that served as a control group or from dams that experienced prenatal transportation stress (PNS). The present study sought to determine if stress endured prenatally would result in long term DNA methylation changes to HPA-axis tissues, and if those changes would be reflected in WBC. A group of 5-year-old Brahman cows having been subjected to prenatal transportation stress (n = 6) were used against a control group of 5-year-old Brahman cows (n = 8) that were not exposed to the same stressor prenatally. Global methylation analyses of HPA-axis tissues to WBC, as well as tissue-to-tissue analyses were conducted using EdgeR software. Results showed tissue specific methylation patterns among the HPA-axis tissues that were not well reflected by WBC. The adrenal cortex and adrenal medulla showed consistency with one another, while the anterior pituitary appeared to be the least affected tissue, with the smallest differences in both control and PNS groups across all comparisons to WBC and other tissues. Otherwise, patterns of methylation were inconsistent when tissues were compared against each other. It is likely the consequences of prenatal stress in mature Brahman cows does not manifest in a global nature. In order to determine consistency between methylation patterns of a tissue and WBC, a change from control to PNS must be apparent and measurable, and to where the patterns of both tissue and WBC correspond in a way that reflects that difference. No such pattern consistency was observed between tissue and WBC, however, a global shift

between control PNS was also not observed. Polar methylation relationships were explored between the control and prenatally stressed groups where LogFC values reflected inverted ratios of differential methylation between HPA-axis tissues and WBC. Genes with differentially methylated CpG sites in the promoter region were targeted and a total of 668 sites were identified as having an inverted ratio of HPA-axis tissue methylation relative to WBC in the control group compared to the prenatally stressed group. Genes such as *FLI1, TINF2, MRE11,* and *BCL2L11* were identified as having multiple differentially methylated sites in their promoter region. While these results do not support the use of WBC for global methylation prediction of DNA in specific neuroendocrine components of the adrenal system in mature Brahman cows, they do propose an alternative perspective for further assessment on how to best characterize the use of WBC as a diagnostic biomarker.

ACKNOWLEDGEMENTS

For this achievement I would like to thank my committee chair, Dr. Riley for his continued support and guidance throughout my time at Texas A&M University. I would also like to thank my committee members Dr. Sanders, Dr. Welsh, and Dr. Davis for their time and input that facilitated my success during my time as a graduate student.

I would also like to thank my close friends and family, and particularly my parents, Carolyn and Alan Collins. Without their continue love and encouragement this endeavor would not have been possible.

CONTRIBUTORS AND FUNDING SOURCES

Contributors

This work was supervised by a dissertation committee consisting of Dr. Riley of the Department of Animal Science, Dr. Welsh of the Department of Animal Science, Dr. Sanders of the Department of Animal Science, and Dr. Davis of the Department of Veterinary Integrative Biosciences.

Dr. Ronald Randel, Dr. Charles Long, Dr, David Riley, and Dr. Thomas Welsh Jr. designed the animal methodologies and provided the tissues for this research.

Funding Sources

This work was supported by the USDA-NIFA [2018-67015-28131], Western Regional Project TEX03212, Hatch Projects H-9022 and H-TEX09377, Texas A&M University One Health Initiative and Texas A&M AgriLife Research, Overton.

NOMENCLATURE

WBC	White Blood Cells
HPA	Hypothalamic-pituitary-adrenal
PNS	Prenatally stressed
AC	Adrenal cortex
AM	Adrenal medulla
PIT	Anterior pituitary
PVN	Paraventricular nucleus of the hypothalamus
MDS	Multidimensional scaling plot
MD	Mean difference plot

TABLE OF CONTENTS

Page

LIST OF FIGURES

Page

LIST OF TABLES

Page

1. INTRODUCTION

Methylation of DNA is an evolutionary mechanism for regulating gene expression in vertebrates. The significance of this process lies in its ability to alter the activity of a DNA sequence without altering the sequence itself (Robertson, 2005). Because of this natural ability to modify a gene's action, understanding this epigenetic mechanism of DNA is of critical importance for improving health and performance of animals. The biochemical process of DNA methylation involves the addition of a methyl group to a DNA base, typically cytosine, at the 5-carbon position often resulting in the long-term repression of transcription (Bird, 1986). Early studies demonstrated the need for control of transcription by way of DNA methylation to inhibit potentially damaging effects of certain DNA sequences (Bird & Taggart, 1980). Although it is an essential function for genomic imprinting, growth and development, and other physiological processes, the fallibility of DNA methylation can have critical health implications (Robertson, 2005). DNA methylation irregularities have been associated with various forms of cancer, immunodeficiencies, metabolic disorders, genetic disorders, and psychiatric disorders, and therefore warrants substantial consideration for health and genetics research (Robertson, 2005; Li et al., 2012; Masliah et al., 2013; Houseman et al., 2015; Kundakovic et al., 2014; Wei et al., 2020).

Nearly all of an individual's genome is subject to DNA methylation and patterns are best observed at the tissue level and can be indicative of physiological status of the sampled region (Ma et al., 2014). Furthermore, the genome is most susceptible to methylation changes during development (Charil et al., 2010). However, many tissues, such as those in the hypothalamus-pituitary-adrenal (HPA) axis, are not easily accessible for sampling. Because of this, new methods for observing methylation differences in targeted tissues are frequently being explored to gain a better understanding of what causes DNA methylation, the effects of DNA methylation, and how

it can be measured or observed without requiring invasive work. In the present study, peripheral blood leukocytes, or white blood cells (WBC), were investigated for their ability to predict or mirror methylation patterns of tissues of the HPA-axis.

Existing evidence for suitability of DNA methylation patterns of a more accessible tissue, such as white blood cells, as a surrogate for DNA methylation patterns of various tissues are conflicting. This study aimed to better characterize both the long-term changes in DNA methylation due to stress during fetal development, as well as determine if the more attainable samples of white blood cells reflect those changes, should they exist. Five-year-old Brahman cows were used for this study and were comprised of a treatment group that was stressed prenatally and a control group that was not stressed. Specifically, the tissues sampled and used in this study were the adrenal medulla, the adrenal cortex, the anterior pituitary, and the paraventricular nucleus of the hypothalamus. The objectives of this study were to,

1) Evaluate correspondence of methylation patterns in CpG sites located on or near promoter regions between HPA-axis tissues and white blood cells within the control group of cows.
2) Evaluate correspondence of methylation patterns in CpG sites located near or on promoter regions between HPA-axis tissues and white blood cells within the prenatally stressed group of cows.
3) Compare the deviations between HPA-axis tissues and white blood cells from the control group to that of the prenatally stressed group and determine if DNA methylation patterns change between case groups in a way that is adequately observable through white blood cells.

4) Further evaluate DNA methylation patterns of the adrenal cortex (AC), adrenal medulla (AM), anterior pituitary (PIT), and hypothalamic paraventricular nuclei (PVN) by performing direct tissue-tissue comparisons (i.e., AC-AM, AC-PIT, AC-PVN, AM-PIT, AM-PVN, and PIT-PVN).

2. LITERATURE REVIEW

2.1. Effects of Prenatal Stress in Humans and Animals

Prenatal exposure to stress has shown to alter physiological functions in the offspring after birth particularly as it relates to stress responses. The HPA-axis serves many important neurological functions such as an individual's ability to cope with and recover from stress as well as regulation of immune system function and metabolism. In cattle, calves having been exposed to stress in utero via trailer transportation showed exaggerated stress responses through increased levels of plasma cortisol (Lay et al., 1997a). Furthermore, pre-weaning dairy calves have shown differing levels of plasma cortisol between groups exposed to intense heat prenatally versus a group exposed to cooling treatments prenatally (Tao et al., 2012). Several studies in humans, mice, pigs, and sheep also support this alteration of HPA-axis function and responsiveness due to prenatal and early life exposure to stress (Gallou-Kabani et al., 2010; Jensen et al., 2012; Braunschweig et al., 2012; Altmann et al., 2012; Cao-Lei et al., 2014; Chadio et al., 2017). The epigenetic mechanisms involved in DNA aberrations of HPA-axis tissues could potentially have major consequences in nervous system regulation as well as growth and development and substantiates a meaningful topic of investigation in livestock production.

A factor commonly pointed to as affecting fetal and early life development is the rate at which glucocorticoids, specifically cortisol, are produced during pregnancy (Davis et al., 2011; Duthie and Reynolds, 2013). Cortisol is naturally elevated in the third trimester of pregnancy, however, there are physiological mechanisms in place that are meant to regulate the amount of glucocorticoids that reach the fetus (Duthie and Reynolds, 2013). Pregnant women who are at risk for preterm delivery are often treated with synthetic glucocorticoids (sGC) despite its association with reduced birth weight. A 2008 study by Kapoor et al., observed the effects of sGC in pregnant

women and found that HPA-axis function alterations are closely associated with children exposed to sGC in utero. Specifically, prenatal exposure to sGC is linked to symptoms of attention-deficit-hyperactivity disorder (ADHD) and these symptoms are attributable to changes in dopamine signaling as a result of sGC exposure. Kapoor et al. (2008) also indicated these results are consistent with those in animal models where prenatal exposure to sGC is associated with behavioral and locomotive differences. Results suggested the changes are likely transgenerational and involve long-term epigenetic modifications to HPA-axis tissues.

Davis et al. (2011) found direct correspondence between elevated maternal cortisol during the late second and third trimesters of pregnancy, with elevated cortisol of the subsequent infants in response to a painful heel-stick blood draw procedure. Elevated cortisol during early pregnancy, as well as psychosocial stress throughout pregnancy, were also associated with a slower behavioral recovery in the infants from the same heel-stick procedure. Conditions such as mode of delivery, medical history, socioeconomic status, race, and sex were ruled out as being explanatory for these elevated infant cortisol levels and stress responses. Results of this study provide strong evidence to support the role of prenatal stress by way of maternal cortisol exposure as having programming influences on the stress regulation physiology of the developing fetus that can be observed after birth.

In humans and other animal species, an enzyme known as 11β-hydroxysteroid dehydrogenase type 2 (*HSD11B2*) serves to regulate the amount of maternal cortisol that ultimately reaches the fetus as a natural mechanism to prevent cortisol influenced programming of the fetal HPA-axis (Duthie and Reynolds, 2013). The action of this enzyme has its limitations to where a higher threshold of maternal stress and disease may still allow undesirable amounts of glucocorticoids to reach the fetus. Consequences of this exposure to maternal glucocorticoids

include lower birth weight, shorter gestation length, susceptibility to neurodevelopmental aberrations, and cardiometabolic diseases later in life (Duthie and Reynolds, 2013). Additionally, HPA-axis dysfunction is also at risk in the mother, with postpartum depression and other mood disturbances being more prevalent in those having experienced prenatal stress (Duthie and Reynolds, 2013).

In juvenile rhesus monkeys, exposure to prenatal stress by way of daily acoustical startle for 25% of their gestation period resulted in behavioral and neuroendocrine alterations of mature offspring (Coe et al., 2003). At 2 to 3 years of age, the offspring of the prenatally stressed monkeys showed greater responsiveness to stress along with higher plasma cortisol levels. Hippocampal volume and neurogenesis in dentate gyrus, or a region of the brain critical for memory formation, was decreased in prenatally stressed monkeys when compared to the control group (Coe et al., 2003). This study provides evidence for aberrant neural development and exaggerated stress reactivity as a result of prenatal stress in a species of nonhuman primate.

Effects of daily restraint during the last 5 weeks of gestation on development and immune function in baby pigs was observed in a 2002 study by Tuchscherer et al. During the first month following parturition, baby pigs produced from gilts having experienced the stress treatment by way of restraint were found to have decreased lymphocyte proliferation as well as reduced thymus weights. Disease prevalence and mortality were significantly increased during the suckling period in the prenatally stressed baby pigs. Control baby pigs were found to always have higher cellular immunity while prenatally stressed baby pigs showed weaker stress hormone reactivity. These results strengthen the notion that prenatal stress has observable consequences on stress response and immune function in subsequent offspring.

Couret et al. (2009) sought to determine the effects of prenatal social stress on the immune and HPA-axis function of baby pigs. Social stress was induced by housing gilts in pairs and interchanging the pairs with unfamiliar individuals in one group, while housing consistent pairs of familiar gilts in the control group. Effects on HPA-axis function as a result of social stress could not be defined as no difference was found in growth rate or plasma cortisol levels between the two groups of offspring. However, immune function was observed to be altered, as total number of white blood cells, lymphocytes, and granulocytes were decreased in the group having experienced prenatal social stress. While these results suggest HPA-axis function was not influenced by this form of prenatal social stress, no deliberate stress tests were imposed upon these offspring, a condition by which a difference in cortisol production and/or stress response may have been observed. The differences in immune function of the offspring provide compelling evidence toward the adverse effects that prenatal stress can induce.

Rats have been the subject of numerous studies that aimed to characterize the effects of early life stress on both the mother and offspring (Charil et al., 2010). Many studies that observed the effects of prenatal stress in rats have found similar results to the previously mentioned studies in the way of inhibited neurological development and greater stress reactivity (Weaver et al., 2002; Charil et al., 2010; Jensen et al., 2012; Ewald et al., 2014; Meaney and Szyf, 2022). Prenatal stress had greater lasting effects in adult rats and mice than other forms of postnatal stress such as premature maternal separation (Estanislau et al., 2005).

Multiple studies in mice and rats have illustrated techniques that may serve to reverse or counteract the effects of prenatal stress in developing offspring (Charil et al., 2010). Environmental enrichment through use of various objects and containers that facilitated cage exploration as well as hiding for protection, along with an exercise wheel, were found to reverse behaviors assumed

to be induced by prenatal stress (Morley-Fletcher et al., 2003). Prior to enhanced environmental enrichment, prenatally stressed rats showed reduced social expression and prolonged corticosterone secretion in response to restraint. Both social and corticosterone secretion responses became aligned with those of the control group following time spent in the enriched environment (Morley-Fletcher et al., 2003). Reduction of hippocampal cell proliferation was observed in prenatally stressed rats by Lemaire et al. (2006), where survival rate, immature neurons, and differentiated new neurons were also observably reduced as compared to the control group. These effects, observed in both young and old groups of prenatally stressed rats, were markedly counteracted by neonatal handling from birth until weaning. These results provide important insight into mechanisms of reversing or counteracting prenatal stress where production characteristics in livestock species may be at risk.

Meaney and Szyf (2022) described the effects of varied licking and grooming of newborn pups by mother rats. When observed for frequency of licking and grooming behaviors, rat mothers were classified as either high or low. Offspring of high frequency licking and grooming by the mother showed reduced plasma adrenocorticotropic hormone (ACTH) and corticosterone responses to acute stress when compared to the responses of offspring from low frequency licking and grooming by the mother. As adults these offspring showed differing behavioral patterns as well, where the offspring of high frequency licking and grooming rats had reduced startle responses and were less hesitant to explore and/or eat when challenged with new environments as compared to the opposing group. To determine if these differences in stress responses are the result of maternal care, or simply inherited from the previous generation, a cross-fostering experiment was conducted in which the offspring of high frequency licking and grooming dams were swapped with the offspring of low frequency licking and grooming dams and vice versa. Results clearly

demonstrated the nongenomic nature of maternal care on the programming of stress response in rat pups. Offspring of the low licking and grooming dams that were reared by high frequency licking and grooming dams were less fearful in novel environments than their counterparts. These results reinforce the consequential nature of DNA methylation changes during early life and development.

The effects of stress on various cattle production metrics related to growth and immunocompetence has been a topic of pronounced importance and thorough investigation for the past several decades (Carroll and Forsberg, 2007). Specifically, transportation stress is known to influence physiological processes related to immune system function, carcass quality, and disease incidence (Fike and Spire, 2006). Lay et al. (1996) sought to determine the effects of both ACTH injection and transportation stress on plasma cortisol levels, plasma cortisol clearance rate, and weight differentiation in pregnant Brahman cows. An initial trial of varying doses of ACTH and saline injections into separate groups of cows showed that while higher doses of ACTH did not affect peak levels of plasma cortisol, higher doses of ACTH did result in a slower clearance rate of plasma cortisol compared to those injected with lower doses of ACTH and even more so compared to those injected with saline. A subsequent trial included induced transportation stress for one group cows, ACTH injection for a second group of cows, and a third control group cows which were treated at 60, 80, 100, 120, and 140 days of gestation. Results showed that ACTH injected cows experienced consistent plasma cortisol peak levels and clearance rates across each treatment, while the transported cows showed the greatest increase of plasma cortisol during the first and second transportation event with plasma cortisol steadily decreasing for every subsequent transportation event. Additionally, shrink, or the difference in initial weight at the start of a stress challenge from the weight at the end of the challenge, was the greatest for transported cows

compared to the other two treatment groups. Shrink, similar to plasma cortisol levels, was greatest in the transported cows in the initial events and steadily decreased for every subsequent transportation event. These results indicate that both exogenous ACTH administration, and induced stress in response to transportation, have clear but differing physiological effects in pregnant cows.

An additional study from Lay et al. (1997b) assigned pregnant Brahman cows to one of three treatment groups: a group that was transported in a stock trailer at various points during their pregnancy, a group that was injected with synthetic ACTH at various points during their pregnancy, and a group that was simply walked through their residing facilities at various points in their pregnancy. The transported test group produced offspring that experienced greater plasma cortisol levels when restrained as suckling calves. When all offspring were injected with synthetic cortisol, the offspring of the transported group showed a slower clearance rate of plasma cortisol as well as an overall greater heart rate through the duration of the test. Results of this study provide strong evidence to support prenatal stress by way of transportation as having a lasting effect on offspring stress regulation. Lay et al. (1997a) obtained blood from fetuses, prior to severance of the umbilical cord, of a treatment group of cows subjected to the same transportation stress previously described, and a control group that was walked through the barn where they resided. Calves were then exsanguinated, and pituitary and adrenal glands were collected. Plasma cortisol from the fetuses showed no difference between transported and control group; however, body weight, pituitary weight, and heart weight were all greater for the transported group relative to the control group. While no differences were detected in the adrenal glands between the treatment and control group, results of this study otherwise suggest prenatal stress may alter the morphological state of the pituitary gland.

2.2. DNA Methylation

While the association between prenatal stress and long-term neuroendocrine, cardiometabolic, and behavioral problems has been well established (Seckl, 2008; Kapoor et al., 2008), the underlying causal physiological mechanisms behind these associations are still being defined. Substantial evidence exists suggesting DNA methylation is a significant contributing factor to lasting and consequential changes in gene expression that influence stress and metabolism (Cao-Lei et al., 2020). DNA methylation plays an essential role in regulation of transcription, embryonic development, chromatic structure, genome stability, and genomic imprinting (Bird, 1986). In this context, DNA methylation refers to the process of adding a methyl group to the 5' carbon of the nitrogenous base cytosine (Bird, 1993). Adenine has also been found to be subject to methylation in mammals and other organisms; however, this mechanism has not been studied as closely and is not as prevalent in mammalian genomes (Wu et al., 2016). The methylation of cytosine is most frequently observed in regions of the genome that are 200 bp or longer, with at least 50% content of Cytosine bound to Guanine by a phosphate group (Gardiner-Garden and Frommer, 1987). These regions of the genome are referred to as CpG islands or CpG sites and, when located in the promoter or exon region of genes, have the ability to derail transcription and silence gene expression (Bird, 1993).

This mechanism of regulating gene expression is one that has been well conserved in complex vertebrate genomes to control growth processes and maintain genome stability (Ehrlich, 1981). Although developed as a genomic evolutionary advantage, disruptions or irregularities of DNA methylation have strong associations with chronic diseases. Knowing this, DNA methylation patterns have great potential to serve as biomarkers for disease presence and/or risk. Methylation of DNA is best observed at the tissue level, which presents limitations for accessing organs or parts

of the body that would require invasive work to reach (Walton et al., 2016). In multiple DNA methylation studies, peripheral blood leukocytes, or white blood cells, have been positioned as a potential surrogate for inaccessible tissues (McKay et al., 2011; Harris et al., 2012; Li et al., 2012; Ma et al., 2014; Huang et al., 2016; Braun et al., 2019; Åsenius et al., 2020).

2.3. DNA Methylation Patterns of Targeted Tissues

To better understand tissue-specific gene expression, Song et al. (2005) used liver, kidney, colon, brain, muscle, and testicular tissues of mice to identify tissue-specific differentially methylated CpG sites. Using restriction landmark genomic scanning (RLGS) and bisulfite sequencing, results of the study showed the greatest discordance in methylation levels between the testis and the other 5 tissues, while the liver, kidney, colon, brain, and muscle tissues were similarly methylated in CpG sites near 7 of the 14 identified genes. These results suggest specific areas of the genome in mice could be targeted to find areas of correspondence between tissues. The tissues used in this study require invasive procedures for sampling, leaving the more accessible peripheral tissues as subject for further investigation.

Hannon et al. (2021) studied DNA methylation patterns of three different peripheral tissues (whole blood, buccal epithelial cells and nasal epithelial cells) and five major blood cell types (granulocytes, monocytes, B cells, CD4+ T cells, CD8+ T cells) from humans where age and whether or not the individual smoked were used to differentiate case groups. The results showed high discordance between cell and tissue types with each sample type having distinct DNA methylation marks across multiple loci. Hannon et al. (2021) concluded that certain traits and/or environmental exposures can be reflected through selective gene expression within certain tissues, but that global disruption cannot necessarily be observed in whole blood samples. However, Houseman et al. (2015) concluded through a review of studies that biological insights still may be

gained from studying DNA methylation in whole blood, despite its heterogeneous nature and potential for confounding cell composition effects.

DNA methylation has been studied most extensively in humans; however, some studies produced findings unique to the animal and inconsistent with what has been observed in humans. Ching et al. (2005) for example, observed through comparative analysis that some, but not all, tissue-specific DNA methylation patterns in mice and rats were consistent with those in humans. Using brain tissues, astrocytes, keratinocytes, and WBC, Ching et al. (2005) found the rho guanine nucleotide exchange factor 17 (*ARHGEF17*) gene showed greater hypermethylation of nearby CpG islands in mice and rats compared to humans. The CpG islands of the SH3 and multiple ankyrin repeat domains 3 (*SHANK3)* gene were similarly methylated between mouse, rat, and human tissues. These findings indicate more refined studies are necessary to understand global DNA methylation patterns in differing species of mammals.

Through cross-species comparisons of paired genes, co-expression was consistent between humans, mice, sheep, goats, yaks, pigs, and chickens but much less consistent with other species such as cattle (Zhou et al., 2020). Zhou et al. (2020) further reported differences in DNA methylation levels across various tissues, as well as differences in developing tissues. This evidence supports the idea that DNA methylation pattern profiles should be considered by species, tissue, and even stage of development. Additionally, Zhou et al. (2020) provided baseline methylation patterns and transcription profiles for bovine somatic cells at a single-base resolution. Although this methylome was specifically characterized within a family of Holstein cattle, and breed differences can likely be expected, these results should prove useful for future DNA methylation studies in a species that has shown distinct pattern differences from other species.

Baik et al. (2014) characterized DNA methylation pattern differences between tissues by observing both intramuscular fat and muscle tissue sourced from the longissimus dorsi muscle in Korean steers. DNA methylation patterns differed in the promoter regions of the two genes, adipogenic peroxisome proliferator-activated receptor gamma isoform 1 *(PPARG1*) and lipogenic fatty acid binding protein 4 *(FABP4*). Specifically, methylation of CpG sites in both genes were observed to be greater in muscle DNA than in intramuscular fat DNA. This information reinforces the criteria of tissue-specific differences and will undoubtedly be useful for better characterization of DNA methylation patterns to potentially serve as biomarkers for cattle.

The previously mentioned study from Meaney and Szyf (2022) demonstrated a molecular basis for the effects of maternal care on stress responses in rat pups and observed greater expression of glucocorticoid receptors (*GR*) in the hippocampus of adult rats reared by high frequency licking and grooming rat mothers. This was attributable to hypermethylation of the nerve growth factor-induced clone A (*NGFIA*) in the offspring reared by low frequency licking and grooming mothers, which inhibited its protein binding abilities which is an important component of transcription processes for *GR*. It was also hypothesized that reversal of *NGFIA* inhibition and/or enhancement of *NGFIA* binding may be possible in the adult rat affected by early life DNA methylation. Histone deacetylases (*HDAC*) inhibitors were used by way of central transfusion to test this hypothesis in offspring of both high and low frequency licking and grooming mothers. Use of the *HDAC* inhibitor resulted in a reversal of *NGFIA* methylation through increased histone acetylation, which resulted in greater binding affinity of *NGFIA*, and therefore greater expression of *GR*. Though tested on a molecular level, these results are consistent with those of Morley-Fletcher et al. (2003) and Lemaire et al. (2006), where environmental enrichment and neonatal handling were used to determine if stress responses could be amended in rats having experienced prenatal stress. These

mechanisms of stress induced methylation correction could have highly impactful therapeutic properties.

2.4. In Utero Conditions Associated with DNA Methylation Changes

Diet and nutrient availability are commonly postured as an affecting mechanism responsible for epigenetic modifications in prenatal and early life development (Thompson et al., 2020). Gallou-Kabani et al. (2010) used mice to evaluate the effects of a high-fat diet during pregnancy on local and global DNA methylation patterns in placental tissues. The control diet, composed of appropriate fat concentration, showed lower methylation levels in male mice than in female mice, and the high-fat diet showed lower methylation levels in female mice only. Diet and sex-specific differential methylation was observed in 30 CpG sites located near one another on chromosome 17. These CpG sites were proposed as having potential influence on binding sites for transcription factors as well as chromatin remodeling. The results support the differential methylation that can be observed between sexes, as well as the in utero conditions affecting DNA methylation and gene expression.

In an effort to understand transgenerational effects of DNA methylation, Braunschweig et al. (2012) used two groups of F0 Swiss Large White pigs and differentiated treatment groups by feeding a standard diet to the control group, and a diet with high amounts of methylating micronutrients to the other. Subsequent F1 and F2 generations were fed the same standard diet recommended for the breed as was fed to the F0 control group. Using tissues from the liver and gluteus muscle, the results regarding DNA methylation in this study were inconclusive. Greater methylation levels of the iodotyrosine deiodinase (*IYD*) gene in the liver of the F2 control group was identified. However, the study was limited to only six promoter regions of differentially methylated genes, and no other significant differences were observed in methylation patterns

between case and control groups nor between liver and muscle tissues. Moreover, methylation patterns of the F0 group were not observed to indicate if the difference in diets caused any methylation differences in the initial generation. The limitations of this study leave the question of transgenerational effects of diets with methylating micronutrients open for further investigation.

A similar study was produced from Jin et al. (2018) where Large White x Landrace F_1 sows were separated into a control group being fed a standard diet and a case group being fed the same standard diet supplemented with methyl donor nutrients (3 g/kg betaine, 15 mg/kg folic acid, 400 mg/kg choline and 150 μg/kg VB_{12}) from mating (artificial insemination by two Landrace boars that were littermates to one another) to delivery. The newborn pigs and subsequent finishing pigs from the sows fed the methyl donor supplement showed greater levels of DNA methylation in the promoter region of the insulin-like growth factor-1 (*IGF-1*) gene in liver tissues as well as greater expression of both the *IGF-1* gene and the IGF-1 receptor (*IGF-1r*) protein in both liver and muscle tissues. These results reinforce in utero conditions as being influential on offspring DNA methylation patterns both immediately after birth and into maturity.

Gene expression effects on offspring in pigs related to nutritional differences were studied by Altmann et al. (2011) using skeletal muscle and liver tissues to target genes essential in methionine metabolism. Three groups of German Landrace sows were assigned diets of low protein concentration, high protein concentration, and the standard recommended protein concentration as the control group. Global liver methylation was significantly influenced by both restricted protein sow diets in fetal tissue and high protein sow diets in finisher pigs. Gene expression in both fetal liver and skeletal muscle tissues showed significant deviation from the control group at both the non-SMC condensin I complex subunit D2 (*NCAPD2)* gene and the non-SMC condensin I complex subunit H (*NCAPH*) gene from sows on restricted protein diets. These

results confirm that both limited and excess protein diets can affect methylation patterns of offspring in pigs, but where long term consequences of these changes still need to be characterized.

Using a sheep model, Zhang et al. (2011) aimed to evaluate the effects of over feeding ewes during the periconceptional period (immediately before conception and into early pregnancy) as well as during late pregnancy. Over feeding during the periconceptional stage resulted in a moderate increase of total body fat in female lambs only, but where other physiological insights could not be gained. However, the ewes that were over-fed in late pregnancy showed greater expression of the Peroxisome proliferator- activated receptor gamma (*PPARG*) gene in placental tissues, as well as an increase of total body fat in postnatal lambs. These results suggest in utero nutrient conditions have potential to cause increased fat deposition as well as impactful genomic programming. A group of ewes who were nutrient restricted during the periconceptional period produced lambs with greater adrenal gland weight, cortisol stress response, and hypermethylation of the insulin like growth factor 2 (*IGF2*). Findings of this study provide evidence of aberrant epigenomic changes from both over feeding and nutrient restriction in utero, where nutrient restriction appears to have more consequential effects on offpsring.

Chadio et al. (2017) also used sheep to assess the epigenetic effects of gestational nutrient restriction on hepatic gluconeogenic enzyme gene expression as well as changes in the glucocorticoid receptor. Three treatment groups were utilized where pregnant ewes in the first group were given a 50% nutrient-restricted diet from Day 0 to 30 of gestation, the second group was given a 50% nutrient-restricted diet from Day 31 to 100 of gestation, and the control group was fed 100% of required nutrients throughout gestation. Significant increased expression of the glucocorticoid receptor and hepatic phosphoenolpyruvate carboxykinase (*PEPCK*) was observed in both case groups compared to the control group. A decrease in methylation of hepatic

gluconeogenic enzyme was observed in the case group that was nutrient-restricted during days 31 to 100 of gestation, with the case group of nutrient restriction during days 0 to 30 also showing a decrease in methylation but to a lesser extent. These findings support the notion of sex-specific methylation changes as a result of in utero conditions but where species-specific criteria should be characterized.

2.5. Effects of Maternal Stress and HPA Axis Function on Developmental Methylation Changes

While the association between prenatal stress and long-term neuroendocrine, cardiometabolic, and behavioral problems have been well established (Seckl, 2008; Kapoor et al., 2008), the underlying causal and physiological mechanisms behind these associations are still being defined. Substantial evidence exists suggesting DNA methylation is a significant contributing factor to lasting and consequential changes in gene expression that influence stress and metabolism in offspring (Cao-Lei et al., 2020). Vidal et al. (2014) failed to detect an association between maternal stress in women and preterm birth. However, using peripheral and cord blood from mother-infant pairs, DNA methylation was measured at multiple differentially methylated regions, and an association between maternal stress and higher infant DNA methylation of the mesoderm specific transcript (*MEST*) gene was found.

Utilizing women who lived through the 1998 Quebec Ice Storm while pregnant, Cao-Lei et al. (2014) aimed to characterize prenatal maternal stress effects on postnatal epigenetic modifications. Using peripheral blood mononuclear cells, T cells, and saliva cells from the subsequent children at ages 8 and 13 years, evidence supporting prenatal stress and its effects on lasting DNA methylation signatures were presented. Specifically, CpG sites near 957 genes associated with immune function showed methylation changes concordant with prenatal maternal

stress, and significant hypermethylation in the secretogranin V (*SCG5*) gene and the lymphotoxin alpha (*LTA*) protein were also observed. The cases were further evaluated for association between prenatal maternal stress and increased central adiposity (waist size-to-height ration) and body mass index (Cao-Lei et al., 2015). Methylation changes from established Type-1 and -2 diabetes mellitus pathways showed concordance with greater central adiposity as well as body mass index, indicating DNA methylation as a mechanism for creating lasting genome programming as a response to early life adversity.

Kundakovic et al. (2014) investigated psychopathology changes during development and used both a mouse and human model to determine if early-life adversity disrupts epigenetic programming that is observable in peripheral tissue data. For the mouse model, in utero bisphenol A (BPA), an endocrine disruptor, was given to pregnant mice as a way to induce lasting epigenetic interference. Lasting DNA methylation changes occurred in the transcriptionally relevant region of the brain derived neurotrophic factor (*BDNF*) gene in both the hippocampus and peripheral blood. Methylation changes of the *BDNF* gene were observed in the placental blood of humans exposed to high maternal BPA. Given that *BDNF* methylation changes have known association with psychiatric disorders (Kundakovic et al., 2014), and that both gene expression and DNA methylation are shown to be altered in both brain and blood tissues, it was posited that this gene may represent a novel biomarker for early psychiatric risk.

Nemoda and Szyf (2017) observed the effects of major depressive disorder in the mother on DNA methylation changes in various tissues including peripheral tissue of newborn cord blood, infant saliva, and adult peripheral blood. It was concluded that prenatal maternal depression can cause DNA methylation changes in the glucocorticoid receptor and the serotonin transporter that are detectable in leukocytes of newborns at birth, and potentially detectable in other tissues as well.

With regard to fetal HPA axis function, Sosnowski et al. (2018) observed through a more recent review of studies that a link exists between prenatal maternal stress, methylation of the nuclear receptor subfamily 3 group C member 1 (*NR3C1*) gene, and infant stress reactivity. Unfortunately, the relevant associations stop there with inconclusive results pertaining to genes identified among the various studies that were used.

Although human studies reveal much about the relationship between prenatal stress and epigenetic modifications, the differences in function of the human HPA-axis during pregnancy may not be reflective of that in livestock species (Glover, 2015). For this reason, animal models are likely more revealing to determine the extent of epigenetic aberrations as a result of prenatal stress. An early study in developmental HPA-axis responsiveness to stress, conducted by Weaver et al. (2002), observed mother rats and early-life care of their pups. An increase in the behaviors of licking, grooming, and arched back nursing of pups was shown to have a dampening effect on the sensitivity of HPA-axis function in the subsequent adult rats. Specifically, the adult rats who received greater frequency of these behaviors from their mothers showed decreased methylation in the exon region of the glucocorticoid receptor which ultimately increased expression of this gene and related transcription factors. Glucocorticoid receptors are an essential component of the negative feedback system that regulates corticotropin releasing hormone levels, suggesting that hypomethylation, and in turn greater expression of, glucocorticoid receptors could result in better mediated HPA-axis function.

Jensen et al. (2012) used Long Evans rats to observe the effects of prenatal stress in the placental 11β-hydroxysteroid dehydrogenase type 2 (*HSD11B2*) gene which is responsible for converting cortisol and corticosterone into inactive metabolites to mitigate the effects of maternal glucocorticoid exposure. The findings of this study suggest that prenatal stress can alter DNA

methylation patterns which can have lasting effects on the expression of the *HSD11B2* gene. Increased DNA methylation was observed at specific CpG sites within the gene's promoter region in the placenta but decreased DNA methylation of CpG sites occurred in the promoter region in fetal hypothalamus tissue. Methylation of the *HSD11B2* gene in the fetal hypothalamus was increased at sites within exon 1. The fetal cortex tissue did not show any changes of DNA methylation within the *HSD11B2* gene. Jensen et al. (2012) reported high correlations of methylation patterns in specific CpG sites within the promoter region and exon 1 of the *HSD11B2* gene between placental and brain tissues, suggesting that placental tissue may be a viable predictor for methylation changes in the brain.

Ewald et al. (2014) utilized a mouse model of Cushing's disease to determine if glucocorticoid induced epigenetic changes would correlate between hippocampus brain tissue and WBC. Stress response was targeted in the FK506 binding protein 5 (*Fkbp5*) gene. Recognizing the study as being limited to several intronic CpGs of a single gene, Ewald et al. (2014) were able to find a significant linear association between DNA methylation and four-week mean plasma corticosterone levels for blood and brain tissues. These results suggest peripheral blood may be viable for assessing changes in brain tissues related to glucocorticoid production, however, further tissue-specific criteria should be outlined for these analyses to be effective. Tissues more relevant to HPA axis function and cortisol production, such as the hypothalamus, pituitary glands, and the adrenal cortex, could potentially have greater insight into glucocorticoid influenced epigenetic modification.

2.6. DNA Methylation Patterns of Blood Compared to Targeted Tissues

In humans, DNA methylation patterns have shown global disruption in cancer and in numerous genetic disorders (Robertson, 2005). Li et al. (2012) reported global methylation of

WBC as differing significantly between healthy controls and cases of various cancers such as pancreatic, breast, bladder, and colorectal. The potential for use of WBC as a biomarker for cancer detection was reinforced by Woo and Kim (2012) who performed a meta-analysis to determine risk of various types of cancers using global DNA hypomethylation levels in peripheral blood leukocytes. While indicating that region and cancer type are important to define for accurate determination of risk, it was ultimately concluded that WBC have great potential as a disease biomarker for cancer in humans. Conversely, Harris et al. (2012) found that WBC DNA methylation patterns have a limited ability for detecting or predicting inflammatory bowel diseases in humans. These findings suggest WBC may serve as a suitable biomarker for some diseases and in some tissues.

Jin (2020) investigated DNA methylation patterns between peripheral blood and breast cancer tissue, as well as between day shift workers and night shift workers. Five genes showed consistent methylation pattern disruption between peripheral blood and breast cancer tissue, with differences also detected between day shift and night shift workers. The aberrant methylation status of the genes, insulin growth factor 2 *(IGF2)*, BReast CAncer Gene *1 (BRCA1)*, glutathione S-transferase Pi *(GSTP1)*, cyclin-dependent kinase inhibitor 2A *(CDKN2A)*, and methylguanine methyltransferase *(MGMT*), could potentially be useful as surrogate markers for breast cancer risk and/or detection, as well as useful for studying the effects of circadian disruption.

Huang et al. (2016) compared DNA methylation patterns of human adipose tissue and blood. They required some correlation between blood and target tissue, as well as this correlation being at least partially attributed to an association with a phenotype of interest. It was concluded that, in the case of adipose tissue, WBC do not adequately reflect DNA methylation patterns, but

that assessment of DNA methylation using tissue specific fine-phenotyping as well as anatomical, histological, and temporal characterization might be appropriate.

This conclusion was upheld by Åsenius et al. (2020) who utilized obesity as a phenotype of interest and compared DNA methylation patterns of blood to that of sperm cells. The relationship was highly discordant and led to the conclusion that human sperm DNA methylation has a unique pattern that is practically uncorrelated with that of respective peripheral blood. Methylation patterns of DNA in human sperm were only nominally correlated with obesity, positioning sperm cells as an unlikely marker for metabolic activity in humans. Wang et al. (2010) utilized obesity as a phenotype of interest and found significantly lower methylation of a CpG island near the tripartite motif-containing protein 3 (*TRIM3*) gene, as well as significantly higher methylation of a CpG island near the ubiquitin associated and SH3 domain containing A (*UBASH3A*) gene in the obese cases compared to non-obese controls. These results indicate that DNA methylation changes may be attributed to obesity and that these changes can be observed in WBC.

DNA methylation patterns in human bone were the subject of a 2021 study by Ebrahimi et al., where blood was investigated as a surrogate. Epigenome-wide DNA methylation at 850,000 CpG sites were observed in both blood and bone tissue, and it was found that a total of 28,549 CpG sites were similarly methylated between tissues. Ebrahimi et al. (2021) concluded that these results indicate that blood methylation patterns may mirror those of human bone to a sufficient degree for DNA methylation studies when access to bone is not practical.

Ma et al. (2014) investigated locus-specific methylation differences between tissues in humans using publicly available data from a childhood asthma study where lymphoblastoid cells and peripheral blood leukocytes were used. A study of postoperative atrial fibrillation where the

atrium, artery, and peripheral blood leukocytes were used was also subjected to further evaluation. Utilizing a quantile normalization model, the study gave the strongest prediction of methylation patterns between WBC to artery tissues followed by WBC to atrium. This might enable non-invasive disease screenings.

Species-specific observations are also important for considering blood as an effective biomarker for specific tissues. McKay et al. (2011) compared DNA methylation patterns in blood to patterns in the liver and kidney of post-partum mice. Folate, which has been shown to alter DNA methylation patterns (McKay et al., 2011), was used in varying amounts to differentiate case groups. Results of this study were consistent with Huang et al. (2016) and Åsenius et al. (2020) in finding limitations of detecting DNA methylation patterns of target tissues through use of peripheral blood leukocytes. More recently, Svoboda et al. (2021) investigated the adverse metabolic effects of perinatal lead exposure. Utilizing paired liver and blood samples from adult mice, thousands of sex-specific cytosines in both tissues were observed, including 44 genomically imprinted loci. There was significant tissue overlap in the genes mapping to differentially methylated cytosines.

2.7. DNA Methylation Patterns of Blood Compared to Various Brain Tissues

Whereas previously mentioned studies may not be able to endorse blood as a viable surrogate for DNA methylation patterns in some target tissues, the idea that species-specific and tissue-specific criteria need greater characterization is upheld. Regarding brain tissues, Horvath et al. (2012) compared age-related DNA methylation changes in brain tissues to whole blood and blood leukocytes. Results showed mean gene expression levels (mRNA abundance) and co-expression relationships are only weakly preserved; however, mean methylation levels showed strong correlations (around $r = 0.9$) between brain and whole blood, while age correlations of CpG

methylation patterns showed moderate correlations (around r = 0.33) between brain and blood tissues. Horvath et al. (2012) utilized ten published data sets to examine regions where CpG sites were consistently methylated between tissues. Significant age-related methylation pattern consistency was noted in CpG sites of genes known to be downregulated in early Alzheimer's disease. The genes found to be differentially methylated based on age are also involved in processes of nervous system development, neuron differentiation, and neurogenesis. Horvath et al. (2012) ultimately concluded that there were age-related co-methylated CpG regions that are consistent between human blood and brain tissues. Masliah et al. (2013) reported concordant methylation changes between blood and brain tissues amongst a specific subset of genes in humans affected with Parkinson's disease. Alzheimer's disease was the specified phenotype for comparing epigenetic variation between blood and brain tissues in the review from Wei et al. (2020). The Amyloid precursor protein (*APP*) gene was the only gene consistently hypermethylated in both brain and peripheral blood.

Although previously mentioned studies show promise for the use of WBC as a biomarker for epigenetic changes in brain tissues, other studies have found contradictory results. Epilepsy patients were used as a subject for comparison of DNA methylation of brain tissue to peripheral blood leukocytes by Braun et al. (2019). Within CpG sites in DNA from tissue of each region of the brain, blood, saliva, and buccal tissue and found that, blood showed the highest correlation to brain methylation patterns at ostensibly significant levels of 20.8%. Braun et al. (2019) reported that brain-peripheral tissue correlations to be inconsistent and indicates that patterns specific to the genomic region of interest should be characterized for most accurate results.

Similarly, Walton et al. (2016) used temporal lobe tissues from Schizophrenia patients to determine if DNA methylation patterns would correlate in peripheral blood. Only 7.9% of CpG

sites as having significant association between blood and brain. Though greater than was predicted by the study, the observed correlation led to the conclusion that DNA methylation markers of WBC cannot reliably predict that of brain tissues. Walton et al. (2016) indicated that a subset of peripheral methylation information specific to tissue or cells, such as blood leukocytes, could potentially be a useful biomarker.

Some age-related DNA methylation pattern alterations can be observed through peripheral blood patterns in mice. For consideration of age-related signatures, Harris et al. (2020) used the hippocampus and WBC of young and aged mice. Only 5 differentially methylated regions were identified gene promoters, and only three were expressed at significantly lower levels in aged mice. Additionally, several transcription factor binding motifs enriched with differentially methylated regions that were common to both the hippocampus and blood tissue were identified.

2.8. Previous Studies Analyzing Stress in Brahman Cows and Offspring

The animals used for the present study were also observed by Price et al. (2015) where several physiological tests were performed on the transported pregnant cows to observe responses to stress from transportation, as well as how variability in temperament can influence those stress responses. Cows were classified as either calm, intermediate, or temperamental, and vaginal temperature, serum cortisol, serum glucose, and serum nonesterified fatty acids were collected before and after each transportation event. Serum cortisol increase following transportation was consistent across all cows of each temperament but was consistently elevated prior to transportation for those classified as temperamental. Vaginal temperature and serum glucose were also elevated post-transportation as opposed to pre-transportation, but this difference did steadily reduced over time with each additional transportation event. This finding was consistent with that of Lay et al. (1996) where habituation to stress challenges was observed through reduction in

physiological responses from repeated occurrences. Changes in serum nonesterified fatty acids were variable across all temperament groups but did not change as a result of repeated transportation events. These results provide insight into the physical manifestations and severity of stress experienced by the pregnant cows that were used for observation of prenatal stress effects in their offspring. Littlejohn et al. (2016) measured temperament and serum cortisol of the (prenatally stressed) PNS, those calves that were gestating during the transportation stress described, and control calves to determine if prenatal stress imposed upon the dam would physically manifest in the offspring. Although there was no difference in birth or weaning weight, temperament scores and serum cortisol levels were consistently elevated in the PNS calves compared to the control calves when measured throughout various points of time prior to weaning.

Tissues from areas of physiological interest, such as those of the adrenal axis require invasive and costly procedures for sampling, and easily obtained alternatives, such as white blood cells (WBC), have been proposed as a possible surrogate for observation of DNA methylation changes. Cattle have sparsely been used as the subject of epigenetic studies aimed toward simplifying identification of DNA methylation changes, despite the applicability to improve production practices. Species specificity is a clear confounding factor when considering previous research in the field, and consequences of DNA methylation should be characterized as such. Therefore, the present study intends to better define the relationship between WBC and HPA axis tissues. This will be achieved through the use of a group of mature Brahman cows that was subjected to prenatal transportation stress, and a control group that was not. Comparison of WBC to each tissue of interest (adrenal cortex, adrenal medulla, anterior pituitary, and paraventricular nucleus of the hypothalamus) in the control was conducted to determine what association, if any, exists. Comparison of WBC to each tissue of interest in the PNS group was also conducted to

determine what association, if any, exists. Results from comparisons within the control group will then be evaluated for correspondence with the results from comparisons within the PNS group, to determine if patterns of DNA methylation change in response to prenatal stress in a way that would indicate a predictive relationship between WBC and tissue. Each tissue of interest will then be compared to one another, to further characterize tissue specific DNA methylation patterns.

3. METHODS

3.1. Animal Procedures

To investigate the relationship between DNA methylation patterns in HPA-axis tissues and peripheral blood leukocytes (white blood cells), as well as comparisons of HPA-axis tissues to one another, data mature Brahman cows (*Bos indicus*) from a comparative DNA methylation experiment were used (Littlejohn et al., 2018; Littlejohn et al., 2020; Baker et al., 2020; Cilkiz et al., 2021). A group of Brahman cows (n = 96) were determined to be pregnant by a day-45 rectal palpation following their last breeding date. Cows were then assigned to one of two treatment groups based on age, parity, and temperament. The treatment group (n = 48) would experience deliberate stress via transportation, and the other group (n = 48) would serve as the control group that would not be subjected to the same stressor while pregnant. The indicated stressor involved 5 transportation occurrences at 60 ± 5, 80 ± 5, 100 ± 5, 120 ± 5, and 140 ± 5 days of gestation. During each occurrence of transportation, the same 2.4m by 7.3m 3-section trailer was utilized and towed by a three-quarter ton truck on smooth highways for a total of 2 hours at a time. This treatment mimicked a previous study regarding prenatal stress that found HPA-axis function to shift in calves having experienced these same conditions in utero (Lay et al., 1997). Control cows were maintained in the same conditions as the stressed cows but were not subjected to the same transportation events.

Both groups were maintained in the same pasture managed under the same nutritional conditions at the Texas A&M AgriLife Research and Extension Center at Overton, and all procedures were done in compliance with the Guide for the Care and Use of Agricultural Animals in Research and Teaching (FASS, 2010) and approved by the Texas A&M AgriLife Research Animal Use and Care Committee. The diet consisted of ad libitum coastal bermudagrass (*Cynodon*

dactylon) in pastures during the summer and fall seasons. The same pastures were overseeded with rye (*Secale cereale*) and ryegrass (*Lolium multiflorum*) Cows were supplemented with coastal bermudagrass hay and a 3:1 corn:soybean meal mix as required depending on forage quality and availability.

Control cows subsequently produced 26 males and 18 females and cow that experienced transportation stress during pregnancy produced 20 males and 21 females. The 39 heifer calves were subsequently entered into the typical development regimen of cows in the herd, which included exposure to bulls for mating at 1 year of age and once per every following year. At 5 years of age, 8 controls and 6 PNS nonpregnant cows from the remaining cows in the groups were harvested at the Rosenthal Meat Science and Technology Center on the Texas A&M University campus. Blood samples were obtained, and leukocytes were stored at –80°C. Tissues obtained from the cows at that time included whole adrenal cortex, adrenal medulla, anterior pituitary, and paraventricular nucleus of the hypothalamus. All were then stored at –80°C.

3.2. DNA Extraction

For methylation analysis, DNA was extracted from 20 mg of each tissue. Sample extraction and digestion protocol was carried out as follows: Tissues were placed in the microcentrifuge and 150 µL of sodium chloride-Tris-EDTA buffer, 25 µL of Proteinase K (20mg/mL) and 25 µL 20% sodium dodecyl sulfate were added. Tissues were gently mixed with the solution and samples were subsequently incubated in a 56°C water bath for 2 hours. The final step involved adding 20 µL of RNAse A (10 mg/mL) to the sample tubes after which the mixtures were incubated at 37˚C for 30 minutes. Purified DNA was then isolated from the digested tissues following the GeneJET Genomic DNA Purification Kit (Thermo Scientific; Waltham, MA, USA) protocol. Following

purification, DNA was quantified with a NanoDrop Spectrophotometer (NanoDrop Technologies, Rockland, DE) and stored at –80˚C.

3.3. DNA Methylation Library Preparation and Sequencing Alignment

Samples of isolated DNA from the extracted tissues were sent to Zymo Research (Irvine, CA) for reduced representation bisulfite sequencing analysis. This process involved DNA digestion with 60 units of TaqαI followed by 30 units of MspI, and then purified with DNA Clean and ConcentratorTM. Ligation to the fragments was then done using adapters containing 5'-methyl-cytosine. Using the ZymocleanTM Gel DNA Recovery KitRe, adapter-ligated fragments of 150 to 250 bp and 250 to 350 bp were recovered and then ligated to the purified DNA fragments followed. Next, the EZ DNA Methylation-LightningTM Kit was used for bisulfite treatment of recovered fragments. Reads were then identified and sequenced from the bisulfite-treated libraries using Illumina base calling. TrimGalore 0.6.4 software was then used for trimming and quality checking based on adapter quality and content, followed by alignment of reads to the *Bos taurus* genome (ARS-UCD1.2; Rosen et al., 2020) using Bismark 0.19.0 (Babrahman Bioinformatics, Cambridge, United Kingdom). The binary alignment map (BAM) files were then quantified and aligned by methylated and unmethylated read totals at each CpG site using using MethylDackel 0.5.0 (Zymo Research).

3.4. Statistical Analyses Between Tissues

Pairwise comparisons of global methylation were performed to evaluate differences between DNA of white blood cells and that of the individually sampled HPA-axis tissues of both the prenatally stressed mature Brahman cows and the control group of mature Brahman cows. These relationships were compared to determine if prenatal stress causes long-term DNA methylation disruption that can be observed within these tissues of mature cows, and if that

disruption is reflected in methylation patterns of the more accessible WBC. Individual CpG sites across the genome, that is, without regard to predefined features, were the focus of subsequent analyses. A bisulfite feature methylation pipeline (SeqMonk) was applied followed by calculation of the information provided by the methylation call tables for the total coverage count, percent methylation, methylated counts, and unmethylated counts. Initial analyses in the software package EdgeR (Robinson et al., 2010) involved filtering for sites with 5x coverage, that is, sites with at least 5 or more read counts within each sample such that adequate sites were utilized for analyses that would be reflective of biological variability in all 14 samples, similar to thresholds utilized in previous livestock methylation studies (Livernois et al., 2021). Data were then fit to a negative binomial (NB) generalized linear model, and differential methylation was assessed using the likelihood-ratio test with the contrast of HPA-axis tissue minus WBC, to circumvent the assumption of normality for log-fold-change and other estimation coefficients (McCarthy et al., 2012). Sites that were always methylated or unmethylated in samples from all animals were removed, as well as any mitochondrial DNA. Filtered sites were then annotated for distance from their closest transcriptional start site relative to the gene on which they were located or the gene to which they were the closest. The false discovery rate (Benjamini and Hochberg, 1995) was controlled at 0.15 to avoid being excessively strict and stifle the potential discovery in this relatively new area of investigation. Analyses were performed for HPA-axis tissues against WBC for both the control and PNS groups (total of 8 sets of results were collected), and corresponding analyses were ultimately compared by treatment to observe both the relationship between methylation patterns of HPA-axis tissues and WBC and how these relationships change, if at all, when involving prenatally stressed cows.

Common dispersion estimates were also calculated for all comparisons. The EdgeR dispersion estimate function fits data to a linear model and uses an empirical Bayes procedure that collects replicate variability information across all loci to estimate locus-specific dispersion estimates (McCarthy et al., 2012; Korneliussen et al., 2014; Feng et al., 2014; Chen et al., 2017). In the case of bisulfite sequencing (BS-seq) data, thousands of loci with replicates of each genomic locus were evaluated. Variance of read counts follows a quadratic mean-variance relationship that uses sequence variability and biological variability combined with the dispersion estimate (Feng et al., 2014). In this case, the quadratic relationship is able to capture all technical factors affecting variability, resulting in a dispersion estimate that only reflects biological characteristics of each locus (Feng et al., 2014; Chen et al., 2017). Furthermore, BS-seq data does not have an apparent mean-variance trend, as is commonly observed in RNA sequencing data, and therefore a common dispersion estimate was generated for all loci using the "estimateDisp" function in EdgeR where the common dispersion estimate is reflective of the variance in methylation for all tissue samples (Feng et al., 2014).

Multidimensional scaling (MDS) plots were generated to provide a visual representation of variability between tissues and WBC within both the control and PNS groups. These plots show the distances between individual samples; each distance represents the average probability that a variable is less than or equal to a designated value (quantile function) in a continuous probability distribution (logistic distribution), also known as the logit function (Al-Aqtash et al., 2015). Log transformed expression values were used to model proportional changes rather than additive changes, and therefore a log base of 2 was used in calculating log-fold-change values, as log2 better fits the NB distribution and is better for detecting smaller, more biologically relevant changes (Changyong et al., 2014). Additional illustration of variability between tissues was

provided by mean difference (MD) plots which were generated for both the control and PNS groups of cows. MD plots are useful for visualizing intensity-dependent trends where variability as well as magnitude of differential methylation are plotted (Ritchie et al., 2015; Chen et al., 2016). The MD plots for data in this study scale the log-fold-change (LogFC) values, which can also be thought of as differences in methylation between samples, against log counts-per-million (LogCPM), which can also be thought of as average abundance or levels of methylation across sites (Ritchie et al., 2015).

3.5. Analysis of Differentially Methylated CpG sites within Promoter Regions

To gain a better understanding of LogFC ratios and their implications within tissue to WBC comparisons, individual CpG sites showing discordance between control and PNS groups were further evaluated. Sites were filtered for associated false discovery rate values of less than or equal to 0.15 (FDR $\leq$ 0.15) and a location of 1,000 base pairs or less upstream, or 500 base pairs or less downstream, of the closest transcription start site. Sites in the control group were then cross referenced with those in the PNS group and the most differentially methylated sites were selected for each tissue to WBC comparison. Selected sites demonstrate opposing LogFC ratios where negative values indicate greater methylation in the promoter region of that gene in WBC while positive values indicate greater methylation in the given HPA-axis tissue. Given that LogFC values represent a ratio, the positive and negative nature of each value can be thought of as a distance from zero, as opposed to a gain or deficit. Those sites having opposing, but symmetric values across zero (i.e., as close as possible to the same numerical distance from zero in each direction) were selected for further evaluation. The reason for this selection method relates to the nature of the LogFC ratio, where the same or similar values in opposing directions

to zero (positive vs. negative) between control and PNS groups indicate inverted ratios, and therefore proportional changes in methylation between treatments.

To qualify as "differentially methylated" in this sense, sites were limited to those that had LogFC values being greater than or equal to 2 for one group, and less than or equal to –2 in the opposing group. Other work evaluating DNA methylation using LogFC values is limited, therefore gene expression studies, which more commonly utilize LogFC, were referenced. The 2019 study from Lee et al., used an absolute LogFC value of 0.15 as the minimal value for differentially expressed genes. Additionally, Guo et al. (2019) used a lower threshold of 1.5 LogFC or lower to characterize genes as being significantly under expressed, and LogFC of 3 or higher as being significantly over expressed. A 2016 publication from Schurch et al. provides guidelines for analyzing and interpreting RNA-seq and differential expression data, and set arbitrary thresholds of 0, 0.3, 1, and 2 for true positive, true negative, false positive, and false negative rates respectively, in relation to the null hypothesis of no differential expression. These studies, along with an understanding of computation of LogFC, supported the threshold of an absolute value of 2 to identify differential methylation between treatment groups

To generate supporting data, EdgeR analyses were conducted for individual tissues to compare treatment effects for these previously selected (and only these) CpG sites within each tissue. Pearson correlation coefficients for mean methylation between tissue to WBC were generated for the genes on which the selected differentially methylated sites were located. These correlation coefficients were estimated for both control and PNS groups. Pearson correlation coefficients may either support the discordance observed in opposing LogFC ratios for the selected genes by way of acceptable negative values (P value ≤ 0.05) or indicate inconclusiveness of differential methylation within those genes.

4. RESULTS

4.1. Comparisons of WBC DNA methylation to DNA methylation of Specific Neuroendocrine Components of the Bovine Adrenal System

4.1.1. Adrenal Cortex

The related count results, percentages, and common dispersion estimates for comparisons of adrenal cortex tissue to WBC in both PNS and control groups can be observed in Table 1. The greatest proportion of sites passing coverage for both the control group at 59.4% and PNS group at 64.1% were found to be not significant, which can also be thought of as similarly methylated in the sense that a large enough difference was not detected to signify either hypomethylation or hypermethylation in favor of one tissue over the other. In both groups of cows, WBC yielded greater methylation concentration at 35% for control and 30.2% for PNS when compared to adrenal cortex tissue. Proportions of differential methylation across all sites filtered were relatively consistent between PNS and control. The common dispersion values of 0.0891 in the control group and 0.0816 in the PNS group indicate only a small degree of variability exists between adrenal cortex tissue and WBC tissue samples. However, the similarity in values between comparisons within the control group and comparisons within the PNS group also indicate the change between the treatments may only be nominal. The proportion of similarly methylated sites may not necessarily reflect the same sites as being similarly methylated withing the control and PNS groups, and therefore the tissues would then reflect those changes in concordance with one another.

To further illustrate differential methylation between tissues, MDS plots were generated which can be seen in Figure 1 for both control and PNS groups. Disparities between tissue types plotted for both the control and PNS groups show high discordance in methylation patterns for

the topmost differentially methylated CpG loci of each adrenal cortex sample. Relating back to the lack of diversity indicated by the common dispersion estimates, this likely stems from the proportion of sites considered not significant, or similarly methylated between groups, rather than from having most of the same sites being hypomethylated and hypermethylated. This could also indicate that patterns of methylation between the tissue types are polarizing in the sense that where hypomethylation occurs in adrenal cortex tissues, hypermethylation is occurring in WBC tissue and vice versa. Closer investigation into individual differentially methylated sites would bring more clarity to this position.

To further consider the variability between adrenal cortex tissues to WBC tissues, MD plots were created which can be seen in Figure 2. Differential methylation of the adrenal cortex tissue WBC is apparent. It can be posited that overall methylation levels, or LogCPM, are greater for WBC compared to adrenal cortex tissues. The MD plots suggest, by way of opposing directionality of blue and red along the y-axis, that both tissues (adrenal cortex and WBC) show significant degrees of differential methylation across sites. This suggests a specific subset of sites may be altered in methylation between the control and PNS groups, but it is not likely that global methylation alters in concordance between control and PNS groups in a consistent fashion that would provide adequate reflection of adrenal cortex tissue methylation through evaluation of WBC tissues. Relative to adrenal cortex tissue, WBC maintained greater abundance of methylation in both treatment groups which limits an identifiable pattern between adrenal cortex tissue and WBC.

Table 1. Counts and percentages of differentially methylated CpG sites and common dispersion estimates for adrenal cortex tissue to white blood cell tissue comparison.

Measurement	Control		PNS[1]	
	Count	Percentage	Count	Percentage
Adrenal cortex[2]	17,713	5.6%	30,615	5.7%
White blood cells[3]	109,780	35%	161,283	30.2%
Not significant[4]	186,838	59.4%	342,482	64.1%
Total	534,380	100%	314,331	100%
Common dispersion estimate[5]	0.0891		0.0816	

[1]Prenatally stressed.

[2]Number and proportion of sites showing greater methylation in adrenal cortex tissues.

[3]Number and proportion of sites showing greater methylation in white blood cells.

[4]Number and proportion of sites without significant differential methylation between tissues.

[5]Squared coefficient of variation in the true abundance of replicates between adrenal cortex tissue and white blood cell tissue.

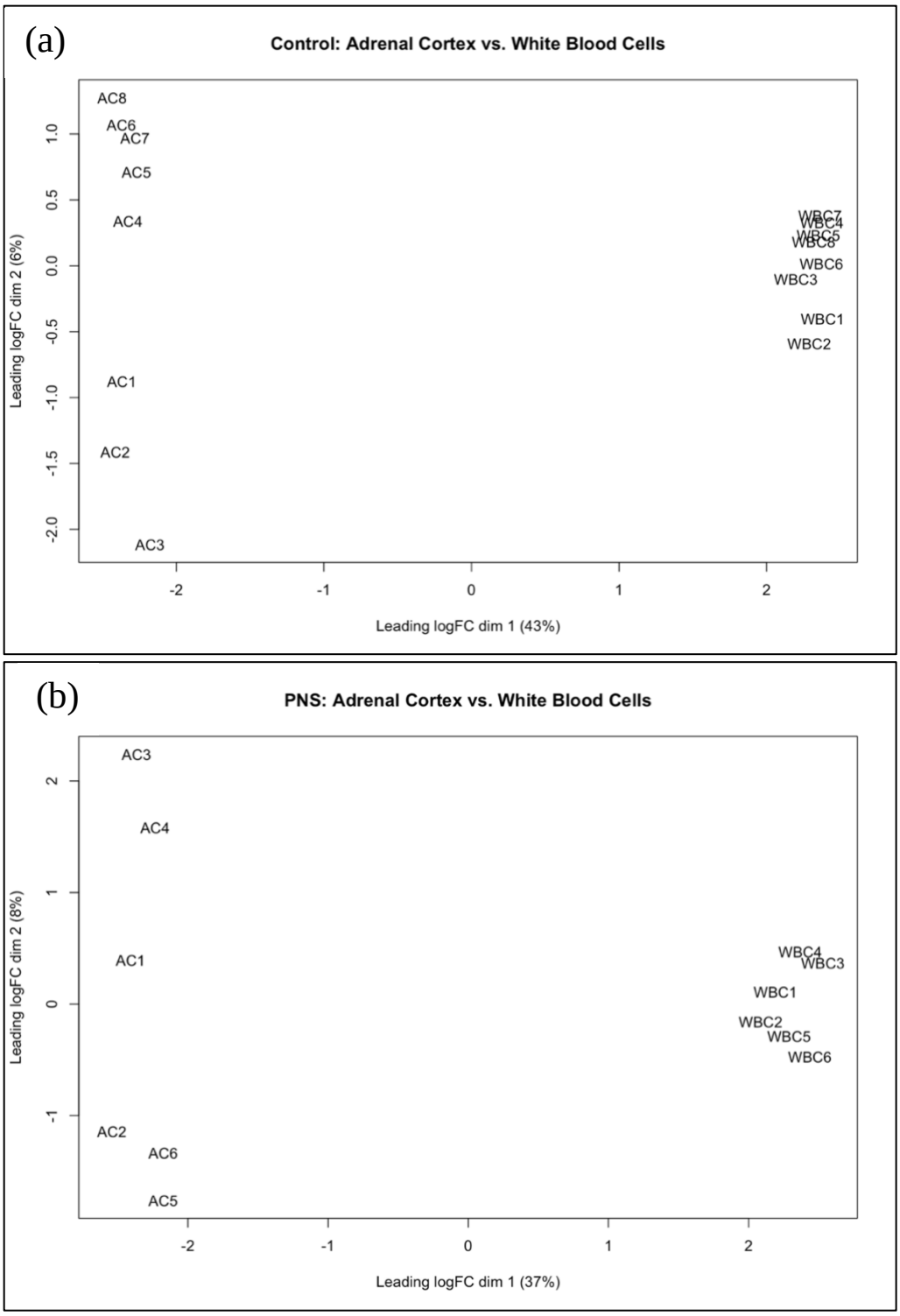

Figure 1. Multidimensional scaling plots for (a) control cows and (b) prenatally stressed (PNS) cows. AC: adrenal cortex. WBC: white blood cells. Sample numbers follow those abbreviations and correspond to the same cows.

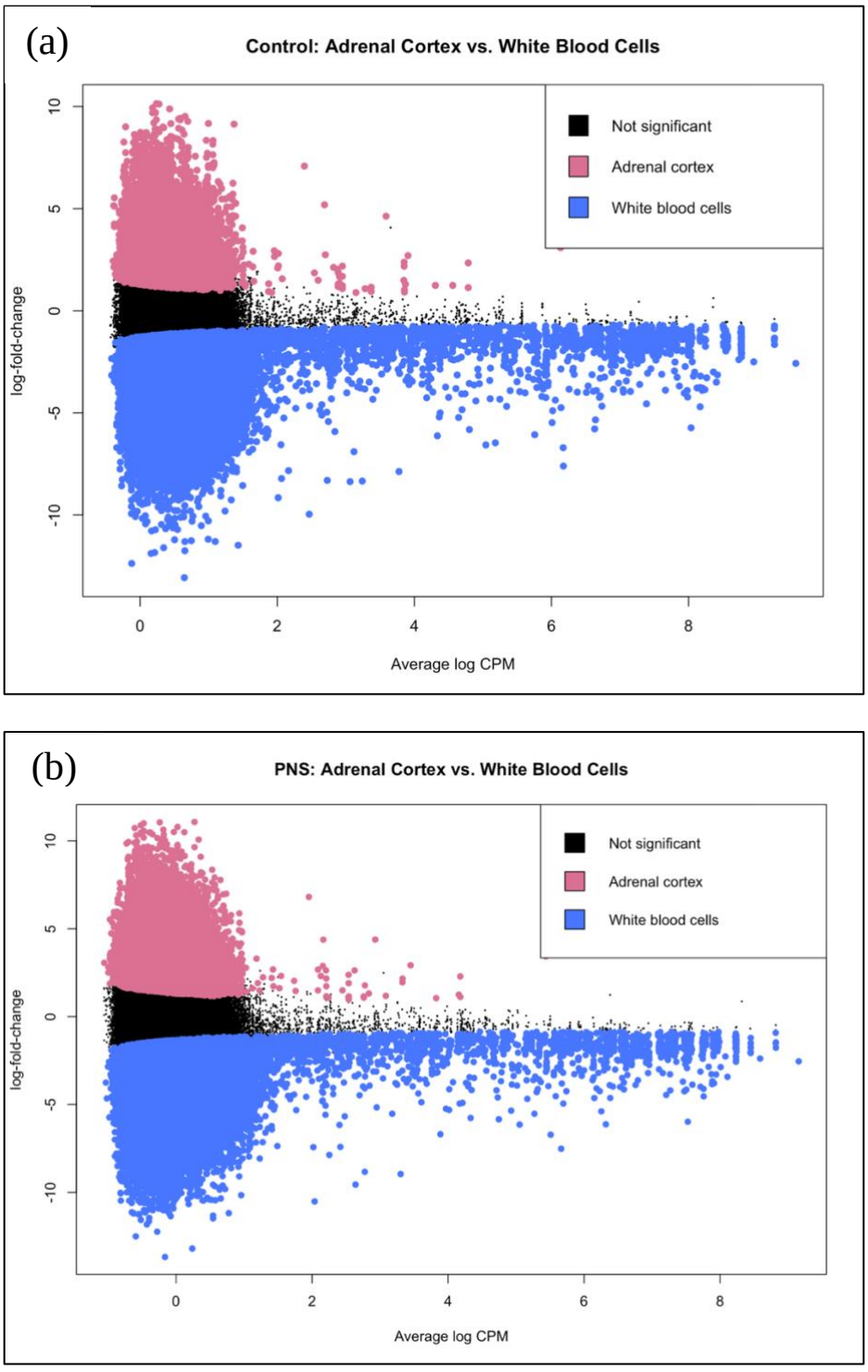

Figure 2. Mean difference plots for (a) control cows and (b) prenatally stressed (PNS) cows. Sites more methylated in the adrenal cortex relative to white blood cells are pink dots; those more methylated in white blood cells relative to the adrenal cortex are blue, and sites not differentially methylated are black.

4.1.2. Adrenal Medulla

The greatest proportion of total sites evaluated in comparisons of the adrenal medulla and WBC were deemed not significant at 56.2% in the control group and 64.1% in the PNS group (Table 2). The lowest percentages were observed in adrenal medulla sites at 4.1% in the control group and 3.7% in the PNS group. The common dispersion estimate of the PNS group is slightly higher at 0.1026 which indicates higher variability among sites of adrenal medulla tissue and WBC tissue when compared to the control group which measured 0.0826. The PNS common dispersion estimate was slightly higher than that of the control group, suggesting an increase in variability among the PNS samples relative to the control group.

To illustrate variability of methylation patterns for the sites with the greatest differences between the adrenal medulla tissues and WBC, MDS plots can be seen in Figure 3, where discordance between adrenal medulla and WBC is apparent for both control and PNS cows. There was greater variability of methylation in WBC in both the control and PNS groups. The MD plots (Figure 4), depict slightly greater abundance of methylation in the PNS group, primarily for WBC but also, to a lesser degree by comparison, for adrenal medulla tissues as well. Results were consistent with the comparisons of adrenal cortex to WBC. Closer evaluation of specific sites will be necessary to understand the concordance between tissues, should any exist. The spread along the y-axis of the MD plots may indicate a polarizing relationship could potentially exist in some CpG sites.

Table 2. Counts and percentages of differentially methylated sites and common dispersion estimates for adrenal medulla tissue to white blood cell tissue comparison.

Measurement	Control		PNS[1]	
	Count	Percentage	Count	Percentage
Adrenal medulla[2]	14,512	4.1%	20,585	3.7%
White blood cells[3]	140,435	39.7%	194,120	34.9%
Not significant[4]	198,886	56.2%	341,645	61.4%
Total	353,833	100%	556,350	100%
Common dispersion estimate[5]		0.0826		0.1026

[1]Prenatally stressed.
[2]Number and proportion of sites showing greater methylation in adrenal medulla tissues.
[3]Number and proportion of sites showing greater methylation in white blood cells.
[4]Number and proportion of sites without significant differential methylation between tissues.
[5]Squared coefficient of variation in the true abundance of replicates between adrenal medulla tissue and white blood cell tissue.

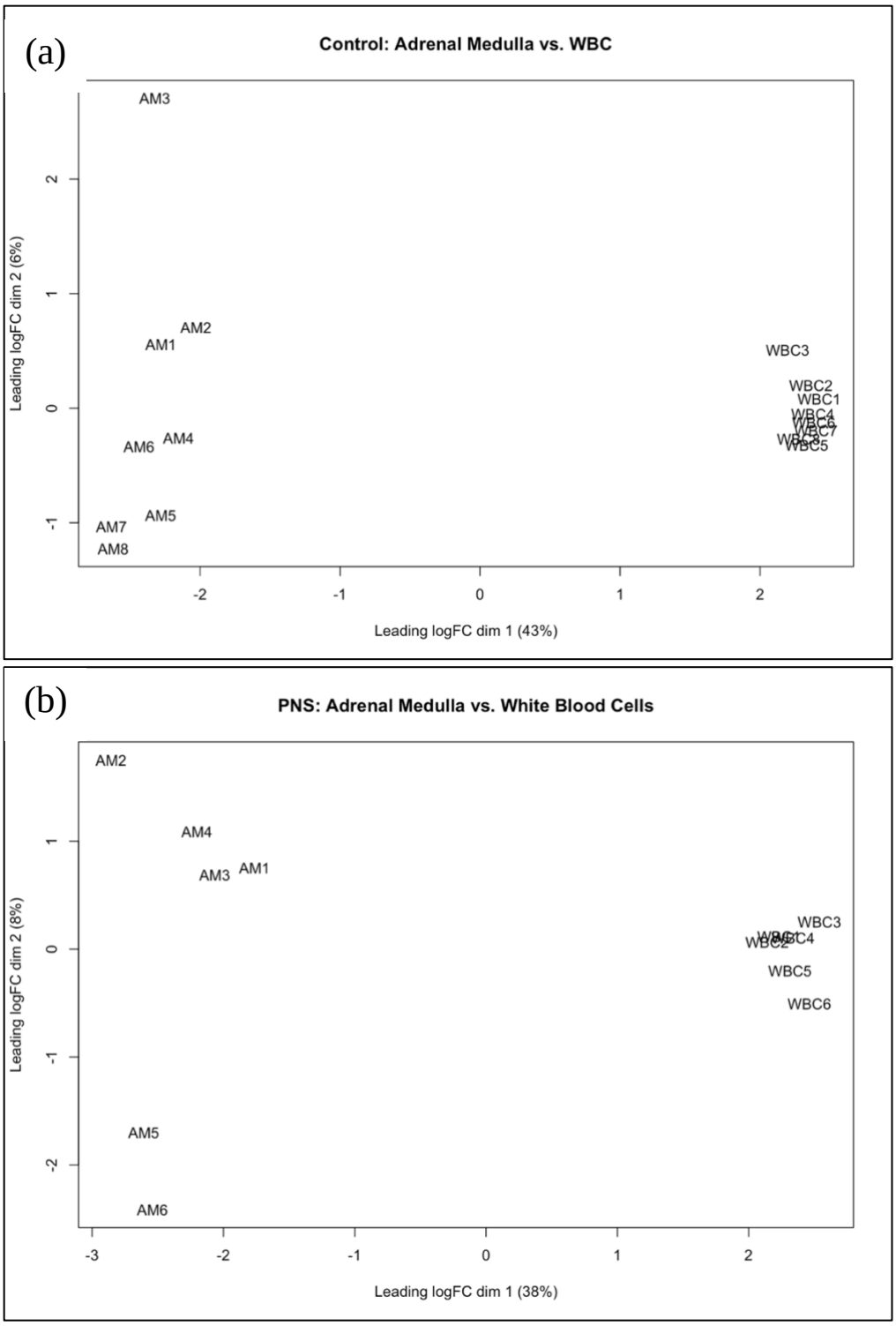

Figure 3. Multidimensional scaling plots for (a) control cows and (b) prenatally stressed (PNS) cows. AM: adrenal medulla. WBC: white blood cells. Sample numbers follow those abbreviations and correspond to the same cows.

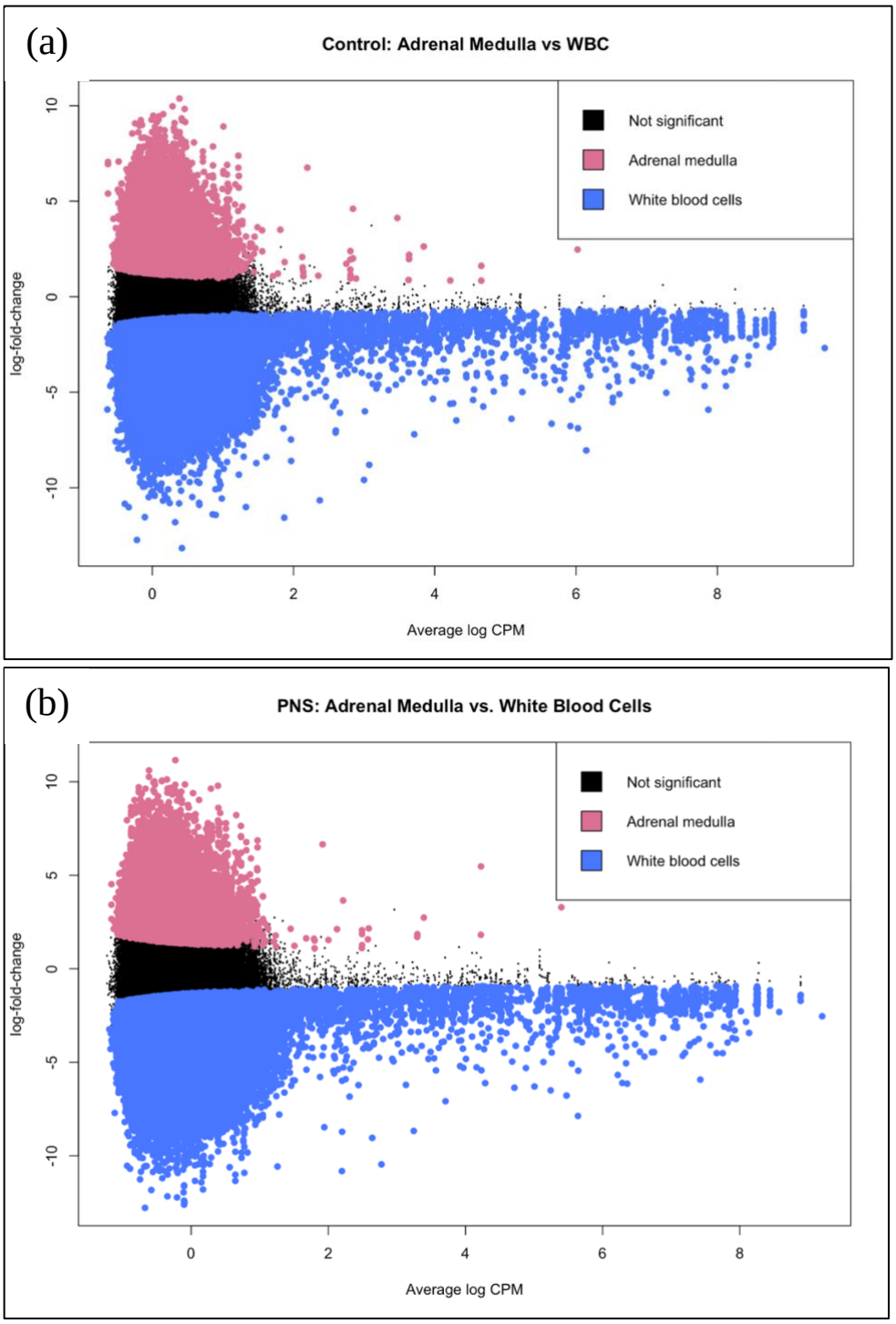

Figure 4. Mean difference plots for (a) control cows and (b) prenatally stressed (PNS) cows. Sites more methylated in the adrenal medulla relative to white blood cells are pink dots; those more methylated in white blood cells relative to the adrenal medulla are blue, and sites not differentially methylated are black.

4.1.3. Anterior Pituitary

Few treatment differences were significant for abundance of methylation of DNA from the anterior pituitary and WBC (Table 3). Unlike the adrenal cortex and adrenal medulla comparisons with WBC, the percentage of sites that were not significant and the percentage of sites more methylated in WBC relative to the anterior pituitary, were similar. In the control group a majority of sites were more methylated in WBC at 50.8%, while sites in the PNS group classified as not significant were similar to the more methylated WBC sites at 48.7% and 48.4% respectively. Greater methylation of the anterior pituitary, relative to WBC methylation, in both groups remained nominal by comparison at 3.3% in control and 2.9% in PNS. Common dispersion estimates indicate the same relationship of variability to the mean when the control group is compared to the PNS group.

The MDS plots for anterior pituitary show high discordance between the anterior pituitary and WBC samples in both control and PNS groups (Figure 5), with high variability among the sites showing the greatest deviation from one another between anterior pituitary tissues and WBC. The LogCPM appears to differ very little between control and PNS groups when viewed within the MD plots (Figure 6). Increased methylation of WBC relative to anterior pituitary was especially noted at high LogCPM values. At low LogCPM values, increased methylation of sites within either anterior pituitary or WBC DNA was more similar; however, there appeared to be more sites hypermethylated in WBC relative to the anterior pituitary. Observable differences in global methylation patterns of anterior pituitary tissues to WBC, when comparing control results to PNS results, remain nominal. This subset of individual sites may be more revealing of mechanisms behind methylation patterns of the relationship between these tissues.

Table 3. Counts and percentages of differentially methylated sites and common dispersion estimates for anterior pituitary tissue to white blood cell tissue comparison.

Measurement	Control		PNS[1]	
	Count	Percentage	Count	Percentage
Anterior pituitary[2]	13,464	3.3%	19,977	2.9%
White blood cells[3]	206,534	50.8%	337,599	48.4%
Not significant[4]	186958	45.9%	340,290	48.7%
Total	406,956	100%	697,866	100%
Common dispersion estimate[5]		0.0759		0.0877

[1]Prenatally stressed.
[2]Number and proportion of sites showing greater methylation in anterior pituitary tissues.
[3]Number and proportion of sites showing greater methylation in white blood cells.
[4]Number and proportion of sites without significant differential methylation between tissues.
[5]Squared coefficient of variation in the true abundance of replicates between anterior pituitary tissue and white blood cell tissue.

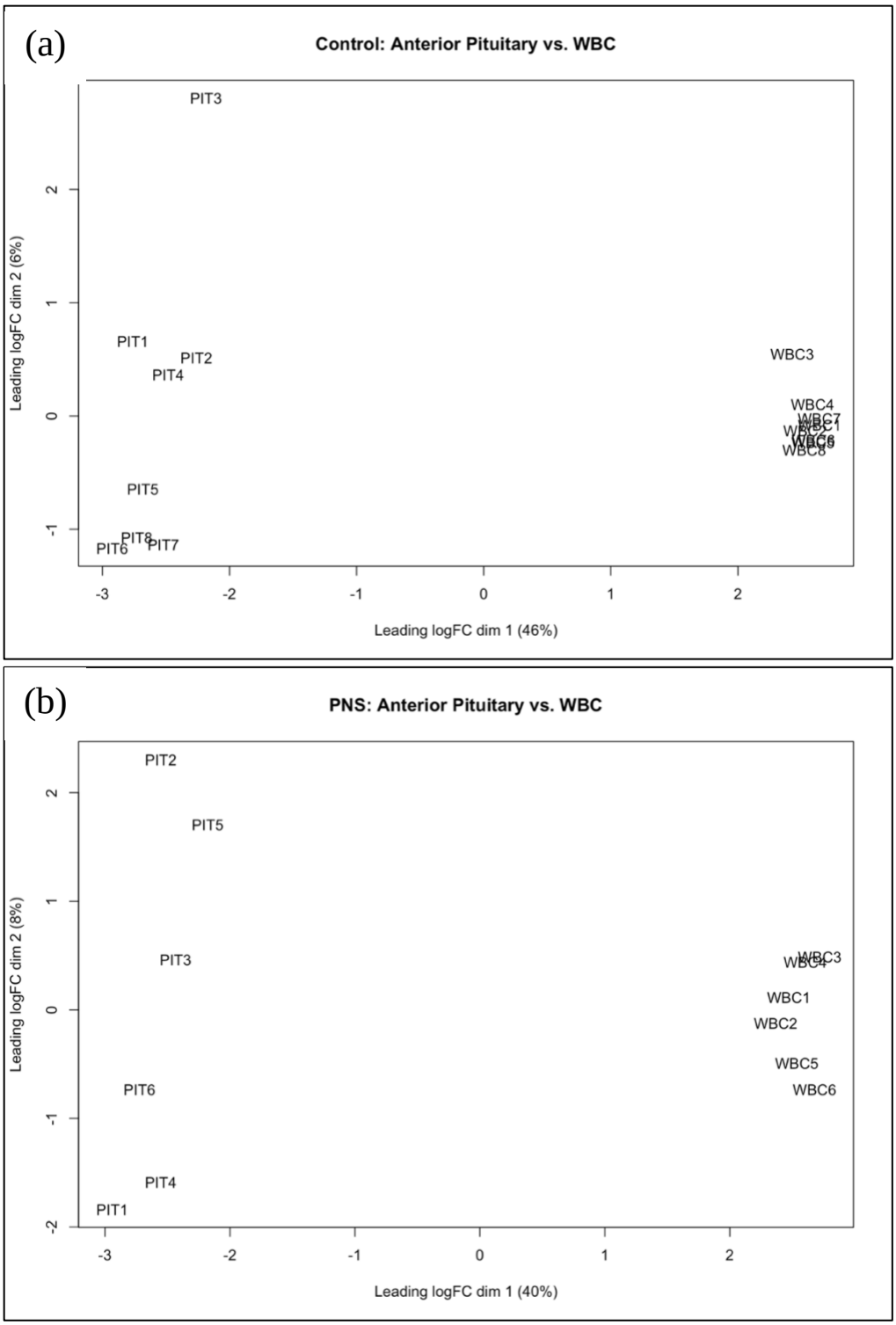

Figure 5. Multidimensional scaling plots for (a) control cows and (b) prenatally stressed (PNS) cows. PIT: anterior pituitary. WBC: white blood cells. Sample numbers follow those abbreviations and correspond to the same cows.

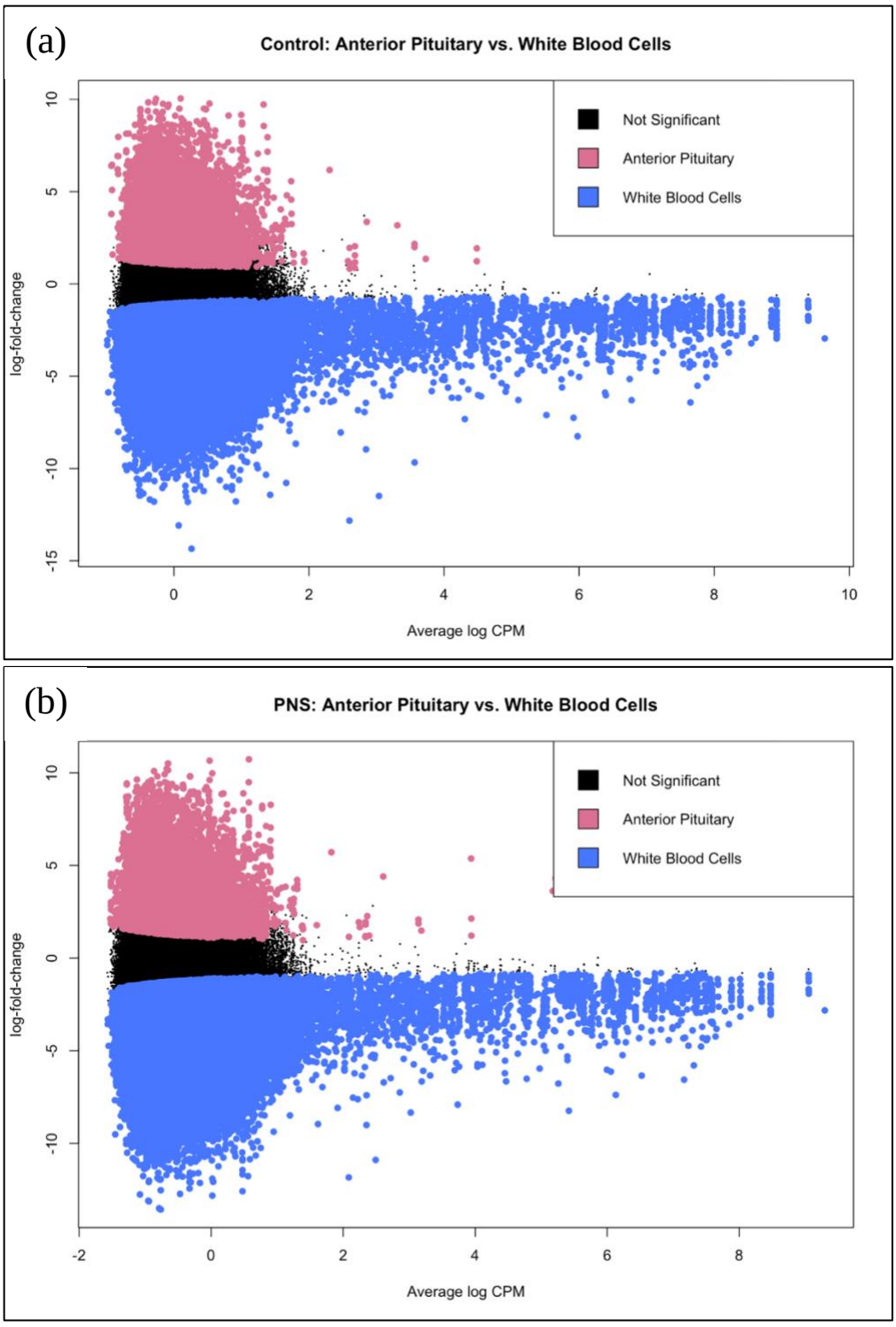

Figure 6. Mean difference plots for (a) control cows and (b) prenatally stressed (PNS) cows. Sites more methylated in the anterior pituitary relative to white blood cells are pink dots; those more methylated in white blood cells relative to the anterior pituitary are blue, and sites not differentially methylated are black.

4.1.4. Paraventricular Nucleus of the Hypothalamus

Results for comparison of the PVN to WBC are relatively consistent with the results from comparisons of WBC with the adrenal cortex, adrenal medulla, and the anterior pituitary (Table 4). The common dispersion measurements indicate slightly greater variability between PVN and WBC in the PNS group at 0.1144, compared to the control group at 0.0737. These values were low, and indicative of minimal variation existing in global methylation patterns between the tissues. Proportions of total counts were also consistent with what has been observed in previously mentioned tissues where the control group showed a majority of sites deemed not significant at 56.3% along with the PNS group at 60.2%. The percentage of sites more methylated in PVN tissue relative to WBC was the lowest in both groups at 3.3% for control and 5.2% for PNS.

Differences between MDS plots were also consistent with what has been observed in the previously analyzed tissues (Figure 7). For both the control and PNS groups, variability among the most differentially methylated CpG loci of each sample was high when comparing PVN to WBC. Mean difference plots for the PVN to WBC comparison suggest that more sites were differentially methylated in the PNS group (Figure 8); this appeared to be consistent with the proportion of sites that had increased methylation in the PVN (Table 4), but not those with increased methylation in WBC. Consistent with previous tissue to WBC comparisons though, WBC shows greater overall abundance in both control and PNS groups. It is particularly notable that for all tissue to WBC comparisons, WBC show greater abundance on the MD plots along with less variability between individuals on the MDS plots. Furthermore, greater differences in methylation between PVN tissues and WBC are also observable by the LogFC measure along the y-axis when comparing control to PNS groups (Figure 7a and 7b). The discordance between

MDS plots and MD plots furthers the notion that investigation into specific differentially methylated sites within tissues may be a better indicator of patterns of correspondence should they exist.

Table 4. Counts and percentages of differentially methylated sites and common dispersion estimates for paraventricular nucleus of the hypothalamus tissue to white blood cell tissue. comparison

Measurement	Control		PNS[1]	
	Count	Percentage	Count	Percentage
PVN[2]	7,198	3.3%	34,418	5.2%
White blood cells[3]	88,726	40.4%	228,901	34.6%
Not significant[4]	123,552	56.3%	397,422	60.2%
Total	219,476	100%	660,741	100%
Common dispersion estimate[5]		0.0737		0.1144

[1]Prenatally stressed.
[2]Number and proportion of sites showing greater methylation in the paraventricular nucleus of the hypothalamus tissues.
[3]Number and proportion of sites showing greater methylation in white blood cells.
[4]Number and proportion of sites without significant differential methylation between tissues.
[5]Squared coefficient of variation in the true abundance of replicates between paraventricular nucleus of the hypothalamus tissue and white blood cell tissue.

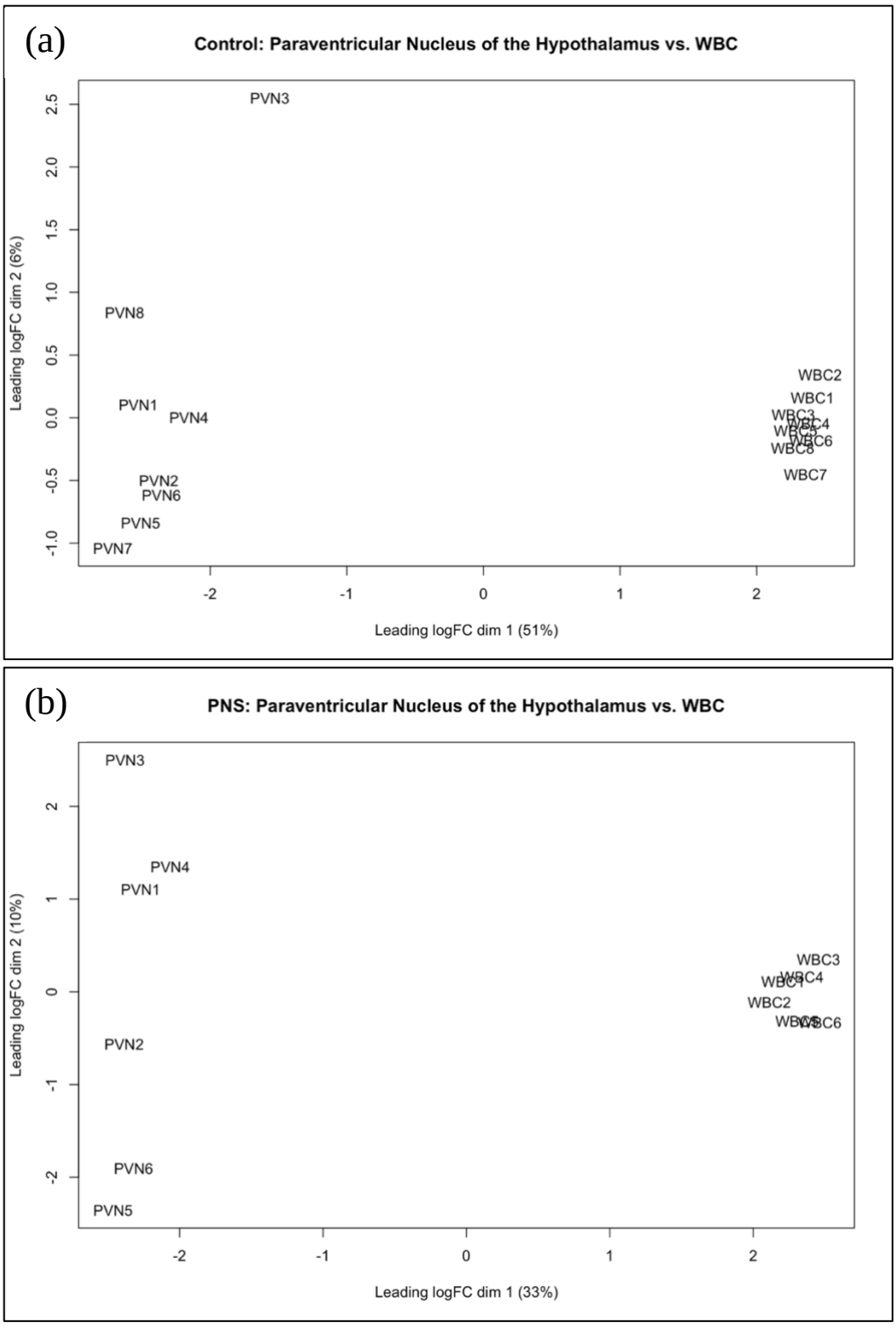

Figure 7. Multidimensional scaling plots for (a) control cows and (b) prenatally stressed (PNS) cows. PVN: paraventricular nucleus of the hypothalamus. WBC: white blood cells. Sample numbers follow those abbreviations and correspond to the same cows.

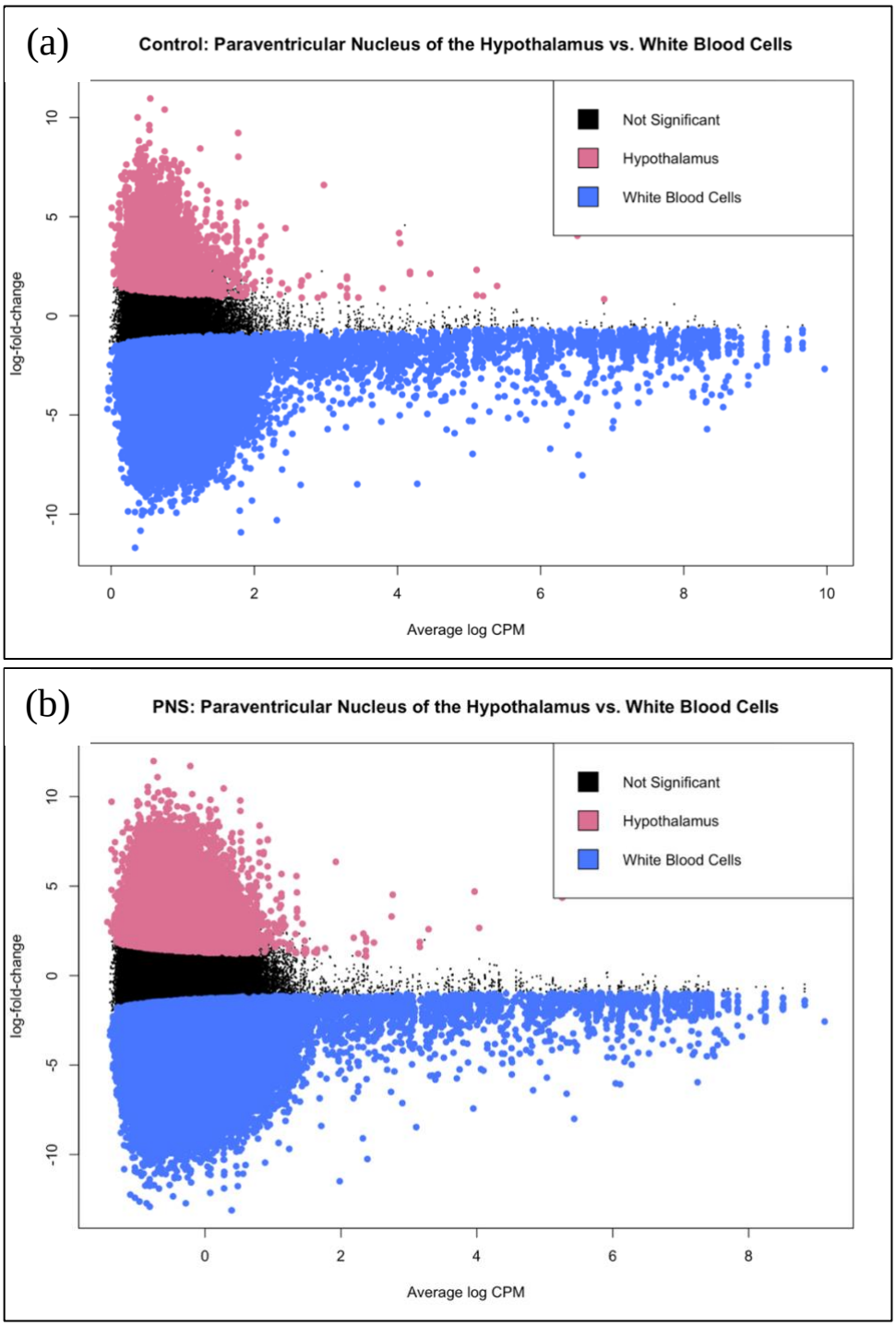

Figure 8. Mean difference plots for (a) control cows and (b) prenatally stressed (PNS) cows. Sites more methylated in the paraventricular nucleus of the hypothalamus relative to white blood cells are pink dots; those more methylated in white blood cells relative to the paraventricular nucleus of the hypothalamus are blue, and sites not differentially methylated are black.

4.2. Global Comparisons Between HPA-Axis Tissues

4.2.1. Adrenal Cortex vs. Adrenal Medulla

The adrenal cortex and adrenal medulla showed large concordance in both global methylation patterns as well as in the control group to PNS group comparisons. The proportion of sites that were not significant for differential methylation was essentially identical for the control group with 94.6% and the PNS group with 94.5% (Table 5). Count results suggest that total methylation differences of the adrenal cortex and adrenal medulla were similar regardless of whether or not prenatal stress is influencing those patterns. The common dispersion estimate is slightly higher for PNS at 0.1907 than the control group at 0.1694, suggesting increased variability in the PNS group relative to the control group.

This is supported by the MDS plots presented in Figure 9. In the control group (Figure 9a) the greatest source of disparities exists between individuals. Adrenal cortex and adrenal medulla samples for individuals were located close to one another. The greatest departures from the group appear to be control individuals 3, 2, and 7, but where the individuals' tissue samples are consistent with one another. A similar trend can be observed in the PNS group where the greatest differences are between individuals, but where tissue deviation is slightly greater than in the control group. Individual 2 from the PNS group is most departed from the rest of the group, but where both tissues remain relatively consistent to each other. Mean difference plots were also consistent with count results (Table 5), showing the majority of the data falling into the not significant range for both control and PNS, but where some distinction still exists between specific sites in both tissues (Figure 10). In contrast to what was observed in the comparisons of tissues with WBC, the not significant sites show heavier concentration along with y-axis with greater abundance along the x-axis in both control and PNS groups (Figure 10). This is

consistent with the high percentage of not significant sites that were found for both control and PNS groups shown in Table 5.

Table 5. Counts and percentages of differentially methylated sites and common dispersion estimates for adrenal cortex tissue to adrenal medulla tissues comparison.

Measurement	Control		PNS[1]	
	Count	Percentage	Count	Percentage
Adrenal Cortex[2]	36,890	3.9%	39,827	4%
Adrenal Medulla[3]	13,931	1.5%	15,028	1.5%
Not Significant[4]	893,104	94.6%	936,517	94.5%
Total	943,925	100%	991,372	100%
Common Dispersion Estimate[5]		0.1694		0.1907

[1]Prenatally stressed.
[2]Number and proportion of sites showing greater methylation in adrenal cortex tissues.
[3]Number and proportion of sites showing greater methylation in adrenal medulla tissues.
[4]Number and proportion of sites without significant differential methylation between tissues.
[5]Squared coefficient of variation in the true abundance of replicates between adrenal cortex tissues and adrenal medulla tissues.

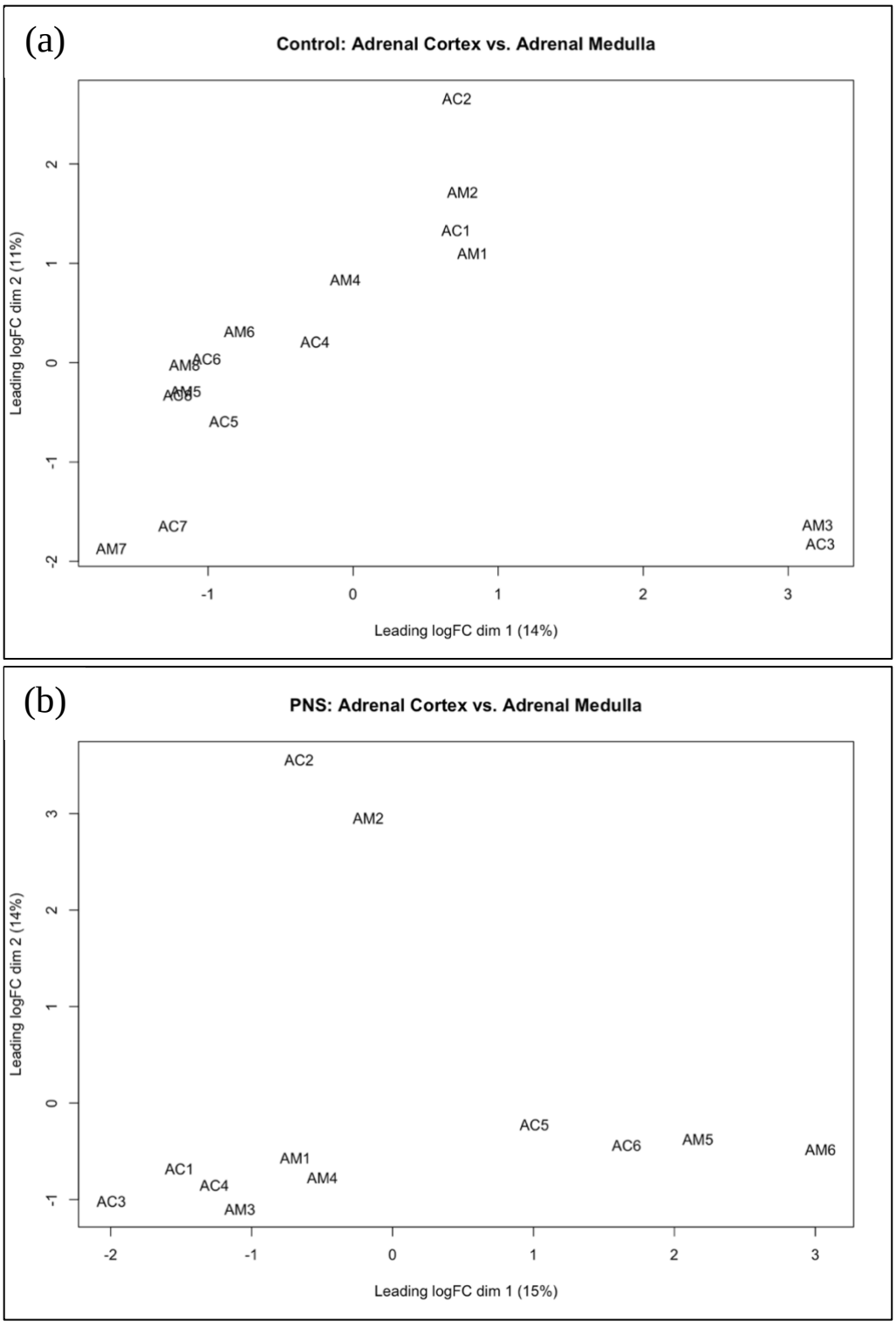

Figure 9. Multidimensional scaling plots for (a) control cows and (b) prenatally stressed (PNS) cows. AC: adrenal cortex. AM: adrenal medulla. Sample numbers follow those abbreviations and correspond to the same cows.

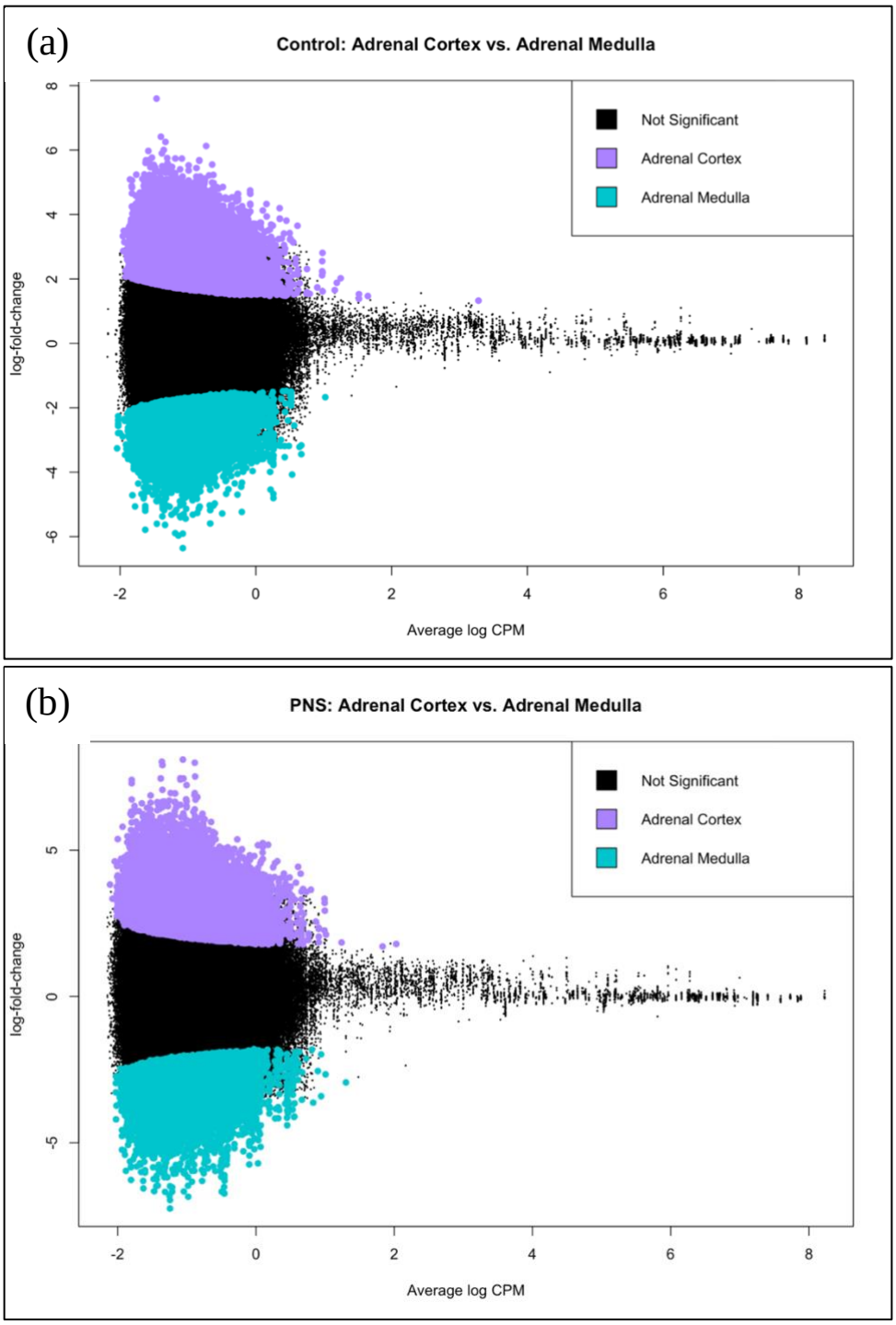

Figure 10. Mean difference plots for (a) control cows and (b) prenatally stressed (PNS) cows. Sites more methylated in the adrenal cortex relative to the adrenal medulla are purple; those more methylated in the adrenal medulla relative to the adrenal cortex are green, and sites not differentially methylated are black.

4.2.2. Adrenal Cortex vs. Anterior Pituitary

Relative to the anterior pituitary, the adrenal cortex shows greater methylation with 23.2% and 22.2% of control and PNS counts respectively (Table 6). Sites deemed not significant, or with small differences in methylation between adrenal cortex and anterior pituitary tissues, still comprise the majority of counts with 73% in the control group and 74.7% of sites in the PNS group. Differences between control and PNS groups were marginal, suggesting prenatal stress may not induce observable changes in methylation in mature Brahman cows. Consistent with most of the previously reported results in the present study, however, the common dispersion estimates increase slightly from control at 0.1392 to PNS at 0.1504 (Table 6), suggesting slightly more variability amongst sites in the PNS group.

The control MDS plot (Figure 11a) shows the greatest distance between tissue types along the x-axis. The next greatest distance can be observed between individuals along the y-axis, but where both tissues of an individual fall relatively close to one another along this axis. As in, where the anterior pituitary sample falls on the y-axis for control individual 3 for example, the adrenal cortex tissue can be seen in a similar location on the y-axis, but on the opposing side of the x-axis. Samples from each individual in both tissues are positioned in a similar order along the y-axis. This is also the case for the MDS plot of the PNS group (Figure 11b). This may indicate a consistency in methylation levels between the adrenal cortex and anterior pituitary within individuals, but where a certain ratio of differential methylation tends to be maintained. Figure 12 also shows the dissimilarities between the two tissues, but also shows the consistency between the control and PNS groups by way of MD plots. Sites deemed not significant in the MD plots are reduced in concentration compared to the adrenal cortex-to-adrenal medulla comparison but is consistent with the count data produced for this comparison of adrenal cortex

to anterior pituitary for both control and PNS groups. Sites more methylated in adrenal cortex DNA show greater abundance of methylation (Figure 12). Sites that were not differentially methylated were the most numerous in comparisons of tissues and were higher in abundance than both tissues individually. Sites more methylated in the anterior pituitary relative to the adrenal cortex display the lowest overall abundance in both control and PNS groups.

Table 6. Counts and percentages of differentially methylated sites and common dispersion estimates for adrenal cortex and anterior pituitary tissues comparisons.

Measurement	Control		PNS[1]	
	Count	Percentage	Count	Percentage
Adrenal Cortex[2]	252,536	23.2%	250,887	22.2%
Anterior Pituitary[3]	40,659	3.8%	34,821	3.1%
Not Significant[4]	790,828	73%	844,577	74.7%
Total	1,084,023	100%	1,130,285	100%
Common Dispersion Estimate[5]		0.1392		0.1504

[1]Prenatally stressed.
[2]Number and proportion of sites showing greater methylation in the adrenal cortex tissues.
[3]Number and proportion of sites showing greater methylation in the anterior pituitary tissues.
[4]Number and proportion of sites without significant differential methylation between tissues.
[5]Squared coefficient of variation in the true abundance of replicates adrenal cortex tissues and anterior pituitary tissues.

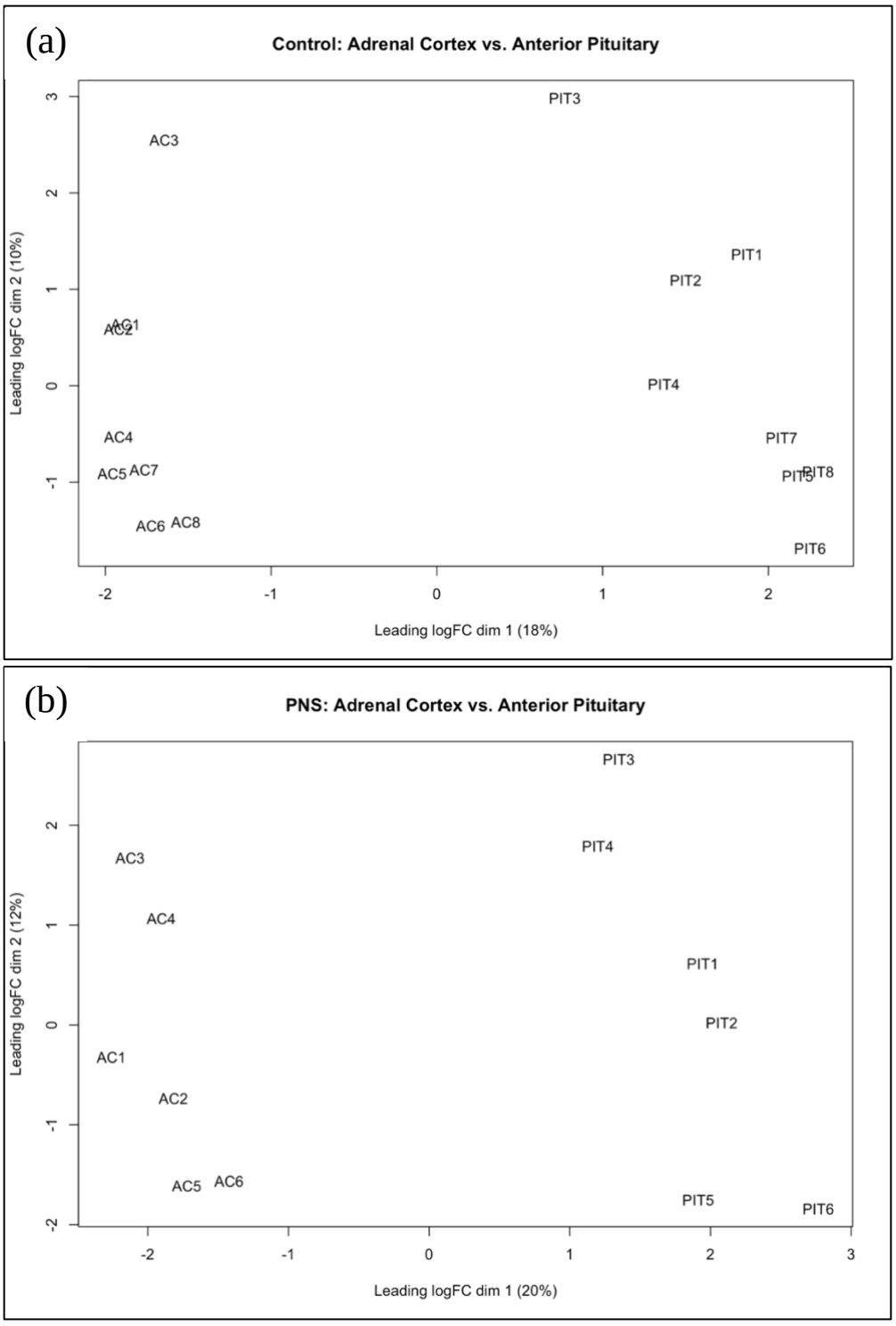

Figure 11. Multidimensional scaling plots for (a) control cows and (b) prenatally stressed (PNS) cows. AC: adrenal cortex. PIT: anterior pituitary. Sample numbers follow those abbreviations and correspond to the same cows.

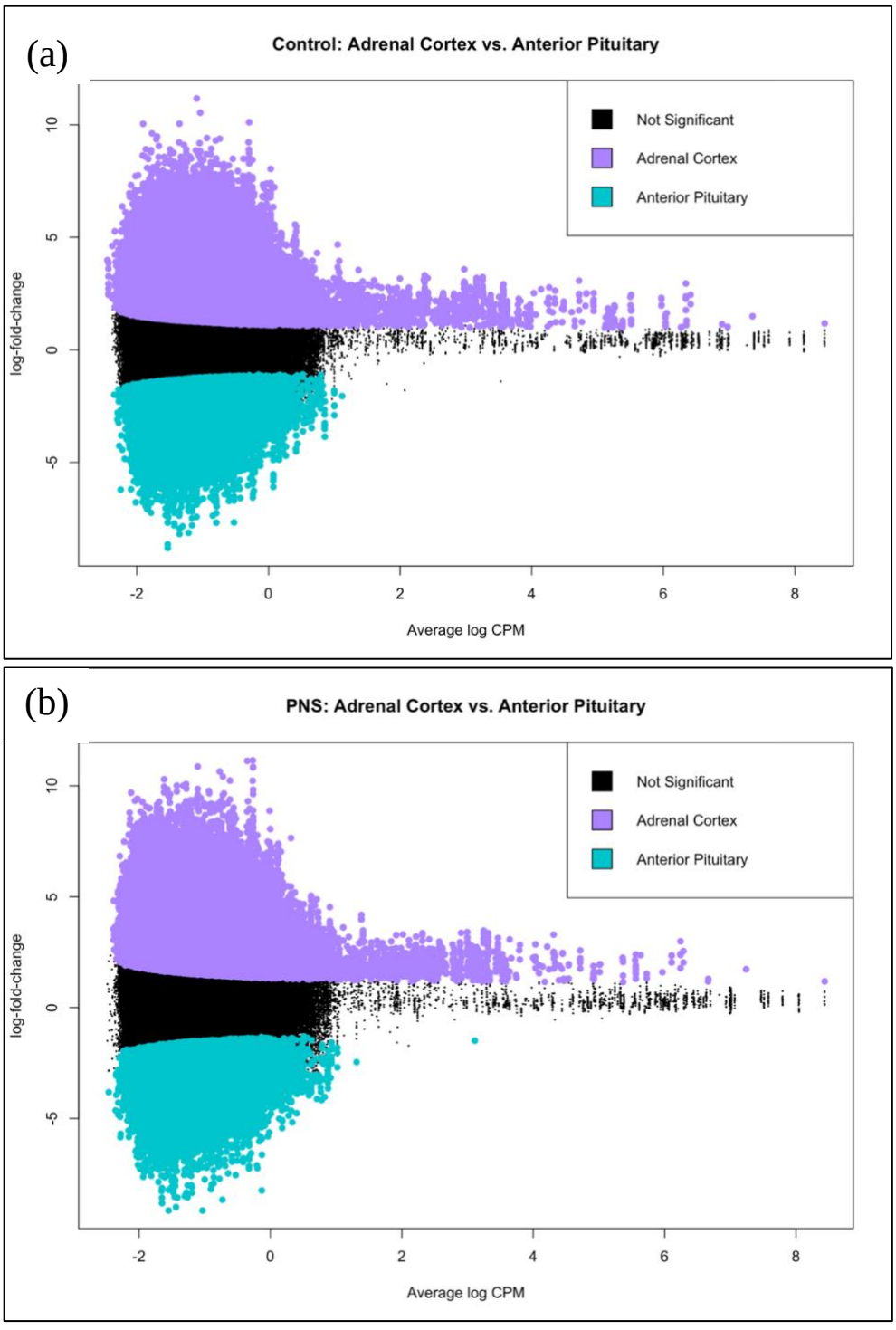

Figure 12. Mean difference plots for (a) control cows and (b) prenatally stressed (PNS) cows. Sites more methylated in the adrenal cortex relative to the anterior pituitary are purple; those more methylated in the anterior pituitary relative to the adrenal cortex are green, and sites not differentially methylated are black.

4.2.3. Adrenal Cortex vs. Paraventricular Nucleus of the Hypothalamus

Sites deemed not significant, or similarly methylated between the tissues, are the dominant proportions of sites (Table 7). Both increased methylation of the adrenal cortex relative to PVN as well as increased methylation of PVN relative to the adrenal cortex make up a greater percentage of sites in the PNS group compared to the control group. Additionally, non-significant sites decrease slightly from 92.8% in the control group to 90% in the PNS group, which suggests some differential methylation between these two tissues may occur as a result of prenatal stress. Greater variability in the PNS group compared to the control group was also observed by common dispersion estimates of 0.1987 and 0.1517 respectively (Table 7).

These changes between control to PNS can also be observed in the MDS plots in Figure 13. Both the control and PNS plots show the greatest distance between tissue types, but there is an observable increase in individual differences in the PNS group, particularly for PVN. Prenatal stress may cause differential methylation of the adrenal cortex relative to PVN and vice versa. The MD plots of Figure 14 also display increased variability from the control to PNS group in both tissues. The concentration of both purple and green sites noticeably increases (quantity of differentially methylated sites) in the PNS group compared to control, and where greater abundance of purple can be seen along the x-axis of the control group, this is slightly reduced in the PNS group.

Table 7. Counts and percentages of differentially methylated sites and common dispersion estimates for adrenal cortex to paraventricular nucleus of the hypothalamus tissue comparison.

Measurement	Control		PNS[1]	
	Count	Percentage	Count	Percentage
Adrenal Cortex[2]	19,671	4.7%	67,331	6.6%
PVN[3]	10,268	2.5%	34,022	3.4%
Not Significant[4]	385,552	92.8%	907,643	90%
Total	415,491	100%	1,008,996	100%
Common Dispersion Estimate[5]		0.1517		0.1987

[1]Prenatally stressed.
[2]Number and proportion of sites showing greater methylation in the adrenal cortex tissues.
[3]Number and proportion of sites showing greater methylation in the paraventricular nucleus of the hypothalamus tissues.
[4]Number and proportion of sites without significant differential methylation between tissues.
[5]Squared coefficient of variation in the true abundance of replicates between adrenal cortex tissues paraventricular nucleus of the hypothalamus tissues.

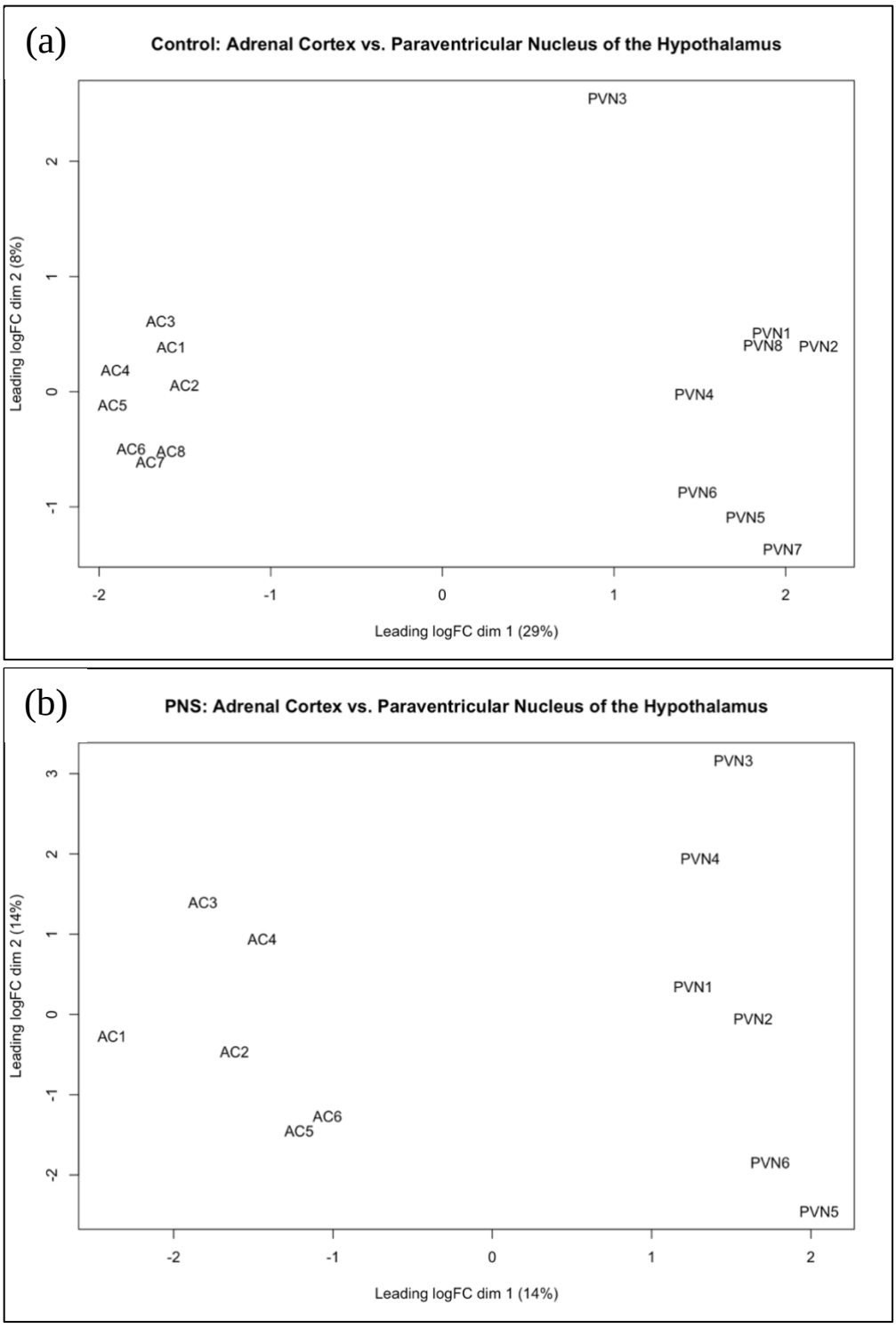

Figure 13. Multidimensional scaling plots for (a) control cows and (b) prenatally stressed (PNS) cows. AC: adrenal cortex. PVN: paraventricular nucleus of the hypothalamus. Sample numbers follow those abbreviations and correspond to the same cows.

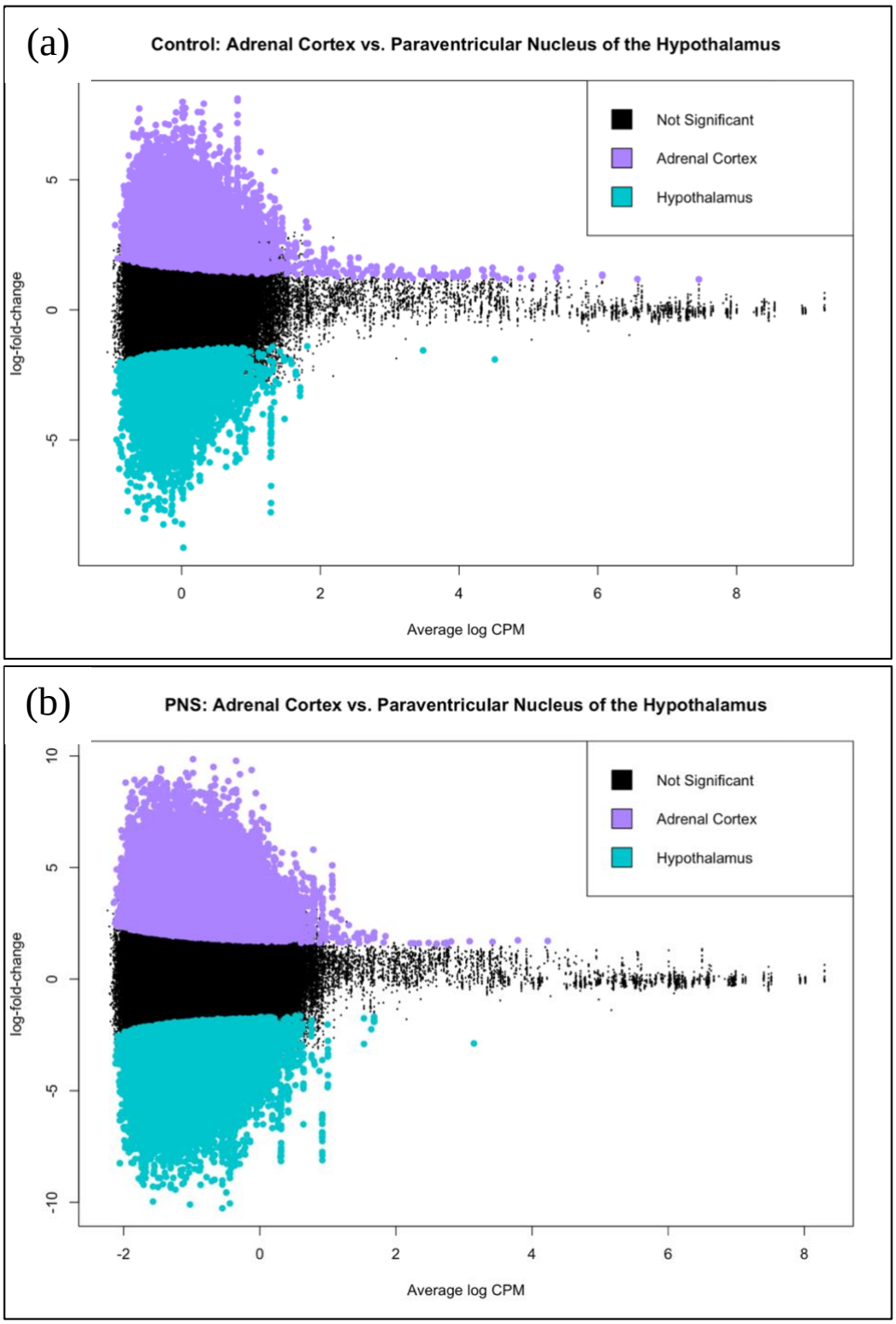

Figure 14. Mean difference plots for (a) control cows and (b) prenatally stressed (PNS) cows. Sites more methylated in the adrenal cortex relative to the paraventricular nucleus of the hypothalamus are purple; those more methylated in the paraventricular nucleus of the hypothalamus relative to the adrenal cortex are green, and sites not differentially methylated are black.

4.2.4. Adrenal Medulla vs. Anterior Pituitary

Due to the high correspondence of methylation patterns of the adrenal cortex adrenal medulla, it may be expected that each tissue's comparison to other tissues could yield similar results. However, unlike the comparisons of adrenal cortex to anterior pituitary across the control to PNS groups, much greater differences between groups can be observed from count analysis of adrenal medulla compared to anterior pituitary (Table 8). Non-significant sites still comprise the majority of sites in both groups, but with the greatest difference observed in tissue-to-tissue comparisons from control to PNS with 73% to 84.8% respectively (Table 8). Sites more methylated in the anterior pituitary relative to the adrenal medulla were lower in PNS by a difference that is somewhat consistent with previously discussed tissue-to-tissue comparisons, sites more methylated in adrenal medulla tissue relative to anterior pituitary tissues were much lower in PNS (12.9%) than control samples (23.2%) (Table 8). The difference in common dispersion estimates was similar to previous tissue comparisons by a margin of about 0.03 with 0.1382 in the control group and 0.1575 in the PNS group (Table 8).

The MDS plots in Figure 15 show the greatest distinction between tissue type followed by distinction of individuals. Differences between tissue types and individuals are both somewhat consistent between the control group and PNS group, but where individual samples were across tissues. Although they are greatly separated along the x-axis, samples from both tissues of individual animals occupy similar y-axis locations. The MD plots displayed by Figure 16 reveal little about pattern differences in the control group relative to the PNS group.

Table 8. Counts and percentages of differentially methylated sites and common dispersion estimates for adrenal medulla and anterior pituitary tissues comparisons.

Measurement	Control		PNS[1]	
	Count	Percentage	Count	Percentage
Adrenal Medulla[2]	204,023	23.2%	151,369	12.9%
Anterior Pituitary[3]	44,192	3.8%	27,406	2.3%
Not Significant[4]	1,019,137	73%	995,916	84.8%
Total	1,267,352	100%	1,174,691	100%
Common Dispersion Estimate[5]		0.1382		0.1575

[1]Prenatally stressed.
[2]Number and proportion of sites showing greater methylation in the adrenal medulla tissues.
[3]Number and proportion of sites showing greater methylation in the anterior pituitary tissues.
[4]Number and proportion of sites without significant differential methylation between tissues.
[5]Squared coefficient of variation in the true abundance of replicates adrenal medulla tissues and anterior pituitary tissues.

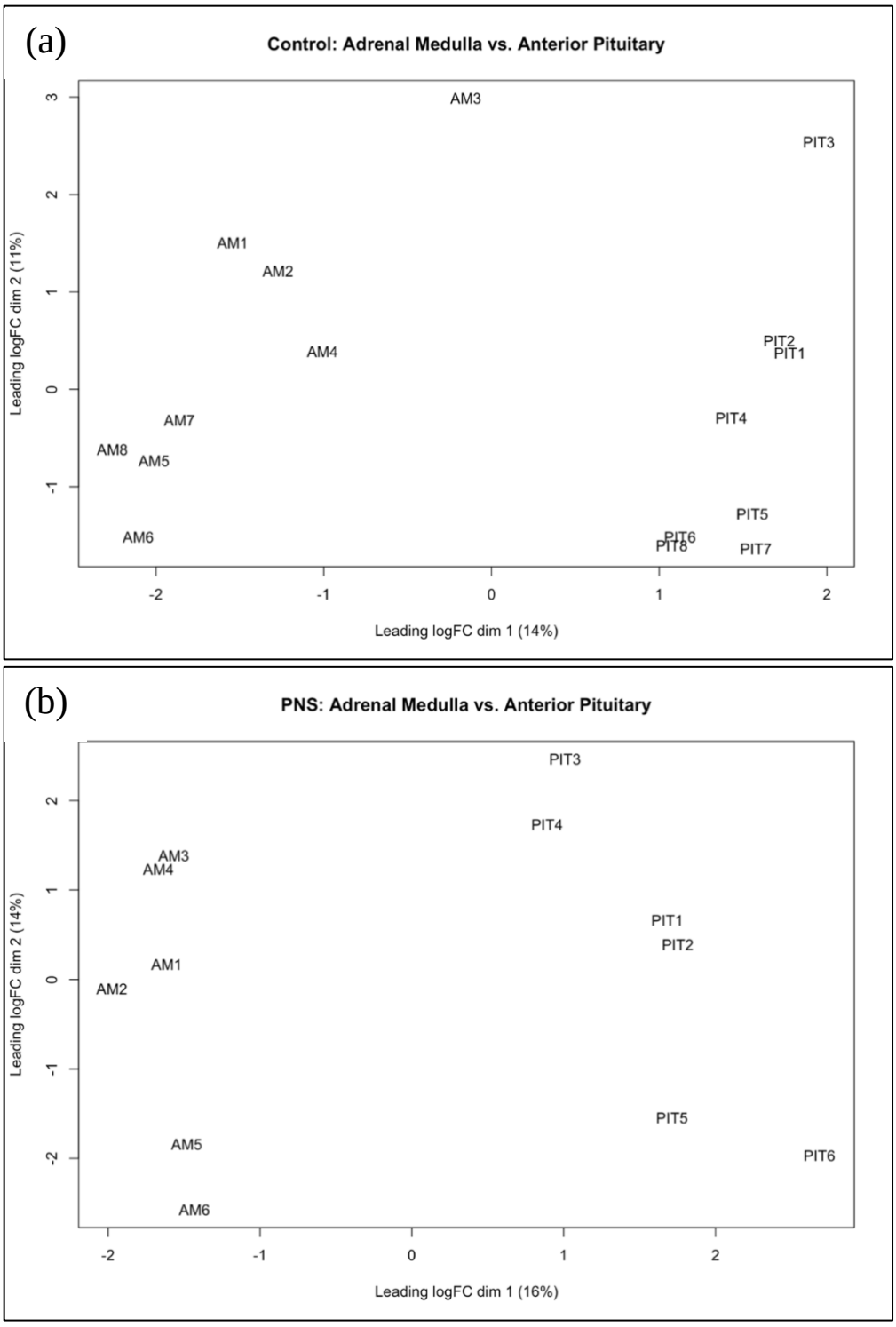

Figure 15. Multidimensional scaling plots for (a) control cows and (b) prenatally stressed (PNS) cows. AM: adrenal medulla. PIT: anterior pituitary. Sample numbers follow those abbreviations and correspond to the same cows.

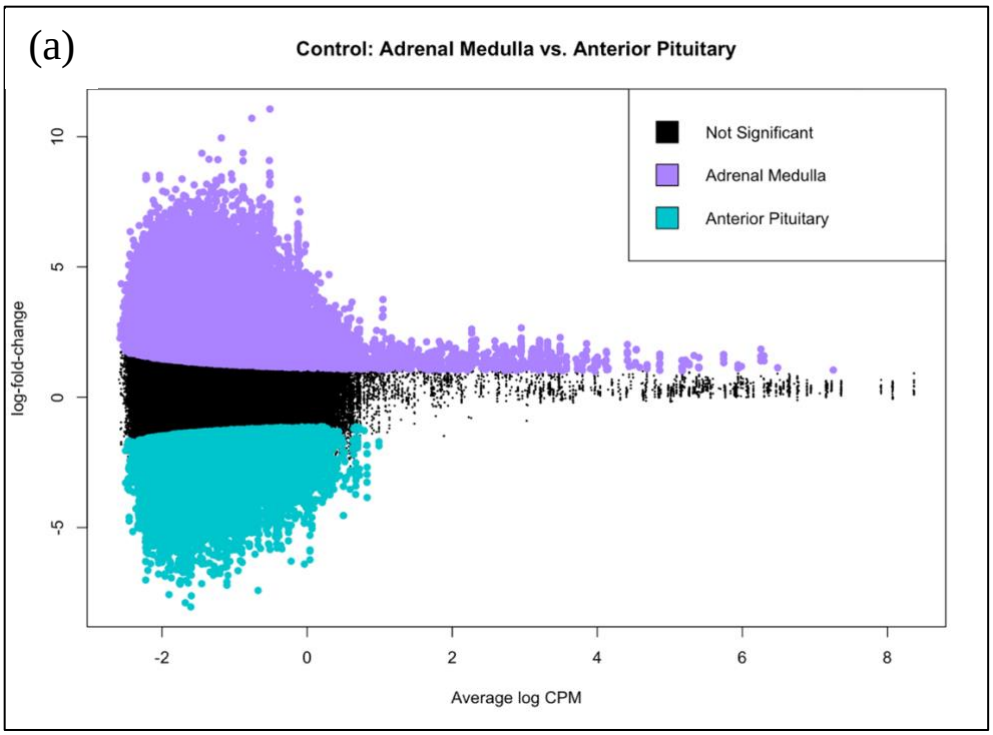

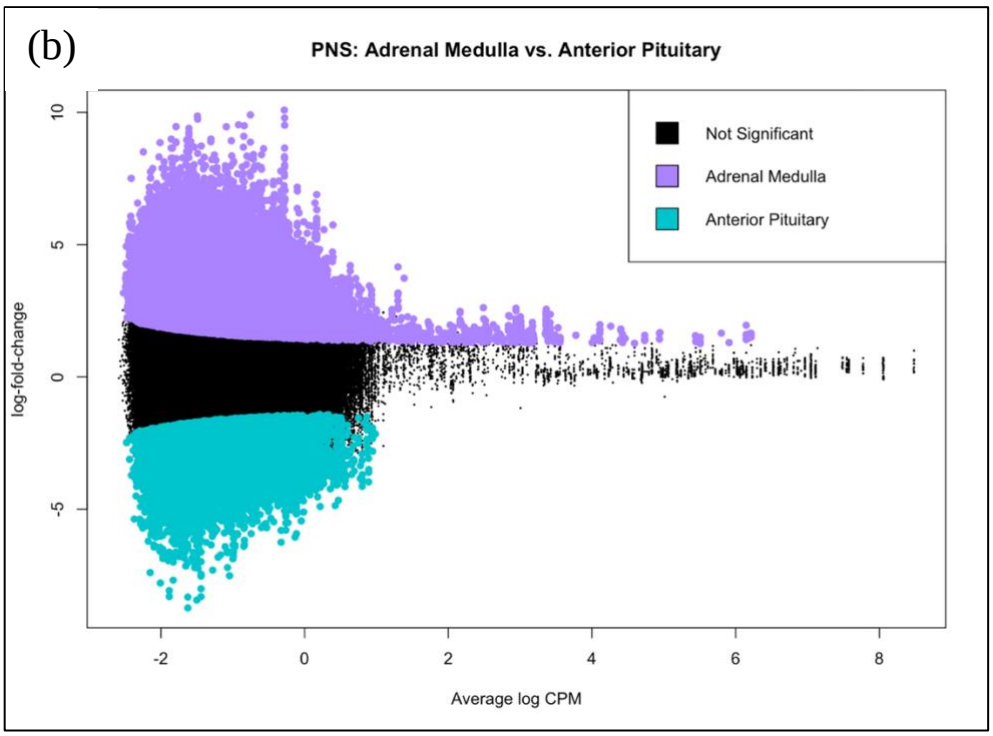

Figure 16. Mean difference plots for (a) control cows and (b) prenatally stressed (PNS) cows. Sites more methylated in the adrenal medulla relative to the anterior pituitary are purple; those more methylated in the anterior pituitary relative to the adrenal medulla are green, and sites not differentially methylated are black.

4.2.5. Adrenal Medulla vs. Paraventricular Nucleus of the Hypothalamus

Based on count percentages, few differences can be observed in adrenal medulla to PVN comparisons from the control group to PNS group. Non-significant sites were the majority of sites in this tissue-to-tissue comparisons with 95.1% in the control group and 95.5% in the PNS group (Table 9). Sites more methylated in the adrenal medulla relative to PVN were similar in the PNS group (2.1%) from the control group (2.5%) (Table 9). This was consistent with the control to PNS differences in sites more methylated in PVN relative to the adrenal medulla with 2.5% and 2.4%, respectively. Common dispersion estimates were consistent with previously reported tissue comparisons at 0.1524 in the control group and 0.1997 in the PNS group (Table 9).

The MDS plots reveal differences between control and PNS groups. Figure 17a indicates a clear contrast in the control group between tissue types across the x-axis with the second largest difference being between individuals along the y-axis. However, no similar separations existed in the MDS plot of the PNS group (Figure 17b). The greatest difference in the MDS plot of the PNS group was among individuals, but where both tissue types show much greater similarity than was observed in the control plot (Figure 17). The MD plots for the adrenal medulla to PVN comparison are less informative about the changes between control and PNS groups (Figure 18). However, these plots do show that PVN methylation in relation to adrenal medulla methylation was slightly greater, with some individual sites deviating from the majority in the control group but is then less prevalent in the PNS group.

Table 9. Counts and percentages of differentially methylated sites and common dispersion estimates for adrenal medulla to paraventricular nucleus of the hypothalamus tissue comparison.

Measurement	Control		PNS[1]	
	Count	Percentage	Count	Percentage
Adrenal medulla[2]	13,782	2.5%	21,896	2.1%
PVN[3]	13,294	2.5%	25,036	2.4%
Not significant[4]	527,335	95.1%	1,009,963	95.5%
Total	554,411	100%	1,056,895	100%
Common dispersion estimate[5]		0.1524		0.1997

[1]Prenatally stressed.
[2]Number and proportion of sites showing greater methylation in the adrenal medulla tissues.
[3]Number and proportion of sites showing greater methylation in the paraventricular nucleus of the hypothalamus tissues.
[4]Number and proportion of sites without significant differential methylation between tissues.
[5]Squared coefficient of variation in the true abundance of replicates between adrenal medulla tissues paraventricular nucleus of the hypothalamus tissues.

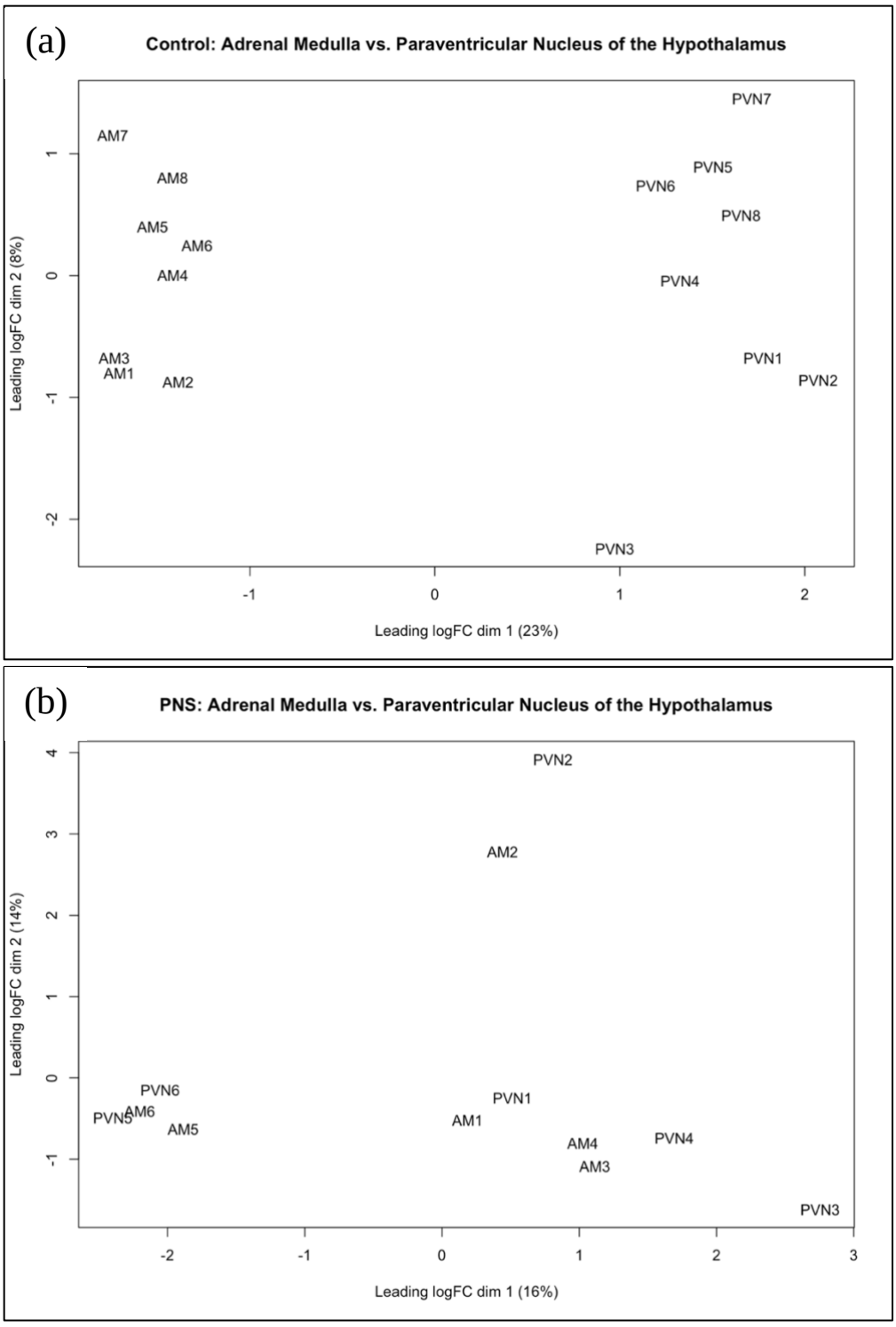

Figure 17. Multidimensional scaling plots for (a) control cows and (b) prenatally stressed (PNS) cows. AM: adrenal medulla. PVN: paraventricular nucleus of the hypothalamus. Sample numbers follow those abbreviations and correspond to the same cows.

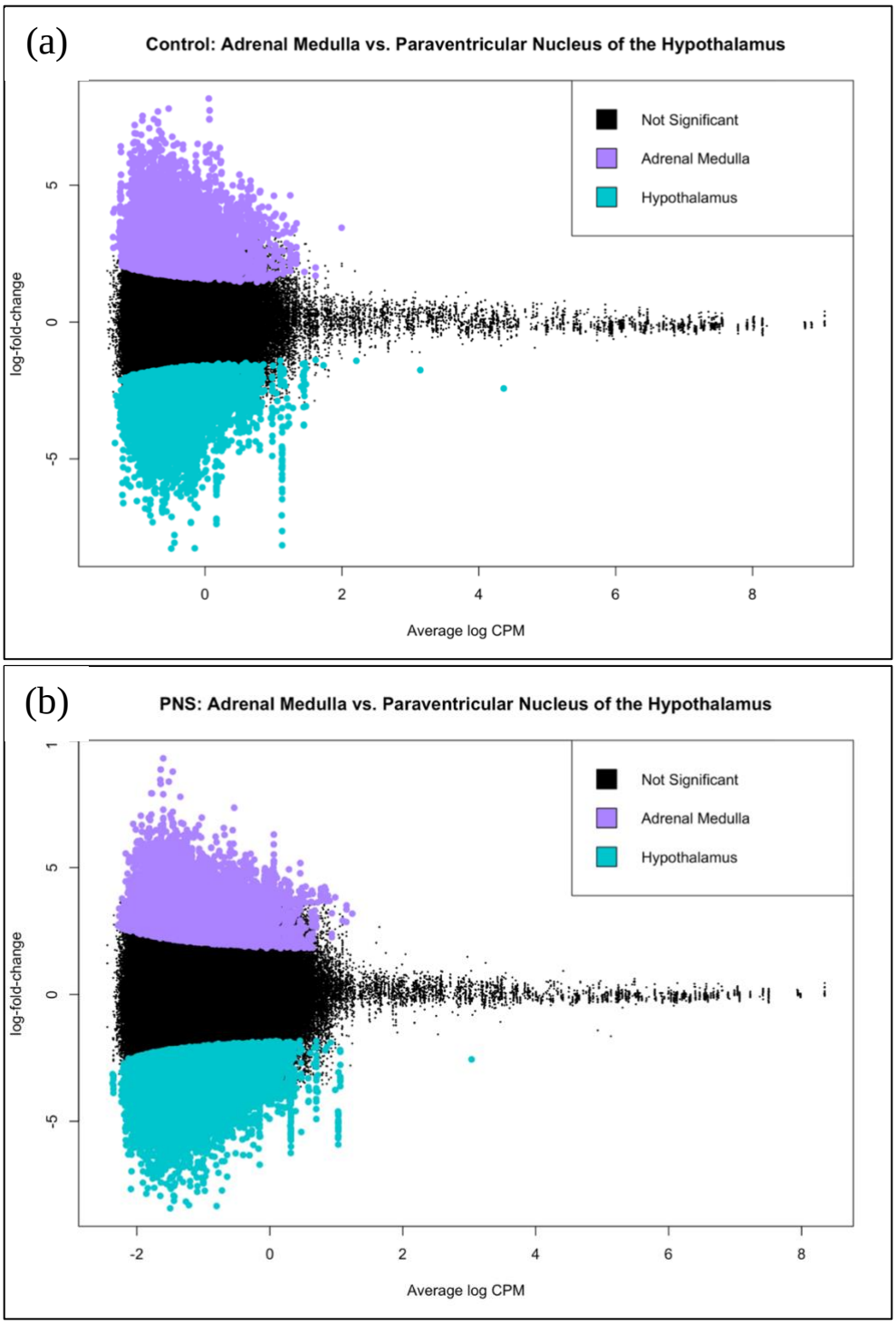

Figure 18. Mean difference plots for (a) control cows and (b) prenatally stressed (PNS) cows. Sites more methylated in the adrenal medulla relative to the paraventricular nucleus of the hypothalamus are purple; those more methylated in the paraventricular nucleus of the hypothalamus relative to the adrenal medulla are green, and sites not differentially methylated are black.

4.2.6. Anterior Pituitary vs. Paraventricular Nucleus of the Hypothalamus

Comparison of the anterior pituitary and PVN highlighted divergence in count proportions largely in sites termed not significant and sites that are more methylated in PVN relative to anterior pituitary (Table 10). Non-significant sites were much higher (87.7%) in the control group; this may be a consequence of prenatal stress. The increase of PVN methylation relative to the anterior pituitary from 9% in the control group to 18.3% in the PNS group may be the primary source of this differential methylation. Especially considering the change in anterior pituitary tissue being more methylated relative to PVN is nominal with 3.4% in the control group and 3.7% in the PNS group (Table 10). Common dispersion estimate treatment differences were similar to those of the other tissue comparisons, with 0.1424 in the control group growing and 0.1703 in the PNS group. This may also be a result of an increased number of differentially methylated sites in the PNS group (Table 10).

The MDS plot of the control group displays a relationship that might be expected where the greatest distinction is seen between tissue types along the x-axis, with the second most difference being amongst individuals along the y-axis (Figure 19a). Interestingly, the spatial relationship between tissue types almost reverses in the PNS group, where PVN sites are mostly sequestered to the right side of the control plot but then fall more to the left of the PNS plot, but with greater spread along the x-axis. Another notable characteristic of these plots is that both samples for each individual align more consistently along the y-axis in the control group than for the PNS group. The two tissues samples of each individual in Figure 19b are substantially distanced from one another, and for some the distance is observable along both axes. The MD plots also show contrast for more methylated sites of anterior pituitary relative to PVN and vice versa in the control plot compared to the PNS plot (Figure 20). Differentially methylated sites

have greater concentration in the PNS plot and PVN shows greater abundance of methylation in both plots.

Table 10. Counts and percentages of differentially methylated sites and common dispersion estimates for anterior pituitary to paraventricular nucleus of the hypothalamus tissue comparison.

Measurement	Control		PNS[1]	
	Count	Percentage	Count	Percentage
Anterior Pituitary[2]	21,271	3.4%	53,408	3.7%
PVN[3]	56,922	9%	267,412	18.3%
Not Significant[4]	551,606	87.7%	1,136,572	78%
Total	629,799	100%	1,457,392	100%
Common Dispersion Estimate[5]		0.1424		0.1703

[1]Prenatally stressed.
[2]Number and proportion of sites showing greater methylation in the anterior pituitary tissues.
[3]Number and proportion of sites showing greater methylation in the paraventricular nucleus of the hypothalamus tissues.
[4]Number and proportion of sites without significant differential methylation between tissues.
[5]Squared coefficient of variation in the true abundance of replicates between anterior pituitary tissues paraventricular nucleus of the hypothalamus tissues.

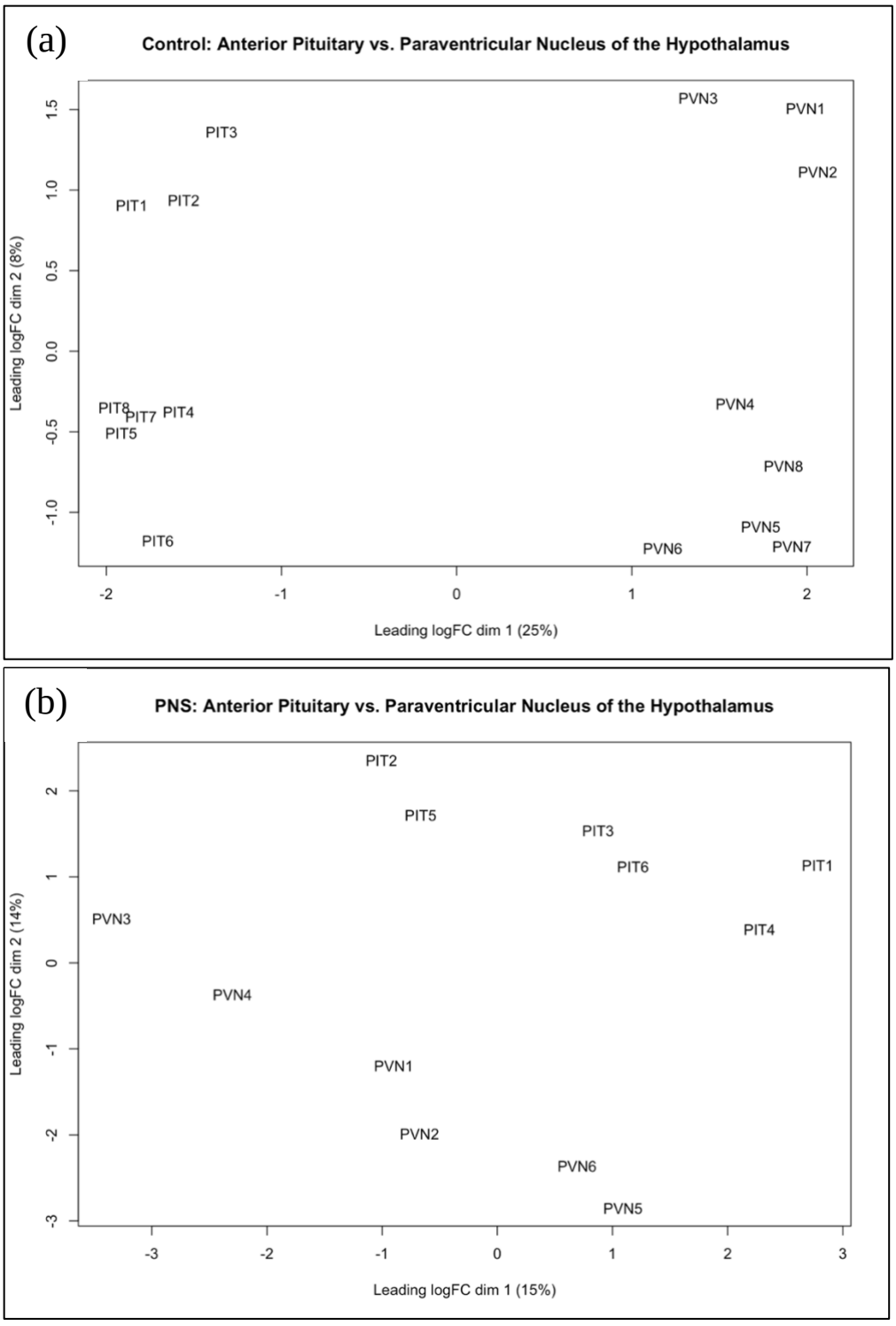

Figure 19. Multidimensional scaling plots for (a) control cows and (b) prenatally stressed (PNS) cows. PIT: anterior pituitary. PVN: paraventricular nucleus of the hypothalamus. Sample numbers follow those abbreviations and correspond to the same cows.

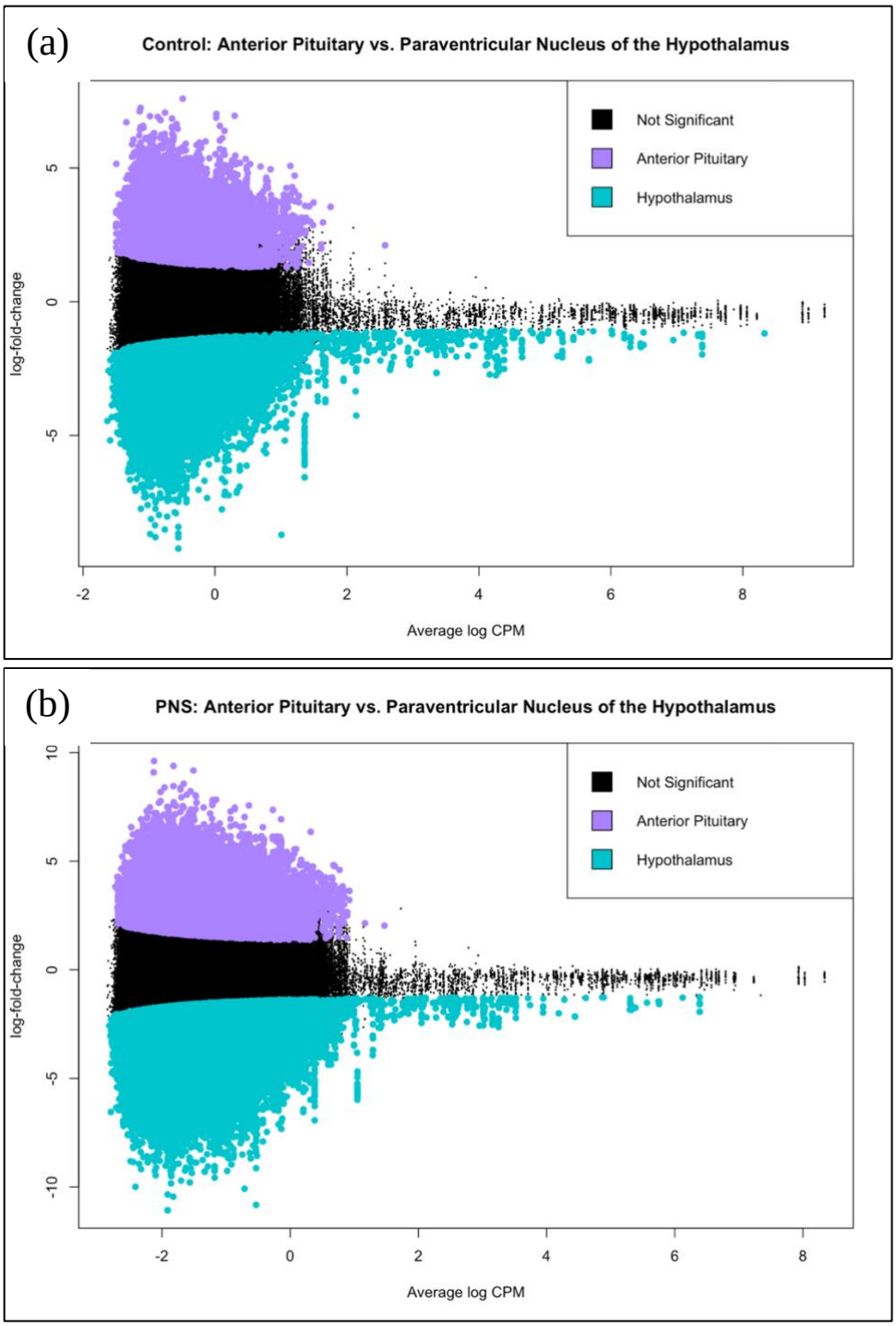

Figure 20. Mean difference plots for (a) control cows and (b) prenatally stressed (PNS) cows. Sites more methylated in the anterior pituitary relative to the paraventricular nucleus of the hypothalamus are purple; those more methylated in the paraventricular nucleus of the hypothalamus relative to the anterior pituitary are green, and sites not differentially methylated are black.

4.3. Top 10 Differentially Methylated Genes of HPA Axis Tissues Compared to WBC

In order to observe trends in DNA methylation data between HPA-axis tissues and WBC, the opposing conditions of the control group and the PNS group were used to determine if the difference in conditions are reflected by a change in methylation patterns of WBC. The common dispersion estimates from the initial analyses indicated that percentages of overall methylation differences between HPA-axis tissues and WBC appears to be similar for both treatments. To identify a suitable pattern for predicting DNA methylation of HPA-axis tissues by way of WBC analysis, two conditions must be met. Comparison of results from control to PNS groups must show an observable change between treatments, and this change must be concordant between the tissue of interest and WBC, where the tissue and WBC change together across treatments. Global analyses of this study do not adequately meet these conditions in a way that would facilitate characterization of HPA-axis tissue methylation patterns by way of WBC. The MDS and MD plots, however, suggest that a degree of polarity in methylation patterns may exist between HPA-axis tissues and WBC. Marginal, but apparent, differences between control data and PNS data exist and merit further investigation of specific CpG sites that could potentially affect gene expression. Therefore, the LogFC values provided by the EdgeR analyses for each CpG site were further evaluated for their corresponding FDR value and proximity to the closest transcription start site.

To supplement these results, direct comparison of control and PNS groups were conducted within each tissue individually at the limited number of identified sites to either support or refute the abundance of methylation of that site within the respective tissue. In the case of control-to-PNS comparisons within tissues, negative values indicate greater methylation within the control group while positive values indicate greater methylation within the PNS

group. Additionally, FDR values were also included to indicate the strength of each LogFC argument, and those with FDR $\geq$ 0.15 were classified as showing no difference in methylation. Because of this only a few sites of each tissue-to-WBC comparison were supported by the corresponding control-to-PNS comparison. These trends of polarity between WBC and HPA-axis tissues present a unique opportunity to further explore differential methylation patterns that have potential for diagnostic value in cattle. Both the location of the selected CpG sites and the observed changes in methylation between the conditions of control and prenatal stress may ultimately be consequential for gene expression and gland function.

4.3.1. Adrenal Cortex

The top 10 sites identified as being most differentially methylated and most biologically relevant, as in those most likely to affect gene expression, transcription, developmental processes, cell proliferation, or apoptosis, for comparisons between adrenal cortex tissue and WBC can be seen in Table 11. The supplemental comparisons of control to PNS within tissue measures for both the adrenal cortex and WBC of the same genes can be seen in Table 12. Genes in the adrenal cortex showed consistently less methylation than WBC in the PNS group as compared to the control group. The genes TERF1-interacting nuclear factor 2 (*TINF2*) and ALX homeobox 3 (*ALX3*) were more methylated (FDR $\leq$ 0.1) in the control group than in the PNS group within the adrenal cortex (Table 12). Meanwhile, core-binding factor subunit beta (*CBFB*) was less methylated (FDR = 0.12) in the control group of WBC when looking at control-to-PNS comparisons in Table 6. All three of these genes have established roles in coding for proteins involved in transcription processes (Simonsson, 2001; Wang et al., 2021; Qi et al., 2021). To support these results, Pearson correlation coefficients were used to illustrate the correspondence between the average methylation of a given gene within both tissue and WBC of both the control

and PNS groups (Table 13). The Fli-1 proto-oncogene, ETS transcription factor (*FLI1*) gene had the greatest negative correlation (r = –0.789; *P* value = 0.057) in the PNS group, which indicated the average methylation of all sites on that gene within the adrenal cortex tissue change in opposition to that of WBC.

4.3.2. Adrenal Medulla

The top 10 differentially methylated sites of the adrenal medulla can be seen in Table 14. The direct control-PNS comparisons within tissue measures can be seen in Table 15. Six of the 10 sites selected in the adrenal medulla were more methylated in adrenal medulla tissue of the PNS group while the other 4 sites were more methylated in WBC of the control group. The LIM domains-containing protein 1 (*LIMD1*) and Ras-related and estrogen-regulated growth inhibitor (*RERG*) genes, which were both more methylated in WBC of the control group and more methylated in adrenal medulla tissue of the PNS group, were also found to be more methylated (FDR = 0.08) within WBC. None of the sites showed a treatment difference within the adrenal medulla (Table 15). Pearson correlation coefficients for the adrenal medulla and WBC comparisons can be seen in Table 16. The only gene with a correlation between adrenal medulla and WBC that was supported by the P value (r = 0.704; *P* value = 0.052) was that of the BCL2 like 11 (*BCL2L11*) gene, which was found to be a strong positive correlation in the control group.

4.3.3. Anterior Pituitary

The top 10 differentially methylated sites of the anterior pituitary are shown in Table 17, while the direct control-PNS comparisons within tissue measures can be seen in Table 18. Four of the 10 sites selected were more methylated in the anterior pituitary tissue in the control group (FDR $\leq$ 0.07), while the other 6 sites were more methylated in the WBC of the PNS group (FDR

≤ 0.09). Within the direct control-PNS within tissue comparisons, the double strand break repair nuclease (*MRE11*) gene was more methylated in the control group of anterior pituitary tissue (FDR = 0.15), while the phosphofurin acidic cluster sorting protein 1 (*PACS1*) gene was more methylated in the control group of WBC (FDR = 0.14). Interestingly, differential methylation of CpG sites in the gene, fibroblast growth factor 20 (*FBG20*) was supported by FDR values for both anterior pituitary and WBC comparisons of control-to-PNS measures (FDR = 0.10 and FDR = 0.06), where WBC had higher methylation in the PNS group, and the anterior pituitary was more methylated in the control group. Of the Pearson correlation coefficients for the anterior pituitary to WBC comparisons that can be seen in Table 19, a negative correlation of sites located on the *MRE11* gene was only somewhat supported by its P value (r = –0.793; *P* value = 0.114). The only other gene that was negatively correlated was the meis homebox 2 (*MEIS2)* which was also negatively correlated (r = –0.712; *P* value = 0.113).

4.3.4. Paraventricular Nucleus of the Hypothalamus

The top 10 differentially methylated sites of PVN to WBC comparisons are detailed in Table 20, and the direct comparisons of treatment groups within tissue measures are presented in Table 21. Four of the 10 sites were more methylated in WBC of the PNS group (FDR ≤ 0.06), while the other 6 sites were more methylated in the PVN in the control group (FDR ≤ 0.13). From the direct treatment comparisons, the TATA-binding protein (*TBP*) was more methylated in the control group of the PVN tissue than in the PNS group (FDR = 0.14). The gene, *FLI1*, which was found to be differentially methylated in the adrenal cortex and adrenal medulla, was also differentially methylated in the PVN. The promoter regions sites of *FLI1* were more methylated in the control group of PVN while being more methylated in the PNS group of WBC (FDR = 0.07 and FDR = 0.14, respectively). Pearson correlation coefficients for PVN to WBC

comparisons are displayed in Table 22. The only gene with a significant positive correlation was in the control group P values: *TBP*, (r = 0.542; P value = 0.165).

4.3.5. Sites with Differential Methylation in Multiple Tissues

Some of the more notable genes identified from the differential methylation comparisons include the *FLI1* gene which was found to be less methylated in the adrenal cortex, adrenal medulla, and paraventricular nucleus of the hypothalamus tissues than in WBC of the prenatally stressed cows. Multiple CpG sites in the promoter region of this gene were differentially methylated in all three tissues. Multiple CpG sites in promoter regions of the *TINF2* gene were less methylated in both the adrenal cortex and anterior pituitary tissues than in WBC of the prenatally stressed cows. More detailed investigation of these genes may be illuminating for potential ramifications of prenatal stress in mature cows. Both the meiotic recombination 11 (*MRE11*) gene and the *BCL2L11* gene were differentially methylated in both the adrenal medulla and anterior pituitary relative to WBC. Greater methylation in the promoter region of *MRE11* was observed in the adrenal medulla and anterior pituitary relative to WBC in the PNS and the opposite was true for the control group. Greater methylation of *BCL2L11* was observed in WBC relative to the adrenal medulla and anterior pituitary relative to WBC in the control group while the opposite was true for the PNS group.

Table 11. Top 10 genes with differentially methylated CpG sites in promoter regions from comparisons of adrenal cortex (AC) tissue to white blood cells (WBC)in the control group and prenatally stressed (PNS) groups. (control AC vs. control WBC *and* PNS AC vs. PNS WBC).

Gene name	**Gene symbol**	**Control LogFC[1]**	**Control FDR[2]**	**PNS LogFC[3]**	**PNS FDR[4]**	**Primary function**
Fli-1 proto-oncogene, ETS transcription factor	*FLI1*	3.67	0.04	– 3.72	0.03	Transcription factor
TERF1 interacting nuclear factor 2	*TINF2*	2.87	0.04	– 2.72	0.06	Telomere repair
Toll interacting protein	*TOLLIP*	2.91	0.05	– 2.61	0.05	Inflammatory signaling
ALX homeobox 3	*ALX3*	2.86	0.02	– 2.26	0.08	Transcription regulation
Core-binding factor subunit beta	*CBFB*	3.25	0.06	– 3.52	0.14	Transcription factor
MYCL proto-oncogene, BHLH transcription factor	*MYCL*	3.57	0.08	– 3.15	0.13	Possible transcription factor
AE binding protein 2	*AEBP2*	3.46	0.08	– 3.24	0.11	Transcription repressor
Solute carrier family 7 member 6 opposite strand	*SLC7A6OS*	3.33	0.07	– 3.32	0.12	Involved in development
Dickkopf WNT signaling pathway inhibitor 1	*DKK1*	2.95	0.13	– 2.83	0.08	Embryonic development
Peroxisomal biogenesis factor 1	*PEX1*	3.21	0.08	– 3.15	0.03	Cytoplasmic protein

[1]Log2 fold change (LogFC) (LogFC)values for comparison of DNA methylation between tissues in the control group of cows, where negative values indicate greater methylation in white blood cells and positive values indicate greater methylation in adrenal cortex tissue.

[2]False discovery rate values associated with the LogFC values in the control group.

[3]Log2 fold change values for comparison of DNA methylation between tissues in the prenatally stressed group of cows, where negative values indicate greater methylation in white blood cells and positive values indicate greater methylation in adrenal cortex tissue.

[4]False discovery rate values associated with the LogFC values in the prenatally stressed group.

Table 12. Treatment comparisons of methylation rates in the top 10 genes with differentially methylated CpG sites in promoter regions selected from evaluations of adrenal cortex (AC) to white blood cells (WBC): within AC between control and prenatally stressed (PNS) cows and within WBC between control PNS cows (control AC vs. PNS AC and control WBC vs. PNS WBC).

Gene name	**Gene symbol**	**AC LogFC[1]**	**AC FDR[2]**	**WBC LogFC[1]**	**WBC FDR[2]**
Fli-1 proto-oncogene, ETS transcription factor	*TINF2*	4.37	0.10	–3.23	0.78
TERF1 interacting nuclear factor 2	*FLI1*	3.22	0.67	–3.44	0.78
Toll interacting protein	*TOLLIP*	2.84	0.67	–2.90	0.78
ALX homeobox 3	*ALX3*	3.64	0.14	–3.96	0.78
Core–binding factor subunit beta	*CBFB*	3.15	0.67	–4.05	0.12
MYCL proto-oncogene, BHLH transcription factor	*MYCL*	3.31	0.67	–2.95	0.78
AE binding protein 2	*AEBP2*	2.53	0.67	–2.81	0.78
Solute carrier family 7 member 6 opposite strand	*SCL7A6OS*	3.05	0.67	–3.17	0.78
Dickkopf WNT signaling pathway inhibitor 1	*DKK1*	3.05	0.67	– 3.16	0.78
Peroxisomal biogenesis factor 1	*PEX1*	2.71	0.67	– 3.47	0.78

[1]Log2 fold change (LogFC) values for comparison of DNA methylation in adrenal cortex tissues between the control and PNS cows, where negative values indicate greater methylation in PNS and positive values indicate greater methylation in the control group.

[2]False discovery rate values associated with LogFC values comparisons between control and PNS cows.

Table 13. Pearson correlation coefficients of adrenal cortex (AC)-white blood cell (WBC) methylation of promoter region CpG sites within identified Top 10 genes (control AC vs. control WBC and prenatally stressed [PNS] AC vs. PNS WBC).

Gene name	**Gene symbol**	**Control**[1]	***P* value**[2]	**PNS**[1]	***P* value**[2]
Fli-1 proto-oncogene, ETS transcription factor	*FLI1*	0.568	0.142	– 0.798	0.057
TERF1 interacting nuclear factor 2	*TINF2*	0.465	0.246	– 0.705	0.118
Toll interacting protein	*TOLLIP*	0.715	0.046	– 0.689	0.130
ALX homeobox 3	*ALX3*	– 0.106	0.803	– 0.283	0.590
Core-binding factor subunit beta	*CBFB*	0.636	0.090	– 0.122	0.818
MYCL proto-oncogene, BHLH transcription factor	*MYCL*	– 0.179	0.671	– 0.658	0.156
AE binding protein 2	*AEBP2*	0.452	0.261	0.544	0.264
Solute carrier family 7 member 6 opposite strand	*SLC7A6OS*	0.061	0.886	0.540	0.269
Dickkopf WNT signaling pathway inhibitor 1	*DKK1*	0.270	0.518	0.018	0.974
Peroxisomal biogenesis factor 1	*PEX1*	0.276	0.509	0.109	0.837

[1]Pearson correlation coefficient estimates for AC-WBC methylation within treatment.

[2]The *P* value associated with the Pearson correlation coefficient to the immediate left.

Table 14. Top 10 genes with differentially methylated CpG sites in promoter regions from comparisons of adrenal medulla (AM) tissue to white blood cells (WBC)in the control group and prenatally stressed (PNS) groups. (control AM vs. control WBC *and* PNS AM vs. PNS WBC).

Gene name	**Gene symbol**	**Control LogFC[1]**	**Control FDR[2]**	**PNS LogFC[3]**	**PNS FDR[4]**	**Primary function**
Fli-1 proto-oncogene, ETS transcription factor	*FLI1*	3.00	0.02	– 2.89	0.05	Transcription Factor
BCL2 like 11	*BCL2L11*	3.06	<0.01	– 3.09	0.02	Telomere repair
Double strand break repair nuclease	*MRE11*	– 3.06	<0.01	3.21	0.06	Apoptosis
Ewing variant transcription factor, ETS family member	*FEV*	– 2.78	0.09	2.78	0.09	Transcription Factor
LIM domain containing 1	*LIMD1*	– 2.89	0.01	3.01	<0.01	Neuroendocrine proteins
Chromogranin A	*CHGA*	– 3.31	0.02	3.39	0.04	Transcription repressor
Zinc finger and BTB domain containing 5	*ZBTB5*	– 2.88	0.03	3.38	<0.01	Growth inhibitor
RAS like estrogen regulated growth inhibitor	*RERG*	– 3.33	<0.01	3.32	0.04	Transcription regulation
HIV-1 Tat interactive protein 2	*HTATIP2*	3.71	<0.01	– 3.25	0.07	Transcription corepressor
Family with sequence similarity 89 member B	*FAM89B*	3.26	0.08	– 3.11	0.05	Transcription corepressor

[1]Log2 fold change (LogFC) values for comparison of DNA methylation between tissues in the control group of cows, where negative values indicate greater methylation in white blood cells and positive values indicate greater methylation in adrenal medulla tissue.

[2]False discovery rate values associated with the LogFC values in the control group.

[3]Log2 fold change values for comparison of DNA methylation between tissues in the prenatally stressed group of cows, where negative values indicate greater methylation in white blood cells and positive values indicate greater methylation in adrenal medulla tissue.

[4]False discovery rate values associated with the LogFC values in the prenatally stressed group.

Table 15. Treatment comparisons of methylation rates in the top 10 genes with differentially methylated CpG sites in promoter regions selected from evaluations of adrenal medulla (AM) to white blood cells (WBC): within AM between control and prenatally stressed (PNS) cows and within WBC between control PNS cows (control AM vs. PNS AM and control WBC vs. PNS WBC).

Gene name	**Gene symbol**	**AM LogFC[1]**	**AM FDR[2]**	**WBC LogFC[1]**	**WBC FDR[2]**
Fli-1 proto-oncogene, ETS transcription factor	*FLI1*	– 2.83	0.67	2.71	0.78
BCL2 like 11	*BCL2L11*	– 2.80	0.67	3.31	0.69
Double strand break repair nuclease	*MRE11*	3.51	0.67	3.98	0.12
Ewing variant transcription factor, ETS family member	*FEV*	2.25	0.67	– 3.01	0.78
LIM domain containing 1	*LIMD1*	3.15	0.67	– 4.00	0.06
Chromogranin A	*CHGA*	2.96	0.66	– 2.86	0.78
Zinc finger and BTB domain containing 5	*ZBTB5*	3.27	0.65	– 2.79	0.78
RAS like estrogen regulated growth inhibitor	*RERG*	3.24	0.65	– 4.29	0.07
HIV-1 Tat interactive protein 2	*HTATIP2*	– 4.37	0.26	3.44	0.78
Family with sequence similarity 89 member B	*FAM89B*	– 3.00	0.67	3.13	0.78

[1]Log2 fold change (LogFC) values for comparison of DNA methylation in adrenal medulla tissues between the control and PNS cows, where negative values indicate greater methylation in PNS and positive values indicate greater methylation in the control group.

[2]False discovery rate values associated with LogFC values of comparisons between control and PNS cows.

Table 16. Pearson correlation coefficients of adrenal medulla (AM)-white blood cell (WBC) methylation of promoter region CpG sites within identified Top 10 genes (control AM vs. control WBC and prenatally stressed [PNS] AM vs. PNS WBC).

Gene name	Gene symbol	Control[1]	*P* value[2]	PNS[1]	*P* value[2]
Fli-1 proto-oncogene, ETS transcription factor	*FLI1*	0.373	0.363	– 0.500	0.313
BCL2 like 11	*BCL2L11*	0.704	0.052	– 0.361	0.482
Double strand break repair nuclease	*MRE11*	0.063	0.882	– 0.499	0.406
Ewing variant transcription factor, ETS family member	*FEV*	0.624	0.098	– 0.423	0.403
LIM domain containing 1	*LIMD1*	0.107	0.801	– 0.233	0.657
Chromogranin A	*CHGA*	0.140	0.742	– 0.236	0.652
Zinc finger and BTB domain containing 5	*ZBTB5*	0.203	0.629	– 0.157	0.767
RAS like estrogen regulated growth inhibitor	*RERG*	0.023	0.957	0.309	0.552
HIV-1 Tat interactive protein 2	*HTATIP2*	– 0.163	0.700	– 0.115	0.828
Family with sequence similarity 89 member B	*FAM89B*	– 0.301	0.469	0.789	0.062

[1]Pearson correlation coefficient estimates for AM-WBC methylation within treatment.

[2]The *P* value associated with the Pearson correlation coefficient estimate to the immediate left.

Table 17. Top 10 genes with differentially methylated CpG sites in promoter regions from comparisons of anterior pituitary (PIT) tissue to white blood cells (WBC)in the control group and prenatally stressed (PNS) groups. (control PIT vs. control WBC *and* PNS PIT vs. PNS WBC).

Gene name	**Gene symbol**	**Control LogFC[1]**	**Control FDR[2]**	**PNS LogFC[3]**	**PNS FDR[4]**	**Primary function**
TERF1 interacting nuclear factor 2	*TINF2*	3.22	0.03	– 3.27	0.04	Telomere repair
BCL2 Like 11	*BCL2L11*	3.45	0.07	– 3.09	<0.01	Apoptosis
MRE11 homolog, double strand break repair nuclease	*MRE11*	– 3.01	<0.01	2.93	0.08	Telomere repair
Zinc finger protein 266	*ZNF266*	– 3.20	0.02	3.51	0.02	Transcription
Meis homeobox 2	*MEIS2*	– 3.99	0.02	3.51	0.02	Transcription
AT-Rich interaction domain 4A	*ARID4A*	– 2.40	0.04	2.88	0.05	Transcription
Fibroblast growth factor 20	*FGF20*	– 3.56	0.09	2.81	0.09	Development
Rac family small GTPase 3	*RAC3*	– 2.97	0.01	2.75	0.07	Cell growth
LDL receptor related protein 8	*LRP8*	2.74	0.05	– 2.78	0.07	Development
Phosphofurin acidic cluster sorting protein 1	*PACS1*	2.72	0.05	– 3.24	<0.01	Cytoplasm

[1]Log2 fold change (LogFC) values for comparison of DNA methylation between tissues in the control group of cows, where negative values indicate greater methylation in white blood cells and positive values indicate greater methylation in anterior pituitary tissue.

[2]False discovery rate values associated with the LogFC values in the control group.

[3]Log2 fold change values for comparison of DNA methylation between tissues in the prenatally stressed group of cows, where negative values indicate greater methylation in white blood cells and positive values indicate greater methylation in anterior pituitary tissue.

[4]False discovery rate values associated with LogFC values in the prenatally stressed group.

Table 18. Treatment comparisons of methylation rates in the top 10 genes with differentially methylated CpG sites in promoter regions selected from evaluations of anterior pituitary (PIT) to white blood cells (WBC): within PIT between control and prenatally stressed (PNS) cows and within WBC between control PNS cows (control PIT vs. PNS PIT and control WBC vs. PNS WBC).

Gene name	**Gene symbol**	**AP LogFC[1]**	**AP FDR[2]**	**WBC LogFC[1]**	**WBC FDR[1]**
TERF1 interacting nuclear factor 2	*TINF2*	– 2.25	0.84	2.61	0.78
BCL2 Like 11	*BCL2L11*	– 2.95	0.84	2.63	0.78
MRE11 homolog, double strand break repair nuclease	*MRE11*	3.06	0.15	– 2.70	0.78
Zinc finger protein 266	*ZNF266*	3.57	0.84	– 3.10	0.76
Meis homeobox 2	*MEIS2*	2.97	0.84	– 2.73	0.78
AT-Rich interaction domain 4A	*ARID4A*	2.58	0.84	– 2.73	0.78
Fibroblast growth factor 20	*FGF20*	3.34	0.10	– 4.58	0.06
Rac family small GTPase 3	*RAC3*	2.86	0.84	– 3.01	0.78
LDL receptor related protein 8	*LRP8*	– 3.33	0.84	2.18	0.78
Phosphofurin acidic cluster sorting protein 1	*PACS1*	– 3.26	0.84	3.57	0.14

[1]Log2 fold change (LogFC) values for comparison of DNA methylation in anterior pituitary tissues between the control cows and PNS cows, where negative values indicate greater methylation in PNS and positive values indicate greater methylation in the control group.

[2]False discovery rate values associated with LogFC values of comparisons between control and PNS cows.

Table 19. Pearson correlation coefficients of anterior pituitary (PIT)-white blood cell (WBC) methylation of promoter region CpG sites within identified Top 10 genes (control PIT vs. control WBC and prenatally stressed [PNS] PIT vs. PNS WBC).

Gene name	**Gene symbol**	**Control**[1]	***P* value**[2]	**PNS**[1]	***P* value**[2]
TERF1 interacting nuclear factor 2	*TINF2*	0.175	0.678	– 0.608	0.200
BCL2 Like 11	*BCL2L11*	0.217	0.605	– 0.316	0.627
MRE11 homolog, double strand break repair nuclease	*MRE11*	0.154	0.716	– 0.793	0.114
Zinc finger protein 266	*ZNF266*	0.388	0.343	– 0.614	0.194
Meis homeobox 2	*MEIS2*	0.290	0.486	– 0.712	0.113
AT-Rich interaction domain 4A	*ARID4A*	– 0.081	0.849	0.416	0.413
Fibroblast growth factor 20	*FGF20*	0.021	0.961	– 0.405	0.426
Rac family small GTPase 3	*RAC3*	0.441	0.274	– 0.390	0.445
LDL receptor related protein 8	*LRP8*	0.080	0.850	– 0.478	0.338
Phosphofurin acidic cluster sorting protein 1	*PACS1*	0.630	0.094	– 0.109	0.838

[1]Pearson correlation coefficient estimates for PIT-WBC methylation within treatment.

[2]The P value associated with the Pearson correlation coefficient to the immediate left.

Table 20. Table 11. Top 10 genes with differentially methylated CpG sites in promoter regions from comparisons of the paraventricular nucleus of the hypothalamus (PVN) tissue to white blood cells (WBC)in the control group and prenatally stressed (PNS) groups. (control PVN vs. control WBC *and* PNS PVN vs. PNS WBC).

Gene name	**Gene symbol**	**Control LogFC[1]**	**Control FDR[2]**	**PNS LogFC[3]**	**PNS FDR[4]**	**Primary function**
Fli-1 proto-oncogene, ETS transcription factor	FLI1	3.77	0.03	– 3.50	<0.01	Transcription factor
Interferon regulatory factor 5	IRF5	– 3.11	0.05	3.03	0.05	Transcription factor
TATA-box binding protein	TBP	– 3.23	0.04	3.58	0.03	Transcription Initiation
Bovine retinoblastoma-like protein 1	RBL1	– 3.15	<0.01	3.45	0.12	Transcription corepressor
Mediator complex subunit 14	MED14	– 3.22	0.07	2.78	0.10	Transcription enhancer
KIT proto-oncogene, receptor tyrosine kinase	KIT	– 3.38	<0.01	2.65	0.13	Cell survival
T-Box transcription factor 18	TBX18	– 2.43	0.07	2.71	0.12	Transcription factor
E2F transcription factor 3	E2F3	3.30	<0.01	– 2.65	0.05	Transcription factor
TNF receptor superfamily member 19	TNFRSF19	2.62	0.03	– 3.34	<0.01	Embryonic development
MAM domain containing glycosylphosphatidylinositol anchor 1	MDGA1	2.52	0.06	– 2.58	0.05	Nervous system development

[1]Log2 fold change (LogFC) values for comparison of DNA methylation between tissues in the control group of cows, where negative values indicate greater methylation in white blood cells and positive values indicate greater methylation in anterior pituitary tissue.

[2]False discovery rate values associated with the LogFC values in the control group.

[3]Log2 fold change values for comparison of DNA methylation between tissues in the prenatally stressed group of cows, where negative values indicate greater methylation in white blood cells and positive values indicate greater methylation in anterior pituitary tissue.

[4]False discovery rate values associated with the LogFC values in the prenatally stressed group.

Table 21. Treatment comparisons of methylation rates in the top 10 genes with differentially methylated CpG sites in promoter regions selected from evaluations of the paraventricular nucleus of the hypothalamus (PVN) to white blood cells (WBC): within PVN between control and prenatally stressed (PNS) cows and within WBC between control PNS cows (control PVN vs. PNS PVN and control WBC vs. PNS WBC).

Gene name	Gene symbol	PVN LogFC[1]	PVN FDR[2]	WBC LogFC[1]	WBC FDR[2]
Fli-1 proto-oncogene, ETS transcription factor	FLI1	– 3.67	0.07	4.73	0.14
Interferon regulatory factor 5	IRF5	3.61	0.59	– 3.28	0.78
TATA-box binding protein	TBP	4.25	0.14	– 3.90	0.78
Bovine retinoblastoma-like protein 1	RBL1	3.97	0.61	– 2.38	0.78
Mediator complex subunit 14	MED14	2.42	0.61	– 3.07	0.73
KIT proto-oncogene, receptor tyrosine kinase	KIT	2.90	0.61	– 3.19	0.78
T-Box transcription factor 18	TBX18	2.87	0.61	– 3.08	0.78
E2F transcription factor 3	E2F3	– 2.76	0.61	3.36	0.78
TNF receptor superfamily member 19	TNFRSF19	– 3.19	0.61	3.25	0.78
MAM domain containing glycosylphosphatidylinositol anchor 1	MDGA1	– 3.18	0.61	2.21	0.78

[1]Log2 fold change (LogFC) values for comparison of DNA methylation in paraventricular nucleus of the hypothalamus tissues between the control cows and PNS cows, where negative values indicate greater methylation in PNS and positive values indicate greater methylation in the control group.

[2]False discovery rate values associated with LogFC values of comparisons between control and PNS cows.

Table 22. Table 13. Pearson correlation coefficients of the paraventricular nucleus of the hypothalamus (PVN)-white blood cell (WBC) methylation of promoter region CpG sites within identified Top 10 genes (control PVN vs. control WBC and prenatally stressed [PNS] PVN vs. PNS WBC).

Gene name	**Gene symbol**	**Control**[1]	***P* value**[2]	**PNS**[1]	***P* value**[2]
Fli-1 proto-oncogene, ETS transcription factor	*FLI1*	0.144	0.733	– 0.581	0.227
Interferon regulatory factor 5	*IRF5*	0.373	0.362	0.274	0.599
TATA-box binding protein	*TBP*	0.542	0.165	– 0.382	0.456
Bovine retinoblastoma-like protein 1	*RBL1*	– 0.302	0.468	0.021	0.969
Mediator complex subunit 14	*MED14*	0.018	0.967	– 0.479	0.336
KIT proto-oncogene, receptor tyrosine kinase	*KIT*	0.370	0.368	– 0.157	0.767
T-Box Transcription Factor 18	*TBX18*	0.138	0.744	– 0.233	0.658
E2F Transcription Factor 3	*E2F3*	0.413	0.309	– 0.381	0.456
TNF Receptor Superfamily Member 19	*TNFRSF19*	0.109	0.797	– 0.592	0.215
MAM Domain Containing Glycosylphosphatidylinositol Anchor 1	*MDGA1*	0.336	0.416	– 0.088	0.868

[1]Pearson correlation coefficient estimates for PVN-WBC methylation within treatment.

[2]*P* value associated with the Pearson correlation coefficient estimates to the immediate left.

5. DISCUSSION

The opposing environmental conditions of a prenatally stressed group of mature Brahman cows and a control group of mature Brahman cows were used to determine if long term changes in DNA methylation patterns of the adrenal cortex, adrenal medulla, anterior pituitary, and hypothalamic paraventricular nuclei could be observed within these tissues as well as WBC. This aspect of the study was used to indicate if a change in DNA methylation patterns of the HPA-axis tissues between the opposing treatments could be mirrored by DNA methylation patterns of WBC to then be used as a diagnostic tool for neuroendocrine functions when sampling of the desired tissue is not reasonable. Initial analyses revealed that, in a global sense, methylation pattern differences between tissue to WBC across control and PNS mature cow comparisons were minimal. When these adrenal axis tissues were subsequently compared to one another, the greatest correspondence could be seen between the adrenal cortex and adrenal medulla relative to the other comparisons, but where predictive relationships could not be characterized based on control to PNS differences. The polarity suggested by the MDS and MD plots led to evaluation of individual CpG sites within promoter regions, and several genes were identified as having inverse methylation ratios of tissue to WBC when the control group was compared against the PNS group. This dynamic between tissue and WBC has not yet been proposed in previous literature but is likely a worthwhile endeavor for better understanding the predictive nature of WBC for DNA methylation patterns of tissues of interest.

5.1. Full Genome Differential Methylation Analyses of Tissues vs. White Blood Cells

White blood cell methylation levels corresponded with each HPA-axis tissue to a degree within either treatment group, as can be observed in the “Not Significant” category of Tables 1 through 4. This term, “Not Significant” refers to sites that were similarly methylated between

tissues, that is sites where the LogFC ratio was between 1 and –1 and with a false discovery rate of $\geq$ 0.15, indicating minimal differences exist in levels of methylation between WBC and tissue at that site. The differences between the control and PNS results were not large enough to suggest DNA methylation patterns change in a concordant manner between HPA-axis tissues and WBC in a way that would facilitate the use of global WBC methylation as a biomarker for prediction of changes in these tissues. However, the global predominance of sites that were not differentially methylated (in a statistical sense) should not be interpreted that the methylation pattern of one tissue would sufficiently predict those of the other.

Huang et al. (2016) provides reasonable criteria to affirm WBC methylation patterns as suitable for predicting specific tissue methylation, where a characteristic or treatment that is suspected of causing epigenetic changes compared against a control that results in a consistent pattern between WBC and the tissue of interest. With this in mind, the results of the current study align with those of Huang et al. (2016), where minimal concordance between human adipose tissue and blood were found. Åsenius et al. (2020) also showed that while methylation patterns WBC could adequately predict obesity in humans, the relationship between sperm cells and WBC was highly discordant, and therefore tissue specific consideration is highly influential in understanding consequences of DNA methylation. Braun et al. (2019) were also unable to confirm predictive relationships of methylation characteristics of blood, saliva, or buccal cells with DNA from any region of the human brain. Still, knowing the tissue specific nature of DNA methylation, WBC cannot be ruled out as a valuable biomarker as there is evidence that supports further investigation, such as that from Woo and Kim (2012), where concordance between WBC and various cancer tissues was identified. Additionally, Ebrahimi et al. (2021) found adequate

correspondence of WBC to bone methylation patterns. Ma et al. (2014) was also able to identify consistencies of methylation characteristics from DNA of atrium, artery, and WBC.

While human studies can provide insight into physiological mechanisms of other mammals, it is still important to consider species-specific differences. There is evidence of discordant methylation patterns between various species of animals and humans, such as that of Ching et al. (2005) where differing patterns between humans, and mice and rats were found by using brain tissues, astrocytes, keratinocytes, and WBC. Zhou et al. (2020) examined methylation patterns of 16 different tissues including, lung, liver, kidney, placenta, ileum, rumen, whole blood, WBC, spleen, ovary, uterus, cortex, adipose, mammary, longissimus dorsi, and heart tissues in numerous species including mice, sheep, goats, yaks, pigs, chickens, and cattle to compare to those in humans. Zhou et al. (2020) identified cross-species methylation characteristics in that work, but notably, not in cattle which was found to have a unique methylome by comparison. This study from Zhou et al. (2020) utilized a family of Holstein cattle and noted that even breed-specific differences may also exist.

Global DNA methylation between certain tissues and WBC may be difficult to characterize, but that specific genes and/or regions of the genome could be targeted that may provide concordant relationships. Ching et al. (2005) identified *ARHGEF17* and *SHANK3* as being similarly methylated genes in brain tissues across mice, rats, and humans. Jin (2020) identified 5 genes as being differentially methylated in breast cancer tissue as compared to healthy breast tissue. Those genes included *IGF2*, *BRCA1*, *GSTP1*, *CDKN2A*, and *MGMT*. Svoboda et al. (2021) used adult mice to observe the metabolic effects of lead exposure and identified 44 imprinted loci that significantly overlapped between liver and blood samples, and ultimately concluded that molecular targets are likely to aid in diagnosis of metabolic disorders.

In humans affected by Parkinson's disease, Masliah et al. (2013) identified the *APP* gene as being consistently hypermethylated between brain tissues and blood. Walton et al. (2016) concluded from studying Schizophrenia patients that specific markers within the genome should be targeted in future research. Harris et al. (2020) also indicated that differentially methylated regions of the genome should be targeted for future evaluation of patterns between hippocampus tissue and WBC.

5.2. Full Genome Differential Methylation Analyses of Tissues vs. Tissues

One comparison of tissue with other tissues with high percentages of similarly methylated sites in both the control and PNS groups were the adrenal cortex and adrenal medulla based on global count analysis. Non-significant sites were the overwhelming majority of each tissue-to-tissue comparison in both control and PNS groups, however, the adrenal tissue comparison showed the second greatest percentage of non-significant sites relative to all other tissue-to-tissue comparisons in both the control and PNS groups. This was further demonstrated by the MDS plots (Figure 9) and MD plots (Figure 10), with the PNS MD plot (Figure 9b) specifically showing greater variation between individuals along the x-axis as compared to the control plot (Figure 9a). Commons dispersion estimates also support some increase in variability of the PNS group in relation to the control group through expression of the ratio of standard deviation to the mean of each respective group squared. The higher common dispersion estimate in the PNS groups supports the notion that the most differentially methylated sites within that group are more numerically distant from one another as compared to the most differentially methylated sites in the control group. It is possible that this enhanced distinction of differential methylation is attributable to the influence of prenatal stress.

Adrenal cortex samples and adrenal medulla samples were well aligned with one another in both the control and PNS groups, which may be due to their proximity and direct inter-involvement of function with one another. Although the hormones produced by the adrenal cortex and adrenal medulla often act in concert with one another, there are still fundamental differences in physiology and function of these glands. Comprised of mesodermal tissue, the adrenal cortex produces steroid hormones while the adrenal medulla is comprised of neuroectodermal tissue and produces catecholamines (Kempná and Flück, 2008). The adrenal medulla only makes up about 10% of the mass of a mature adrenal gland and is considered a modified sympathetic ganglion due to its role in sympathetic nervous system (Kempná and Flück, 2008). It may be the case that those sites expressing greater differential methylation between tissues are more central to the function and effectiveness of each gland, and the sites found to be similarly methylated are less critical for development and/or function. It may also be the case that methylation patterns happen in an inconsistent pattern between individuals where certain influences create an expectation for a degree of differential methylation but where location and consequence of that methylation are less predictable.

Both the adrenal cortex and adrenal medulla had similar relationships with PVN where more than 90% of sites in the control and PNS groups were considered not significant. Although the adrenal cortex-anterior pituitary comparisons were relatively consistent between the control and PNS groups, the adrenal medulla-to-anterior pituitary comparisons had considerable differences between the control and PNS groups. Specifically, relative to the control group, sites considered not significant were 11.8% greater in the PNS group and sites with greater methylation in the adrenal medulla relative to the anterior pituitary were 10.3% lower in the PNS group relative to the control group (Table 8). In this case it would appear that methylated sites

between the adrenal medulla and anterior pituitary become less distinct from one another where prenatal stress has been induced. However, the common dispersion estimates continue to suggest that differences in samples become greater in the PNS group relative to the control group of this tissue-to-tissue comparison. It is possible that while some proportion of similarly methylated sites remains when comparing control to PNS, the sites comprising those proportions may not necessarily be the same.

The adrenal medulla is the most disconnected from direct communication with the other relevant glands in the HPA-axis. Considered a critical component of the sympathetic-adrenal-medullary (SAM) system, the adrenal medulla has been described as reacting independently from activities of the HPA-axis. Schommer et al. (2003) characterized the response and habituation patterns of the HPA-axis and SAM system in response to repeated psychosocial stress in humans and found that the two have distinct functioning in this regard. The HPA-axis was quicker to habituate its response to repeated psychosocial stress which manifested in a gradual reduction of salivary free cortisol, plasma cortisol, ACTH, and heart rate after every stress challenge. In contrast, the adrenal medulla functions by way of acetylcholinergic input that regulates enzymes of the gland that converts tyrosine to catecholamines. These hormones, referred to as norepinephrine and epinephrine, were produced in consistent levels across stress challenges, with no decrease observed and therefore no habituation to stress response occurred (Schommer et al., 2003). These contrasts in functionality may be attributable to the inconsistency of correspondence in methylation patterns of the adrenal medulla in relation to the other HPA-axis tissues where the adrenal medulla may have a distinct and independent response to stress.

The anterior pituitary and PVN, had different methylation count statistics corresponding to control and PNS groups. Specifically, sites considered not significant decreased by 9.7% in

the PNS group relative to the control group, which seemed to be primarily compensated by a 9.3% increase in sites more methylated in PVN tissue relative to anterior pituitary tissue in the PNS group compared to the control group. As has been consistent across all tissue-tissue comparisons, the common dispersion estimates suggest greater variability across sites in the PNS group compared to the control group and the comparison of anterior pituitary to PVN was no different. Considerable evidence exists that supports differential methylation of the hypothalamus in response to stress, particularly in the growing brain (Jensen et al., 2012; Shutoh et al., 2012; Cheong et al., 2018; Shen et al., 2020). While the anterior pituitary showed the least differential methylation between the control group to PNS group relative to the other tissues, the relationship of this gland to the others observed is well documented, and therefore would likely be impacted by a residual effect of methylation changes in the other tissues if nothing else.

5.3. Differentially Methylated CpG Site Identification and Analysis

Due to the lack of insight from global methylation analyses, differential methylation of specific CpG sites were considered. When looking at the MD plots, the spread along the y-axis where LogFC values are displayed is relatively proportional for each HPA-axis tissue to WBC comparison, suggesting polarity of methylation levels may exist between tissues. To better comprehend this dynamic of the relationships of tissue with WBC, a closer inspection of differentially methylated sites between treatment groups was executed. Based on the LogFC calculations, a single value that is found to be positive in one group, but negative in the other group, amounts to a directly inverted ratio. In the case of HPA-axis tissue to WBC tissue comparisons, the ratio being measured is the number of methylated sites having passed coverage on each gene within the tissues and WBC. This means when a positive value in the control group is reflected by a value of similar magnitude yet negative in the PNS group, or vice versa, one of

two things are happening. Either methylation of WBC or the tissue increases so greatly in one treatment group (control or PNS) relative to the other that it becomes multiple times higher than its value in the opposing treatment group resulting in an inverted ratio (i.e., if site "x" has control tissue = 1 and WBC = 2, then LogFC = log2(1/2) and control LogFC of x = – 1 . And, if PNS tissue = 4 and WBC = 2, then LogFC = log2(4/2) and PNS LogFC of x = 1). The alternative is one tissue (WBC or HPA-axis tissue) is not only elevated in one treatment group relative to the other, but methylation of the opposing tissue has also lowered at a proportional rate in the same treatment group, which would also result in an inverted ratio (i.e., if site "y" control tissue = 1 and WBC = 2, then LogFC = log2(1/2) and control LogFC of y = – 1. And, if PNS tissue = 2 and WBC = 1, then LogFC = log2(2/1) and PNS LogFC of y = 1). Should the latter scenario be true, identification of sites for which the methylation patterns are inverted may provide insight into use of WBC for HPA-axis tissue diagnostics. Visual inspection of the MD and MDS plots suggest such polarity between tissues may exist, making levels of hypomethylation in WBC of one group (control or PNS) proportional to hypermethylation of a given tissue in the other group.

After filtering for sites located in promoter regions of genes and with corresponding false discovery rate values of ≤ 0.15, a limited number of differentially methylated sites remained that facilitated closer observation of potential gene expression mechanisms taking place. This left a total of 165 sites in the adrenal cortex, 164 sites in the adrenal medulla, 205 sites in the anterior pituitary, and 134 sites in the paraventricular region of the hypothalamus. It is important to note as well though that several genes were found to have multiple differentially methylated sites in their promoter regions. Genes with multiple CpG sites in their promoter region were treated as preferential for further analysis.

5.4. Genes With Differentially Methylated Sites in Multiple Tissues

Among the more compelling results of this analysis were the number of genes with differentially methylated CpG site(s) in their promoter region that are involved in transcription regulation. Of the top 10 differentially methylated genes for each tissue (37 total), 54% were implicated as having some role in transcription processes. Among those genes involved in transcription is the Fli-1 proto-oncogene, ETS transcription factor (*FLI1*) where multiple differentially methylated CpG sites were found within the adrenal cortex, adrenal medulla, and paraventricular nucleus of the hypothalamus. The *FLI1* gene is a member of the E26 transformation-specific family of transcription factors and has been linked to numerous biological functions related to tumorigenesis as well as immune and inflammatory responses (Wang et al., 2021; Prasad et al., 1992). Dysfunction of *FLI1* also has known involvement in the development of several diseases including various cancers, lupus, systemic sclerosis, and sepsis (Cui et al., 2009; Mathenia et al., 2010; Noda et al., 2014; Wang et al., 2021). Although it is a rare phenomenon, *FLI1* has even been found to be positively expressed in tumor cells of primary Ewing sarcoma or primitive neuroectodermal tumor of the adrenal gland in humans (Zhang et al., 2016). *FLI1* codes for sequence specific DNA binding transcriptional activators and suppression or overexpression of this gene has consequential effects on the genes for which it regulates transcription (Prasad et al., 1992). A specific example from Wang et al. (2021) shows that *FLI1* regulates the expression of granulocyte-macrophage colony-stimulating factor (*GM-CSF*) in T-cells and endothelial cells. Originally identified as a cell differentiation mediator, *GM-CSF* has been observed to rapidly multiply during inflammatory and autoimmune reactions in endothelial cells and is linked to chronic inflammatory conditions as well as different forms of cancer (Becher et al., 2016). An increase in *FLI1* expression is directly linked to increased expression of *GM-CSF* and directly impacts the regulatory responsibilities of *GM-CSF* (Wang et al., 2021).

In the context of the present study, multiple CpG sites in the promoter region of *FLI1* were observed to be differentially methylated in the adrenal cortex, adrenal medulla, and PVN tissues relative to WBC. The prenatally stressed cows were hypomethylated at the *FLI1* promoter region in the adrenal and PVN tissues relative to WBC, while the control cows had the opposite relative methylation. It may be that higher levels of methylation at the promoter site of *FLI1* in WBC correspond with a lower level of methylation of the same site in adrenal and PVN tissues as a result of prenatal stress. Given that both under and overexpression of *FLI1* has associated physiological consequences, the full implications of this differential methylation will require further exploration of the gene's role in HPA-axis function in cattle. Still, it can be speculated that a certain level of *FLI1* methylation occurs naturally to prevent its overexpression, and the consequences of prenatal stress may have led to inadequate methylation of this gene in adrenal and PVN tissues. In lieu of distinct characterization of this gene's specific role in HPA-axis function, *FLI1* does offer a compelling candidate gene for future investigation of differential methylation patterns in these tissues.

Both the meiotic recombination 11 (*MRE11*) gene and the BCL2 like 11 (*BCL2L11*) gene were differentially methylated in both the adrenal medulla and anterior pituitary relative to WBC. In humans, *MRE11* has multiple established roles in telomere maintenance and repair, double strand break repair, DNA damage response, and re-sectioning of broken DNA ends, all of which are critical for maintaining genome stability (Lu et al., 2021). Furthermore, *MRE11* is a member of the *MRE11-RAD50-NBS1* complex which is involved in numerous DNA repair pathways (Bian et al., 2019). Mutations of the *MRE11* gene that result in a lack of expression of this gene are linked to various types of cancers including colorectal cancer and breast cancer (Giannini et al., 2002; Bartkova et al., 2008). Furthermore, non-functioning variants of *MRE11*

have been implicated as causal for Ataxia-Telangiectasia-like disorder. This disorder develops during childhood and is characterized progressive cerebellar degeneration and ionizing radiation hypersensitivity (Stewart et al., 1999). In the present study, *MRE11* was found to be more methylated in both the anterior pituitary and adrenal medulla relative to WBC in the PNS group, and where WBC were more methylated relative to these tissues in the control group. Given the consequential nature of aberrant *MRE11* expression that has been established, increased methylation of this gene, and therefore likely suppressed expression of this gene, may ultimately be harmful to the functionality of these organs, and this may be attributable to the prenatal stress endured by this group of cows. Although extensive evidence for the ramifications of this genes malfunction exists in humans, minimal work has been done to study this gene in other species, and its functionality, or lack thereof, has yet to be defined in cattle.

Conversely, *BCL2L11* was more methylated in WBC than in the adrenal medulla and anterior pituitary of the PNS group, while the opposite was found for the control group. Because of the role of *BCL2L11* in regulation apoptosis in T – and B – cells, increased methylation of this gene in WBC may result in unfavorable health outcomes (Nieters et al., 2012). In humans and in mice, variants leading to reduced expression of *BCL2L11* have a well-established role in lymphomagenesis which often results in cancer related to tissues and organs that produce, store, and transport WBC (Egle et al., 2004; Witzig et al., 2011; Nieters et al., 2012). A study in Indian cattle utilized two native breeds, Tharparkar and a crossbred referred to as Vrindavani, to observe genetic variation related to heat stress tolerance (Khan et al., 2021). Tharparkar is a dairy breed with the greatest heat tolerance, disease resistance, tick resistance, and general hardiness of all other purebred cattle in India (Khan et al., 2021). The crossbred, Vrindavani, is described as having the greatest milk production and reproduction parameters relative to other crossbreds and

purebreds including Tharparkar and was developed by crossing Hariana cows (indigenous to India) with Holstein-Friesian, Brown Swiss and Jersey bulls in different combinations (Khan et al., 2021). Milk production in Vrindavani cattle suffers under antagonistic heat conditions and was therefore used to help identify genetic characteristics of Tharparkar cattle that aid in their heat tolerance (Khan et al., 2021). The *BCL2L11* gene was found to be differentially expressed between the two breeds with upregulation in Vrindavani cattle and downregulation in Tharparkar cattle (Khan et al., 2021). This aligns with observed activation of apoptosis during heat stress, where Tharparkar is ultimately less affected due in part to the downregulation of *BCL2L11* which has an established role in regulating apoptosis (Khan et al., 2021). This information reinforces the consequential nature of abnormal *BCL2L11* expression in not just humans, but also in cattle, and substantiate the genes candidacy for further assessment of DNA methylation patterns that may affect transcription of this gene.

Finally, TERF1 interacting nuclear factor 2 (*TINF2*) was found to be differentially methylated in the adrenal cortex and anterior pituitary. Relative to WBC, *TINF2* showed greater methylation in adrenal cortex and anterior pituitary tissues of the control group, while the opposite was observed in the PNS group. The primary function of *TINF2* is regulation of telomere length, but also has characteristics of a housekeeping gene within its proximal promoter region (Simonsson, 2001). This gene is without a canonical TATA box but is comprised of several GC boxes, which are potential binding sites for ubiquitous transcription factors, and align with its subjection to promoter region methylation in the present study (Simonsson, 2001). Several deleterious and non-functioning mutations of *TINF2* have been identified in humans that are associated with dyskeratosis congenita, which is a disease characterized by pulmonary fibrosis, bone marrow failure, and development of solid tumors (Fukuhara et al., 2013; Hoffman

et al., 2016; Du et al., 2018). Additionally, *TINF2* is particularly well associated with bone marrow failure as well as with aplastic anemia (Du et al., 2018). He et al. (2020) identified a frameshift mutation of *TINF2* in a large family affected with papillary thyroid carcinoma and melanoma. This mutation stifled the ability of *TINF2* to properly bind to telomeric repeat binding factor 2 (*TERF2*) which directly binds to telomeric DNA. Furthermore, telomere length of those with cancer and carrying this mutation was significantly longer than that of the healthy controls and those with the same mutation but without cancer. Abnormal function of *TINF2*, which plays a critical role in shelterin complex and telomere maintenance, is likely impactful in diseases related to apoptosis regulation, as has been shown in previous studies on shelterin genes and the influence of telomere length on cancer risk (Maciejowski and de Lange, 2017; He etl al., 2020). Despite the role of *TINF2* not yet being characterized in cattle, aberrant expression of this gene has been clearly linked to several physiological disorders and may become problematic when methylation patterns deviate from what would be considered normal or expected.

5.4.1. Differentially Methylated Sites in Adrenal Cortex to WBC Comparisons

Another gene coding for transcriptional regulating proteins is Aristaless-like homeobox 3 (*ALX3*) that was also found to be differentially methylated at multiple sites in its promoter region in adrenal cortex tissue compared to WBC. Similar to *FLI1*, *ALX3* was found to be hypomethylated in adrenal cortex tissue and hypermethylated in WBC of the prenatally stressed cows, versus the hypomethylation observed in WBC and hypermethylation of adrenal cortex tissue in the control cows. Based on previous studies investigating *ALX3*, it again may be that hypomethylation of *ALX3* within adrenal cortex tissue is ultimately a consequence of prenatal stress. Qi et al. (2021) showed how overexpression of *ALX3* is causative of overexpression of cell division cycle 25A (*CDC25A*) which regulates cell proliferation and requires a degree of

silencing to inhibit promotion of damaging cells. By way of increased histone H3 trimethylation at lysine 4 (*H3k4me3*) demethylation, *ALX3* positively influenced the transcription of *CDC25A* which resulted in cell cycle progression of cervical cancer. In opposition to these findings however, Wimmer et al. reported in 2002 that preferential methylation of *ALX3* was observed in late-stage neuroblastoma tumors. While both methylation status and regulatory function of *ALX3* have clear consequences, the ramifications of *ALX3* expression are yet to be fully understood particularly in the context of neuroendocrine functions.

Like *FLI1*, another transcription factor that influences expression of *GM-CSF* is the core-binding factor subunit beta (*CBFB*) which was also found to have several differentially methylated sites in its promoter region. This gene has also been implicated in the pathogenesis of cancer cells, specifically breast cancer, and where mutations of this gene or under or overexpression are influential in cancer cell proliferation and survival (Hsu et al., 2022). Consistent with the previously mentioned transcription factors, *CBFB* showed greater methylation in WBC than adrenal cortex tissue in the prenatally stressed group, with greater methylation in adrenal cortex tissue than WBC of the control group. Another gene involved in transcription, whose downregulation has shown to be beneficial in combating the growth of cancer cells, is the proto-oncogene, bHLH transcription factor (*MYCL*) (Qin et al., 2019). The overexpression of *MYCL* has been observed in several different malignancies in humans but is particularly prevalent in gastric cancer cells (Qin et al., 2019; Chen et al., 2015). This gene was also hypomethylated in the adrenal cortex tissue of the prenatally stressed cows. Also following this trend of hypomethylation in the adrenal cortex of prenatally stressed cows, along with evidence of beneficial downregulation, is the AE binding protein 2 (*AEBP2*) gene. Zhang et al. (2019) showed not only how a failure in degradation of the transcription regulator, *AEBP2* is

linked to ovarian cancer cell tumorigenesis, but also how the genetic knockout of *AEBP2* leads to inhibition of ovarian cancer cell proliferation and a greater sensitivity to cisplatin therapeutics.

5.4.2. Differentially Methylated Sites in the Adrenal Medulla to WBC Comparisons

Another member of the ETS transcription family that was differentially methylated in the adrenal medulla to WBC comparisons is the fifth Ewing variant transcription factor, ETS family member (*FEV*). Lui et al. (2017) found that *FEV* was expressed in fetal hematopoietic cells and was necessary for self-renewal of hematopoietic stem cells, but also that *FEV* was silenced after birth. Further testing in this study showed, however, that in pediatric acute lymphoid leukemia and acute myeloid leukemia that *FEV* was expressed in the cancerous cells. In adult, postnatally developed leukemia samples *FEV* was found to rarely be expressed, but almost always expressed in pediatric samples indicating that *FEV* expression in leukemia cells may be of prenatal origin. For further analysis, samples were taken from pediatric leukemia cases from groups of children, teenagers, and young adults. Nearly all samples in children, and all samples from teenagers and young adults tested positive for *FEV* expression. Finally, tests of *FEV* knockout in this study showed how *FEV* silencing impairs leukemia-propagating abilities of leukemic stem cells.

Regarding the present study, *FEV* was more methylated in adrenal medulla tissue than in WBC of the prenatally stressed group, and more methylated in WBC of the control group. Given that both lymphoid leukemia and myeloid leukemia are blood-cell related cancers, as well as the results of Lui et al. (2017), it may be expected that *FEV* would be under expressed in WBC of other adult animals such as cattle. Because prenatal stress is consequential to the adult animal's health, it is possible that repression of *FEV* in WBC was not adequately regulated. Though prenatal conditions were not discussed in the 2017 study from Liu et al., the prenatal origins of pediatric leukemia may have similar underlying mechanisms of a lack of adequate repression of

FEV in WBC. Then *FEV* may have potential as a diagnostic biomarker for evidence of improper prenatal conditions and/or WBC related disease. The role of *FEV* in the adrenal medulla and neuroendocrine function has yet to be defined, so it may also be that this differential methylation can be attributed to functionality of these systems rather than WBC. A rare case of prostatic-carcinoma with neuroendocrine differentiation was found by Febres-Aldana et al. in 2020 in which a fusion of *FEV* with EWS RNA Binding Protein 1 (*EWSR1*) was implicated as the cause. Fusions of transcription factors of the ETS family, for which *FEV* is a member, with *EWSR1* are the source of various cancers that belong to the Ewing family of tumors. In this case the authors were admittedly unsure of a definitive diagnosis due to the ambiguous and unique nature of the phenotype. Therefore, it may still be that *FEV* aberrations within neuroendocrine cells present unfavorable outcomes, but further characterization of this relationship will ultimately be required.

5.4.3. Differentially Methylated Sites in the Anterior Pituitary to WBC Comparisons

In the anterior pituitary, a gene known as meis homeobox 2 (*MEIS2*), encodes for a protein that is a member of the three amino acid loop extension (*TALE*) homebox family which are highly conserved proteins that serve as transcription regulators and have been implicated in numerous functions related to development. In the context of the present study, *MEIS2* was found to be more methylated in WBC of the control group, and more methylated in anterior pituitary tissue of the PNS group. The hypermethylation of *MEIS2* has shown to be consequential in cases of various cancers including thyroid cancer and prostate cancer. Nørgaard et al. (2019) found low *MEIS2* transcriptional expression was significantly associated with poor biochemical recurrence-free survival in three independent radical prostatectomy cohorts. Additionally, Wen et al. (2021) observed significant downregulation of MEIS2 in thyroid cancer

cells, whereas when overexpressed *MEIS2* was shown to inhibit cell proliferation and induce apoptosis of cancerous cells. When under expressed, *MEIS2* has clear consequences; however, this gene's role in HPA-axis function is not yet characterized .

Also differentially methylated in the anterior pituitary is the 4A AT-rich interaction domain (*ARID4A*) which was more methylated in WBC of the control group and more methylated in anterior pituitary tissue of the PNS group. The protein encoded by this gene is a ubiquitously expressed, DNA-binding nuclear protein with transcriptional repression activity (Wu et al., 2013; Zhang et al., 2021; Ren et al., 2022). Both suppression of gene expression and epigenetic imprinting are known functions of *ARID4A*, in addition to likely serving as a tumor suppressor in human prostate and breast cancer (Zhang et al., 2021). With particularly high expression in neuronal cells and the cerebral cortex, this gene is thought to be a critical element for neuronal development and function in humans (Wu et al., 2006; Zhang et al., 2021). This gene also has established imprinting responsibilities, and dysfunction in this role is linked to leukemia and Prader-Willi syndrome (Wu et al., 2006; Zhang et al., 2021). The involvement of *ARID4A* in Prader-Willi syndrome further supports the notion that this gene is part of neuronal development as Prader-Willi syndrome is an imprinted neurodevelopmental disorder (Zhang et al., 2021). Clearly *ARID4A* is important in numerous contexts of human physiology, and the ramifications of aberrant expression are broadly affecting. While limited work has been done regarding this gene and its function in cattle, future research of bovine anterior pituitary genetic function may benefit from particular consideration of this gene.

5.4.4. Differentially Methylated Sites in the PVN to WBC Comparisons

The paraventricular nucleus of the hypothalamus also displayed differential methylation in genes involved with transcription. Specifically, the Interferon regulatory factor 5 (*IRF5*) gene

which is known to be a critical transcription factor for inflammatory and immune responses (Ni et al., 2022). Within this role, *IRF5* is responsible for regulation of proliferation and differentiation of T-cells as well as enhancement of polarization of macrophages towards inflammatory manifestations. This gene has been associated with several autoimmune diseases including lupus in humans and mice, inflammatory bowel disease, and ankylosing spondylitis (AS) (Almuttaqi et al., 2019; Song et al., 2020; Ni et al., 2022). Gene promoter methylation of IRF5 was shown to be lower in patients with AS and was able to identify AS patients from non-AS patients. Alternatively, overexpression and activation were observed in peripheral blood mononuclear cells of patients with systemic lupus, which was supported by mice that were protected from the onset and severity of lupus when lacking *IRF5* (Song et al., 2020). Ultimately these results indicate that aberrant methylation patterns of *IRF5* may serve a critical role in proper immune response regulation of multiple species.

An important and consequential gene that was found to be differentially methylated in the paraventricular nucleus of the hypothalamus is the TATA-box binding protein (*TBP*). This gene is a necessary component for all transcription events in eukaryotes and is thought to function as an assembly platform that recruits general transcription factors, as well as RNA polymerase, for formation of pre-initiation complexes that are suitable for transcription (Hardivillé et al., 2020; Ravarani et al., 2020). Among the consequences associated with dysfunctional TBP includes the reprogramming of cellular metabolism and that results in significant alterations in lipid storage (Hardivillé et al., 2020). Another differentially methylated transcription factor found in the paraventricular nucleus of the hypothalamus to WBC comparisons was the RB transcriptional corepressor like 1 (*RBL1*) gene. This gene is known to operate as a tumor suppressor in epidermal and lung cancer (Lázaro et al., 2019). Specifically, suppression of *RBL1* is linked to

large-cell neuroendocrine cell carcinoma as well as small-cell lung carcinoma, with greater association to large-cell neuroendocrine cell carcinoma (Lázaro et al., 2019). The *RBL1* gene has also shown that hypermethylation in its promoter region results in low expression of its encoded protein which is thought to cause radio-resistance of 3D carcinoma cells (Pan et al., 2017). Both *TBP* and *RBL1* were more methylated in WBC of the control group, but more methylated in the paraventricular nucleus of the hypothalamus in the PNS group.

5.5. Limitations Related to Animal Samples and Procedures

In the present study, one of the main limiting factors is of course sample size, due to the costly nature of obtaining the desired tissue samples which in this case required harvesting of the animals. Additionally, the age at which the cows used in this study were harvested was also limiting as very few other studies exist that allow for comparison, as well as the affecting condition being far removed in time from when the cows were ultimately harvested. Cilkiz et al. (2021) was able to observe the differences between methylation patterns of lymphocytes at 28 days of age in these prenatally stressed cows and compare to methylation patterns of lymphocytes at 5 years of age in the same cows. While certain canonical pathways related to growth and development and nervous system function appeared to maintain differential methylation in the PNS group compared to the control group, differential methylation was also observed in the day 28 WBC vs. the 5-year-old WBC. This suggests that while a degree of differential methylation is maintained into adulthood as a result of prenatal stress, some degree of differential methylation is not maintained and/or patterns can further alter as the animal ages. Nonetheless this study is at least a starting point for better understanding long term methylation changes in mature cattle. Particularly as stress response and HPA-axis function are a critical component of life and therefore influential on production of beef, understanding DNA

methylation changes in adult Brahman cattle is still a significant physiological mechanism that warrants a thorough understanding. Furthermore, DNA methylation has shown to pass between generations which makes observance of these patterns for breeding animals particularly critical (Joo et al., 2018). Transgenerational effects of DNA methylation are just starting to be studied and will likely be a popular target for future epigenetic research (Braunschweig et al., 2012).

Regarding the processing of tissue samples, reduced representation bisulfite sequencing (RRBS) has historically been the most commonly used technique for DNA methylation of cytosine studies (Fraga and Esteller, 2002). While RRBS is cost and resource effective, along with having a narrow scope of analysis that is limited to the bases of interest (CpG sites) that allows for simple library construction (Meissner et al., 2002), this method is not without its limitations. Aside for CpG rich fragments, other methylated genomic regions are excluded from analysis. Additionally, RRBS is unable to differentiate between 5-methylcytosine (5-mC) and 5-hydroxymethylcytosine (5-hmC). More importantly though, RRBS is somewhat inefficient at converting all unmethylated cytosine into uracil, which is the primary mechanism by which methylated cytosine sites are totaled (Fraga and Esteller, 2002). Due to these shortcomings in RRBS analyses, a considerable margin of error must be considered when evaluating results. Several supplementary methods have been developed in response to these challenges, such as Tn5mC-seq, which uses transposase-based in vitro shotgun library construction to assemble complex sequencing libraries from minimally sized DNA fragments (Adey and Shendure, 2012). Additionally, the Post-bisulfite adaptor tagging (PBAT) and terminal deoxyribonucleotidyl transferase (TdT)-assisted adenylate connector-mediated ssDNA (TACS) ligation methods provide improvements to bisulfite sequencing by increasing the number of unamplified reads

from small amounts of DNA through (PBAT) and increases the lengths of library fragments through TACS (Miura et al., 2012).

As technologies and interest in DNA methylation has continued to advance, a demand for bisulfite-free methods became more prevalent. The ten-eleven translocation (TET)-assisted pyridine borane sequencing (TAPS) method was recently described, where detection of modifications with high sensitivity and specificity are achievable without affecting unmethylated cytosines while also preserving DNA fragments of 10 kb or longer (Lui et al., 2020). Evidence showing TAPS as resulting in higher mapping rates, more even coverage, and lower sequencing costs supports this method as being more comprehensive and efficient than previously described methods. This method was further refined for more thorough mapping ability and is referred to as long-read Tet-assisted pyridine borane sequencing (lrTAPS) (Lui et al., 2020).

Furthermore, as an alternative to chemical methods, which can be subject to bias sequencing data, an enzymatic deamination method has also been recently developed. Through a series of enzymatic reactions, enzymatic methyl-seq (EM-seq) is able to detect both 5-mC and 5-hmC (Sun et al., 2021). Initially, the enzymes TET2 and T4-BGT convert 5-mC and 5-hmC into products that can withstand deamination into uracil from the third and final enzyme of the process, APOBEC3A. Moreover, due to its ability to develop libraries from as little as 100 pg of DNA, EM-seq has been shown to outperform bisulfite libraries with better coverage, distribution, sensitivity, and accuracy of cytosine methylation rates (Sun et al., 2021). While RRBS is still a viable and popular method for DNA methylation research, these improved and more refined techniques are worth consideration for future studies of a similar nature.

Another dynamic worth considering for DNA methylation research is that aside from cytosine, the base adenine is also subject to methylation. Adenine admittedly is much lower in

abundance compared to 5-mC which makes it difficult to detect with less sensitive sequencing methods, and therefore has been considered much less by researchers (Wu et al., 2016). Referred to as 6-methyladenosine (6-mA), this modification occurs in both prokaryotes and eukaryotes and performs functions related to restriction modification systems, transcription, transposition, and repair. Originally discovered in bacteria, 6-mA has more recently been shown to have a complex role in eukaryotes which is continually being investigated and better understood. Evidence exists that shows 6-mA's presence in mammalian brain tissue, its presence in gene promoter regions, and its ability to repress gene expression, similar to 5-mC. Particularly as it relates to HPA-axis function, 6-mA's presence in brain tissue may make it also worth prioritizing in future epigenetic research.

5.6. Limitations Related to EdgeR Data and Differentially Methylated Sites

The use of EdgeR is common for RNA sequencing and differential gene expression analyses but is still a relatively new approach for DNA methylation analysis (Chen et al., 2017). For this reason, there are limited published results to compare to at this point. Additionally, differences detected between the control group and PNS group proved to be minimal, and when reported for global methylation between tissues, whatever differences did exist were not well reflected by the results. It is of course also possible that these results are reflective of the minimal changes that persisted between treatment groups, but that conclusion will need to be upheld by further published studies where a phenotype of interest is clearly defined that provides differing results in the control and treatment groups that are able to reflect concordance or discordance of methylation patterns between a tissue of interest and WBC. Furthermore, the use of 5x coverage being controlled at an FDR of ≤ 0.15 may have created too narrow of conditions for the analysis

to strongly reflect patterns between treatment groups. Broader criteria could prove to be more effective for finding and characterizing methylation patterns.

Regarding the evaluation of differentially methylated CpG sites in the promoter region of genes, this idea that methylation may be inversely related between WBC and HPA-axis tissues has not been considered before. The likelihood of this being a true relationship of methylation patterns is contingent on further investigation of these genes and/or these specific sites to either bolster or refute the results presented here. Caveats against over interpretation of results include the sample size of the data, the age of the cows, the degree of induced prenatal stress, the discordance of global methylation patterns, the novelty of the idea that polarity exists within methylation patterns, and other confounding environmental factors. Still, this study does provide an alternative dynamic for consideration of biomarker design and function and creates additional routes to consider for future methylation pattern evaluations.

The existing evidence of tissue specific methylation, while limited in cattle, is substantial in other species, particularly humans, mice, and rats. Consistent patterns, tissues, and genes eligible for targeting remain elusive and challenging to identify. It may also be worth considering that changes in DNA methylation can be affected by environment but may also be more random than has previously been considered. Numerous genes and genomic regions have been implicated in differential methylation studies; however, few have been supported by repeated studies to confirm the relationship. An expected condition, such as some form of prenatal stress, may cause changes in DNA methylation, but that those changes may not necessarily be designated to the same gene or genomic region within DNA of different tissues every time. The degree to which the affecting condition is implemented may also dictate the amount and location of methylation. This may provide an explanation as to why some studies have found high

correspondence in methylation between blood and tissues, while others have not. It is most likely that patterns of DNA methylation are highly nuanced, tissue-specific, species-specific, and possibly even breed-specific, which makes for a challenging mechanism to characterize. What is clear, however, is that DNA methylation is consequential for numerous species and affects numerous physiological functions and is therefore a worthwhile science to continually pursue.

6. CONCLUSION

In summary, global methylation analyses for both the PNS and control groups showed little consistency in terms of WBC methylation pattern correspondence to HPA-axis tissue methylation patterns. While WBC and HPA-axis tissues did consistently show a degree of association across analyses, the global differences between the PNS and control group did not contrast enough to suggest a predictive relationship between WBC and the tissues of interest. For global WBC analysis to be a viable utility for predicting methylation patterns in HPA-axis tissues a defined phenotype or condition must produce a distinct difference when compared to a control group, and where WBC and the tissue of interest reflect this difference consistently with one another.

When comparing HPA-axis tissues to one another, additional insights for methylation pattern changes in the system as a whole were limited. Still, dysfunction of the HPA-axis does not require aberrations of the genome in each tissue to create consequential stress regulation in an adult animal. What can be deduced is that methylation patterns between these tissues are variable, and based on the physiological stress tests induced on these cows at a young age by Littlejohn et al. (2020), and the lasting changes in methylation of the lymphocytes from 28 days of age to 5 years of age in the PNS group by Cilkiz et al. (2021), evidence of dysregulation of HPA-axis function in these cows remains compelling and justifies prenatal stress as an area for concern in cattle production.

The advantage of using a statistical software such as EdgeR for methylation analyses is the illustration of both similar methylation and differential methylation. While consistencies in the data were not able to clearly define a global pattern between WBC and the tissues of interest in the present study, the polarity between samples did offer an alternative dynamic for

investigation of differential methylation. Based on the ratios reflected by the LogFC values, a number of sites were inversely related between WBC and HPA-axis tissues. It may be the case that, as a consequence of prenatal stress, hypomethylation in WBC could reflect hypermethylation in the tissue of interest at that site and vice versa. Although this particular type of relationship has yet to be explored in this context, the mathematical change in the relationship of WBC and tissue methylation between the PNS and control groups is irrefutable, and the genes identified are potentially consequential if subjected to aberrant methylation. Many of the sites identified as having this inverted relationship can be found in the promoter region of genes related to transcription regulation and telomere maintenance. Those genes responsible for transcription regulation may be affected in a manner that reduces or enhances their expression within a given tissue which could result in irregular expression of other genes for which the prior genes are responsible for maintaining. Evidence exists that suggests dysfunction of the transcription factors identified here, as well as dysfunction of the genes responsible for telomere maintenance, has resulted in various physiological malfunctions and have been associated with various forms of cancer in both the tissues of interest and WBC.

Based on the results provided by the present study, the most productive endeavors will likely be targeting methylation and/or expression of specific genes that either have established roles in the proper function of the tissues of interest or have shown some pattern of association between WBC and HPA-axis tissues for which a phenotype or influential condition has been characterized. Genes directly related to the proper function of each tissue may not change in a way that is observable in WBC, and therefore it is proposed that genes such as *FLI1*, *TINF2*, *MRE11*, *BCL2L11*, or any of the others having shown a relationship with WBC in this study, could be useful for focus in future investigations. To rule out WBC as a useful biomarker of

methylation changes in other physiological systems at this point is not necessarily justified, however, adjustments to methodology and strategies for identifying these patterns may ultimately be required to better characterize the predictive value of this relationship.

REFERENCES

Adey, A. and J. Shendure. 2012. Ultra-low-input, tagmentation-based whole-genome bisulfite sequencing. Genome Res. 22(6), 1139 – 1143. DOI: 10.1101/gr.136242.111

Al-Aqtash, R., F. Famoye, and C. Lee. 2015. On generating a new family of distributions using the logit function. J, Probab. Stat., 13(1), 135 – 152.

Altmann, S., E. urani, M. Schwerin, C. C. Metges, K. Wimmers, and S. Ponsuksili. 2012. Maternal dietary protein restriction and excess affects offspring gene expression and methylation of non-SMC subunits of condensin I in liver and skeletal muscle. Epigenetics, 7(3), 239 – 252. DOI: 10.4161/epi.7.3.19183

Almuttaqi, H. and I. A. Udalova. 2019. Advances and challenges in targeting IRF5, a key regulator of inflammation. FEBS J., 286(9), 1624 – 1637. DOI: 10.1111/febs.14654

Åsenius, F., T. J. Gorrie-Stone, A. Brew, Y. Panchbhaya, E. Williamson, L. C. Schalkwyk, V. K. Rakyan, M. L. Holland, S. J. Marzi, and D. J. Williams. 2020. The DNA methylome of human sperm is distinct from blood with little evidence for tissue-consistent obesity associations. PLoS Genet., 16(10), e1009035. DOI: 10.1371/journal.pgen.1009035

Baik, M., T. T. T. Vu, M. Y. Piao, and H. J. Kang. 2014. Association of DNA methylation levels with tissue-specific expression of adipogenic and lipogenic genes in longissimus dorsi muscle of Korean cattle. Asian-Australas. J. Anim. Sci., 27(10), 1493 – 1498. DOI: 10.5713/ajas.2014.14283

Baker, E. C., K. Z. Cilkiz, P. K. Riggs, B. P. Littlejohn, C. R. Long, T. H. Welsh Jr., R. D. Randel, and D. G. Riley. 2020. Effect of prenatal transportation stress on DNA methylation in Brahman heifers. Livest. Sci., 240, 104 – 116. DOI: 10.1016/j.livsci.2020.104116

Bartkova, J., J. Tommiska, L. Oplustilova, K. Aaltonen, A. Tamminen, T. Heikkinen, M. Mistrik, K. Aittomäki, C. Blomqvist, P. Heikkilä, and J. Lukas. 2008. Aberrations of the MRE11–RAD50–NBS1 DNA damage sensor complex in human breast cancer: MRE11 as a candidate familial cancer-predisposing gene. Mol. Oncol., 2(4), 296 – 316. DOI: 10.1016/j.molonc.2008.09.007

Becher, B., S. Tugues, and M. Greter. 2016. GM-CSF: from growth factor to central mediator of tissue inflammation. Immunity, 45(5), 963 – 973. DOI: 10.1016/j.immuni.2016.10.026

Benjamini, Y., and Y. Hochberg. 1995. Controlling the false discovery rate: a practical and powerful approach to multiple testing. J. R. Stat. Soc., Series B (Methodological) 57(1):289 – 300. DOI: 10.1111/j.2517-6161.1995.tb02031.x

Bian, L., Y. Meng, M. Zhang, and D. Li. 2019. MRE11-RAD50-NBS1 complex alterations and DNA damage response: implications for cancer treatment. Molecular Cancer, 18(1), 1 – 14. DOI: 10.1186/s12943-019-1100-5

Bird, A. P. 1986. CpG-rich islands and the function of DNA methylation. Nature, 321(6067), 209 – 213. DOI: 10.1038/321209a0

Bird, A. P. 1993. Functions for DNA methylation in vertebrates. In Cold Spring Harbor Symposia on Quantitative Biology (Vol. 58, pp. 281 – 285). Cold Spring Harbor Laboratory Press. DOI:10.1101/SQB.1993.058.01.033

Bird, A. P., and M. H. Taggart. 1980. Variable patterns of total DNA and rDNA methylation in animals. Nucleic Acids Res, 8(7), 1485 – 1497. DOI: 10.1093/nar/8.7.1485

Braun, P. R., S. Han, B. Hing, Y. Nagahama, L. N. Gaul, J. T. Heinzman, A. J. Grossbach, L. Close, B. J. Dlouhy, M. A. Howard III, H. Kawasaki, J. B. Potash, and G. Shinozaki. 2019. Genome-wide DNA methylation comparison between live human brain and peripheral tissues within individuals. Transl. Psychiatry, 9(1), 1 – 10. DOI: 10.1038/s41398-019-0376y

Braunschweig, M., V. Jagannathan, A. Gutzwiller, and G. Bee. 2012. Investigations on transgenerational epigenetic response down the male line in F2 pigs. PloS one, 7(2), p.e30583. DOI: 10.1371/journal.pone.0030583

Cao-Lei, L., K. N. Dancause, G. Elgbeili, R. Massart, M. Szyf, A. Liu, D. P. Laplante and S. King. 2015. DNA methylation mediates the impact of exposure to prenatal maternal stress on BMI and central adiposity in children at age 13½ years: Project Ice Storm. Epigenetics, 10(8), 749 – 761. DOI: 10.1080/15592294.2015.1063771

Cao-Lei, L., R. Massart, M. J. Suderman, Z. Machnes, G. Elgbeili, D. P. Laplante, M. Szyf, and S. King. 2014. DNA methylation signatures triggered by prenatal maternal stress exposure to a natural disaster: Project Ice Storm. PloS one. 9(9), e107653. DOI: 10.1371/journal.pone.0107653

Cao-Lei, L., S. R. De Rooij, S. King, S. G. Matthews, G. A. S. Metz, T. J. Roseboom, and M. Szyf. 2020. Prenatal stress and epigenetics. Neurosci. Biobehav. Rev. 117, 198 – 210. DOI: 10.1016/j.neubiorev.2017.05.016

Carroll, J. A. and N. E. Forsberg. 2007. Influence of stress and nutrition on cattle immunity. Vet. Clin. North Am. Food Anim. Pract., 23(1), 105 – 149. DOI: 10.1016/j.cvfa.2007.01.003

Chadio, S., B. Kotsampasi, S. Taka, E. Liandris, N. Papadopoulos, and E. Plakokefalos. 2017. Epigenetic changes of hepatic glucocorticoid receptor in sheep male offspring undernourished in utero. Reprod. Fertil. Dev., 29(10), 1995 – 2004. DOI: 10.1071/RD16276

Changyong, F. E. N. G., W. A. N. G. Hongyue, L. U. Naiji, C. H. E. N. Tian, H. E. Hua, and L. U. Ying. 2014. Log-transformation and its implications for data analysis. Shanghai Arch. Psychiatry, 26(2), 105 – 109. DOI:10.3969/j.issn.1002-0829.2014.02.009

Charil, A., D. P. Laplante, C. Vaillancourt, and S. King. 2010. Prenatal stress and brain development. Brain Res. Rev., 65(1), 56 – 79. DOI: 10.1016/j.brainresrev.2010.06.002

Chen, S., J. Tang, L. Huang, and J. Lin. 2015. Expression and prognostic value of Mycl1 in gastric cancer. Biochem. Biophys. Res. Commun., 456(4), 879 – 883. DOI: 10.1016/j.bbrc.2014.12.060

Chen, Y., A. T. Lun, and G. K. Smyth. 2016. From reads to genes to pathways: differential expression analysis of RNA-Seq experiments using Rsubread and the edgeR quasi-likelihood pipeline. F1000Research, 5.DOI: 10.12688/f1000research.8987.2

Chen, Y., B. Pal, J. E. Visvader, and G. K. Smyth. 2017. Differential methylation analysis of reduced representation bisulfite sequencing experiments using edgeR. F1000Research, 6.

Cheong, A., S. A. Johnson, E. C. Howald, M. R. Ellersieck, L. Camacho, S. M. Lewis, M. M. Vanlandingham, J. Ying, S. M. Ho, and C. S. Rosenfeld. 2018. Gene expression and DNA methylation changes in the hypothalamus and hippocampus of adult rats developmentally exposed to bisphenol A or ethinyl estradiol: a CLARITY-BPA consortium study. Epigenetics, 13(7), 704 – 720. DOI: 10.1080/15592294.2018.1497388

Cilkiz, K. Z., E. C. Baker, P.K. Riggs, B. P. Littlejohn, C. R. Long, T. H. Welsh Jr., R. D. Randel, and D. G. Riley. 2021. Genome-wide DNA methylation alteration in prenatally stressed

Brahman heifer calves with the advancement of age. Epigenetics, 16(5), 519 – 536. DOI: 10.1080/15592294.2020.1805694

Coe, C. L., M. Kramer, B. Czéh, E. Gould, A. J. Reeves, C. Kirschbaum, and E. Fuchs. 2003. Prenatal stress diminishes neurogenesis in the dentate gyrus of juvenile rhesus monkeys. Biol. Psychiatry, 54(10), 1025 – 1034. DOI: 10.1016/S0006-3223(03)00698-X

Cui, J. W., L. M. Vecchiarelli-Federico, Y. J. Li, G. J. Wang, and Y. Ben-David. 2009. Continuous Fli-1 expression plays an essential role in the proliferation and survival of F-MuLV-induced erythroleukemia and human erythroleukemia. Leukemia, 23(7), 1311 – 1319. DOI: doi.org/10.1038/leu.2009.20

Couret, D., A. Jamin, G. Kuntz-Simon, A. Prunier, and E. Merlot. 2009. Maternal stress during late gestation has moderate but long-lasting effects on the immune system of the piglets. Vet. Immunol. Immunopathol., 131(1-2), 17 – 24. DOI: 10.1016/j.vetimm.2009.03.003

Davis, E. P., L. M. Glynn, F. Waffarn, and C. A. Sandman. 2011. Prenatal maternal stress programs infant stress regulation. J. Child Psychol. Psychiatry, 52(2), 119 – 129. DOI: 10.1111/j.1469-7610.2010.02314.x

Du, H., Y. Guo, D. Ma, K. Tang, D. Cai, Y. Luo, and C. Xie. 2018. A case report of heterozygous TINF2 gene mutation associated with pulmonary fibrosis in a patient with dyskeratosis congenita. Medicine, 97(19), e0724. DOI: 10.1097/MD.0000000000010724

Duthie, L. and R. M. Reynolds. 2013. Changes in the maternal hypothalamic-pituitary-adrenal axis in pregnancy and postpartum: influences on maternal and fetal outcomes. Neuroendocrinology, 98(2), 106 – 115. DOI: 10.1159/000354702

Ebrahimi, P., H. Luthman, F. E. McGuigan, and K. E. Akesson. 2021. Epigenome-wide cross-tissue correlation of human bone and blood DNA methylation–can blood be used as a surrogate for bone? Epigenetics, 16(1), 92 – 105. DOI: 10.1080/15592294.2020.1788325

Egle, A., A. W. Harris, P. Bouillet, and S. Cory. 2004. Bim is a suppressor of Myc-induced mouse B cell leukemia. Proc. Natl. Acad. Sci., 101(16), 6164 – 6169. DOI: 10.1073/pnas.040147110

Ehrlich, M. and R. Y. H. Wang. 1981. 5-Methylcytosine in eukaryotic DNA. Science, 212(4501), 1350 – 1357. DOI: 10.1126/science.6262918

Estanislau, C. and S. Morato. 2005. Prenatal stress produces more behavioral alterations than maternal separation in the elevated plus-maze and in the elevated T-maze. Behav. Brain Res., 163(1), 70 – 77. DOI: 10.1016/j.bbr.2005.04.003

Ewald, E. R., G. S. Wand, F. Seifuddin, X. Yang, K. L. Tamashiro, J. B. Potash, P. Zandi, and R. S. Lee. 2014. Alterations in DNA methylation of Fkbp5 as a determinant of blood–brain correlation of glucocorticoid exposure. Psychoneuroendocrinology, 44, 112 – 122. DOI: 10.1016/j.psyneuen.2014.03.003

Febres-Aldana, C. A., K. Krishnamurthy, R. Delgado, J. Kochiyil, R. Poppiti, and A. M. Medina. 2020. Prostatic carcinoma with neuroendocrine differentiation harboring the EWSR1-FEV fusion transcript in a man with the WRN G327X germline mutation: A new variant of prostatic carcinoma or a member of the Ewing sarcoma family of tumors? Pathol. Res. Pract., 216(2), 152758. DOI: 10.1016/j.prp.2019.152758

Federation of Animal Science Societies (FASS). 2010. Guide for the care and use of agricultural animals in research and teaching. 3rd ed. FASS, Champaign, IL.

Feng, H., K. N. Conneely, and H. Wu. 2014. A Bayesian hierarchical model to detect differentially methylated loci from single nucleotide resolution sequencing data. Nucleic Acids Res., 42(8), e69 – e69. DOI: 10.1093/nar/gku154

Fike, K. and M. F. Spire. 2006. Transportation of cattle. Vet. Clin. North Am. Food Anim. Pract, 22(2), 305 – 320. DOI: 10.1016/j.cvfa.2006.03.012

Fraga, M. F. and M. Esteller. 2002. DNA methylation: a profile of methods and applications. Biotechniques, 33(3), 632 – 649. DOI: 10.2144/02333rv01

Fukuhara, A., Y. Tanino, T. Ishii, Y. Inokoshi, K. Saito, N. Fukuhara, S. Sato, J. Saito, T. Ishida, H. Yamaguchi, and M. Munakata. 2013. Pulmonary fibrosis in dyskeratosis congenita with TINF2 gene mutation. Eur. Respir. J., 42(6), 1757 – 1759. DOI: 10.1183/09031936.00149113

Gardiner-Garden, M. and M. Frommer. 1987. CpG islands in vertebrate genomes. J. Mol. Biol., 196(2), 261 – 282. DOI: 10.1016/0022-2836(87)90689-9

Giannini, G., E. Ristori, F. Cerignoli, C. Rinaldi, M. Zani, A. Viel, L. Ottini, M. Crescenzi, S. Martinotti, M. Bignami, and L. Frati. 2002. Human MRE11 is inactivated in mismatch repair-deficient cancers. EMBO Rep., 3(3), 248 – 254. DOI: 10.1093/embo-reports/kvf044

Glover, V., 2015. Prenatal stress and its effects on the fetus and the child: possible underlying biological mechanisms. In Perinatal programming of neurodevelopment (269 – 283). Springer, New York, NY. DOI: 10.1007/978-1-4939-1372-5_13

Guo, Y., T. Van Schaik, N. Jhamat, A. Niazi, M. Chanrot, G. Charpigny, J. F. Valarcher, E. Bongcam-Rudloff, G. Andersson, and P. Humblot. 2019. Differential gene expression in bovine endometrial epithelial cells after challenge with LPS; specific implications for genes involved in embryo maternal interactions. PloS one, 14(9), e0222081. DOI: 10.1371/journal.pone.0222081

Hannon, E., G. Mansell, E. Walker, M. F. Nabais, J. Burrage, A. Kepa, J. Best-Lane, A. Rose, S. Heck, T. Moffitt, A. Caspi, L. Arseneault and J. Mill. 2021. Assessing the co-variability of DNA methylation across peripheral cells and tissues: Implications for the interpretation of findings in epigenetic epidemiology. PLoS genetics, 17(3), e1009443. DOI: 10.1371/journal.pgen.1009443

Hardivillé, S., P. S. Banerjee, E. S. S. Alpergin, D. M. Smith, G. Han, J. Ma, C. C. Talbot Jr, P. Hu, M. J. Wolfgang, and G. W. Hart. 2020. TATA-box binding protein O-GlcNAcylation at T114 regulates formation of the B-TFIID complex and is critical for metabolic gene regulation. Mol. Cell, 77(5), 1143 – 1152. DOI: 10.1016/j.molcel.2019.11.022

Harris, A. R., D. Nagy-Szakal, N. Pedersen, A. Opekun, J. Bronsky, P. Munkholm, C. Jespersgaard, P. Andersen, B. Melegh, G. Ferry, T. Jess, and R. Kellermayer. 2012. Genome-wide peripheral blood leukocyte DNA methylation microarrays identified a single association with inflammatory bowel diseases. IBD., 18(12), 2334 – 2341. DOI: 10.1002/ibd.22956

Harris, C. J., B. A. Davis, J. A. Zweig, K. A. Nevonen, J. F. Quinn, L. Carbone, and N. E. Gray. 2020. Age-associated DNA methylation patterns are shared between the hippocampus and peripheral blood cells. Front. genet, 11, 111. DOI: 10.3389/fgene.2020.00111

He, H., W. Li, D. F. Comiskey, S. Liyanarachchi, T. T. Nieminen, Y. Wang, K. E. DeLap, P. Brock, and A. de la Chapelle. 2020. A truncating germline mutation of TINF2 in individuals with thyroid cancer or melanoma results in longer telomeres. Thyroid, 30(2), 204 – 213. DOI: 10.1089/thy.2019.0156

Hoffman, T. W., J. J. Van der Vis, M. F. M. van Oosterhout, H. W. Van Es, D. A. Van Kessel, J. C. Grutters, and C. H. M. van Moorsel. 2016. TINF2 gene mutation in a patient with pulmonary fibrosis. Case Rep. Pulmonol., 2016, 1310862. DOI: 10.1155/2016/1310862

Horvath, S., Y. Zhang, P. Langfelder, R. S. Kahn, M. P. Boks, K. van Eijk, L. H. van den Berg, R. A. Ophoff. 2012. Aging effects on DNA methylation modules in human brain and blood tissue. Genome Biol., 13(10), 1 – 18. DOI: 10.1186/gb-2012-13-10-r97

Huang, Y. T., S. Chu, E. B. Loucks, C. L. Lin, C.B. Eaton, S. L. Buka, and K. T. Kelsey. 2016. Epigenome-wide profiling of DNA methylation in paired samples of adipose tissue and blood. Epigenetics, 11(3), 227 – 236. DOI: 10.1080/15592294.2016.1146853

Hsu, C. H., H. P. Ma, J. R. Ong, M. S. Hsieh, V. K. Yadav, C. T. Yeh, T. Y. Chao, W. H. Lee, W. C. Huang, K. T. Kuo, and I. H. Fong. 2022. Cancer-Associated Exosomal CBFB Facilitates the Aggressive Phenotype, Evasion of Oxidative Stress, and Preferential Predisposition to Bone Prometastatic Factor of Breast Cancer Progression. Disease markers, 2022. DOI: 10.1155/2022/844662

Jin, Y. 2020. Blood DNA methylation as a surrogate epigenetic biomarker in study of night shift work and breast cancer (Doctoral dissertation, Yale University).

Jin, C., Y. Zhuo, J. Wang, Y. Zhao, Y. Xuan, D. Mou, H. Liu, P. Zhou, Z. Fang, L. Che, and S. Xu. 2018. Methyl donors dietary supplementation to gestating sows diet improves the growth rate of offspring and is associating with changes in expression and DNA methylation of insulin-like growth factor-1 gene. Journal of animal physiology and animal nutrition, 102(5), 1340 – 1350. DOI: 10.1111/jpn.12933

Joo, J. E., J. G. Dowty, R. L. Milne, E. M. Wong, P. A. Dugué, D. English, J. L. Hopper, D. E. Goldgar, G. G. Giles, and M. C. Southey. 2018. Heritable DNA methylation marks associated with susceptibility to breast cancer. Nat. Commun., 9(1), 1 – 12. DOI: 10.1038/s41467-018-03058-6

Kapoor, A., S. Petropoulos, and S. G. Matthews. 2008. Fetal programming of hypothalamic–pituitary–adrenal (HPA) axis function and behavior by synthetic glucocorticoids. Brain Res. Rev., 57(2), 586 – 595. DOI: 10.1016/j.brainresrev.2007.06.013

Khan, R. I. N., A. R. Sahu, W. A. Malla, M. R. Praharaj, N. Hosamani, S. Kumar, S. Gupta, S. Sharma, A. Saxena, A. Varshney, and P. Singh. 2021. Systems biology under heat stress in Indian cattle. Gene, 805, 145908. DOI: 10.1016/j.gene.2021.145908

Korneliussen, T. S., A. Albrechtsen, and R. Nielsen. 2014. ANGSD: analysis of next generation sequencing data. BMC Bioinform., 15(1), 1 – 13. DOI: 10.1186/s12859-014-0356-4

Kundakovic, M., K. Gudsnuk, J. B. Herbstman, D. Tang, F. P. Perera, and F. A. Champagne. 2014. DNA methylation of BDNF as a biomarker of early-life adversity. PNAS, 112(22), 6807 – 6813. DOI: 10.1073/pnas.1408355111

Lay Jr, D. C., R. D. Randel, T. H. Friend, J. A. Carroll, T. H. Welsh, Jr., O. C. Jenkins, D. A. Neuendorff, D. M. Bushong, and G. M. Kapp. 1997a. Effects of prenatal stress on the fetal calf. Domest. Anim. Endocrinol. 14, 73 – 80. DOI:10.1016/S0739-7240(96)00115-4.

Lay Jr, D. C., R. D. Randel, T. H. Friend, O. C. Jenkins, D. A. Neuendorff, D. M. Bushong, E. K. Lanier, and M. K. Bjorge. 1997b. Effects of prenatal stress on suckling calves. J. Anim. Sci., 75(12), 3143 – 3151. DOI: 10.2527/1997.75123143x

Lay Jr, D. C., T. H. Friend, R. D. Randel, O. C. Jenkins, D. A. Neuendorff, G. M. Kapp, and D. M. Bushong. 1996. Adrenocorticotropic hormone dose response and some physiological effects of transportation on pregnant Brahman cattle. J. Anim. Sci., 74(8), 1806 – 1811. DOI: 10.2527/1996.7481806x

Lázaro, S., M. Pérez-Crespo, C. Lorz, A. Bernardini, M. Oteo, A. B. Enguita, E. Romero, P. Hernández, L. Tomás, M. A. Morcillo, and J. M. Paramio. 2019. Differential development of large-cell neuroendocrine or small-cell lung carcinoma upon inactivation of 4 tumor suppressor genes. Proc. Natl. Acad. Sci., 116(44), 22300 – 22306. DOI: 10.1073/pnas.1821745116

Lee, C. J., H. Ahn, D. Jeong, M. Pak, J. H. Moon, and S. Kim. 2020. Impact of mutations in DNA methylation modification genes on genome-wide methylation landscapes and downstream gene activations in pan-cancer. BMC Med. Genet., 13(3), 1 – 14. DOI:10.1186/s12920-020-0659-4

Lemaire, V., S. Lamarque, M. Le Moal, P. V. Piazza, and D. N. Abrous. 2006. Postnatal stimulation of the pups counteracts prenatal stress-induced deficits in hippocampal neurogenesis. Biol. Psychiatry, 59(9), 786 – 792. DOI: 10.1016/j.biopsych.2005.11.009

Li, L., J. Y. Choi, K. M. Lee, H. Sung, S. K. Park, I. Oze, K. F. Pan, W. C. You, Y. X. Chen, J. Y. Fang, K. Matsuo, W. H. Kim, Y. Yuasa, and D. Kang. 2012. DNA methylation in

peripheral blood: a potential biomarker for cancer molecular epidemiology. J. Epidemiol., 22(5), 384 – 394. DOI: 10.2188/jea.JE20120003

Littlejohn, B. P., D. M. Price, J. P. Banta, A. W. Lewis, D. A. Neuendorff, J. A. Carroll, R. C. Vann, T. H. Welsh Jr, and R. D. Randel. 2016. Prenatal transportation stress alters temperament and serum cortisol concentrations in suckling Brahman calves. J. Anim. Sci., 94(2), 602 – 609. DOI: 10.2527/jas.2015-9635

Littlejohn, B. P., D. M. Price, D. A. Neuendorff, J. A. Carroll, R. C. Vann, P. K. Riggs, D. G. Riley, C. R. Long, T. H. Welsh Jr., and R. D. Randel. 2018. Prenatal transportation stress alters genome-wide DNA methylation in suckling Brahman bull calves. J. Anim. Sci., 96(12), 5075 – 5099. DOI: 10.1093/jas/sky350

Littlejohn, B. P., D. M. Price, D. A. Neuendorff, J. A. Carroll, R. C. Vann, P. K. Riggs, D. G. Riley, C. R. Long, R. D. Randel, and T. H. Welsh Jr. 2020. Influence of prenatal transportation stress-induced differential DNA methylation on the physiological control of behavior and stress response in suckling Brahman bull calves. J. Anim. Sci., 98(1), p.skz368. DOI: 10.1093/jas/skz368

Liu, T. H., Y. J. Tang, Y. Huang, L. Wang, X. L. Guo, J. Q. Mi, L. G. Liu, H. Zhu, Y. Zhang, L. Chen, and X. Liu. 2017. Expression of the fetal hematopoiesis regulator FEV indicates leukemias of prenatal origin. Leukemia, 31(5), 1079 – 1086. DOI: 10.1038/leu.2016.313

Lu, R., H. Zhang, Y. N. Jiang, Z. Q. Wang, L. Sun, and Z. W. Zhou. 2021. Post-Translational Modification of MRE11: Its Implication in DDR and Diseases. Genes, 12(8), 1158. DOI: 10.3390/genes12081158

Ma, B., E. H. Wilker, S. A. Willis-Owen, H. M. Byun, K. C. Wong, V. Motta, A. A. Baccarelli, J. Schwartz, W. O. C. M. Cookson, K Khabbaz, M. A. Mittleman, M. F. Moffatt, and Liang, L. 2014. Predicting DNA methylation level across human tissues. Nucleic Acids Res., 42(6), 3515 – 3528. DOI: 10.1093/nar/gkt1380

Maciejowski, J. and T. de Lange. 2017. Telomeres in cancer: tumour suppression and genome instability. Nat. Rev. Mol. Cell Biol., 18(3), 175 – 186. DOI: 10.1038/nrm.2016.171

Masliah, E., W. Dumaop, D. Galasko, and P. Desplats. 2013. Distinctive patterns of DNA methylation associated with Parkinson disease: identification of concordant epigenetic changes in brain and peripheral blood leukocytes. Epigenetics, 8(10), 1030 – 1038. DOI: 10.4161/epi.25865

Mathenia, J., E. Reyes-Cortes, S. Williams, I. Molano, P. Ruiz, D. K. Watson, G. S. Gilkeson, and X. K. Zhang. 2010. Impact of Fli-1 transcription factor on autoantibody and lupus nephritis in NZM2410 mice. Clin. Exp. Immunol., 162(2), 362 – 371. DOI: 10.1111/j.1365-2249.2010.04245.x

McCarthy, D. J., Y. Chen, and G. K. Smyth. 2012. Differential expression analysis of multifactor RNA-Seq experiments with respect to biological variation. Nucleic Acids Res., 40(10), 4288 – 4297. DOI: 10.1093/nar/gks042

Meaney, M. J. and M. Szyf. 2022. Environmental programming of stress responses through DNA methylation: life at the interface between a dynamic environment and a fixed genome. Dialogues Clin. Neurosci., 7(2), 103 – 123. DOI: 10.31887/DCNS.2005.7.2/mmeaney

Meissner, A., A. Gnirke, G. W. Bell, B. Ramsahoye, E. S. Lander, and R. Jaenisch. 2005. Reduced representation bisulfite sequencing for comparative high-resolution DNA methylation analysis. Nucleic Acids Res., 33(18), 5868 – 5877. DOI: 10.1093/nar/gki901

Miura, F., Y. Enomoto, R. Dairiki, and T. Ito. 2012. Amplification-free whole-genome bisulfite sequencing by post-bisulfite adaptor tagging. Nucleic Acids Res. 40(17), e136 – e136. DOI: 10.1093/nar/gks454

Morley-Fletcher, S., M. Rea, S. Maccari, and G. Laviola. 2003. Environmental enrichment during adolescence reverses the effects of prenatal stress on play behaviour and HPA-axis reactivity in rats. Eur. J. Neurosci., 18(12), 3367 – 3374. DOI: 10.1111/j.1460-9568.2003.03070.x

Nemoda, Z., and M. Szyf. 2017. Epigenetic alterations and prenatal maternal depression. Birth Defects Res. 109(12), 888 – 897. DOI: 10.1002/bdr2.1081

Ni, M., Y. Chen, X. Sun, Y. Deng, X. Wang, T. Zhang, Y. Wu, L. Yu, S. Xu, H. Yu, and Z. Shuai. 2022. DNA methylation and transcriptional profiles of IRF5 gene in ankylosing spondylitis: A case-control study. Int. Immunopharmacol., 110, 109033. DOI: 10.1016/j.intimp.2022.109033

Nieters, A., L. Conde, S. L. Slager, A. Brooks-Wilson, L. Morton, D. R. Skibola, A. J. Novak, J. Riby, S. M. Ansell, E. Halperin, and T. D. Shanafelt. 2012. PRRC2A and BCL2L11 gene variants influence risk of non-Hodgkin lymphoma: results from the InterLymph consortium. Am. J. Hematol., 120(23), 4645 – 4648. DOI: 10.1182/blood-2012-05-427989

Noda, S., Y. Asano, S. Nishimura, T. Taniguchi, K. Fujiu, I. Manabe, K. Nakamura, T. Yamashita, R. Saigusa, K. Akamata, and T. Takahashi. 2014. Simultaneous downregulation of KLF5 and Fli1 is a key feature underlying systemic sclerosis. Nat. Commun., 5(1), 1 – 17. DOI: 10.1038/ncomms6797

Nørgaard, M., C. Haldrup, M. T. Bjerre, S. Høyer, B. Ulhøi, M. Borre, and K. D. Sørensen. 2019. Epigenetic silencing of MEIS2 in prostate cancer recurrence. Clin. Epigenetics, 11(1), 1 – 14. DOI: 10.1186/s13148-019-0742-x

Pan, D., Y. Chen, Y. Du, Z. Ren, X. Li, and B. Hu. 2017. Methylation of promoter of RBL1 enhances the radioresistance of three dimensional cultured carcinoma cells. Oncotarget, 8(3), 4422 – 4435. DOI: 10.18632/oncotarget.12647

Prasad, D. D. K., V. N. Rao, E. Shyam, and P. Reddy. 1992. Structure and expression of human Fli-1 gene. Cancer Res., 52(20), 5833 – 5837.

Price, D. M., A. W. Lewis, D. A. Neuendorff, J. A. Carroll, N. C. Burdick Sanchez, R. C. Vann, T. H. Welsh Jr, and R. D. Randel. 2015. Physiological and metabolic responses of gestating Brahman cows to repeated transportation. J. Anim. Sci., 93(2), 737 – 745. DOI: 10.2527/jas.2013-7508

Qi, J., L. Zhou, D. Li, J. Yang, H. Wang, H. Cao, Y. Huang, Z. Zhang, L. Chang, C. Zhu, and J. Zhan. 2021. Oncogenic role of ALX3 in cervical cancer cells through KDM2B-mediated histone demethylation of CDC25A. BMC cancer, 21(1), 1 – 15. DOI: 10.1186/s12885-021-08552-7

Qin, P., H. Wang, F. Zhang, Y. Huang, and S. Chen. 2019. Targeted silencing of MYCL1 by RNA interference inhibits migration and invasion of MGC-803 gastric cancer cells. Cell Biochem. Funct., 37(4), 266 – 272. DOI: 10.1002/cbf.3395

Ravarani, C. N., T. Flock, S. Chavali, M. Anandapadamanaban, M. Babu, and S. Balaji. 2020. Molecular determinants underlying functional innovations of TBP and their impact on transcription initiation. Nat. Commun., 11(1), 1 – 16. DOI: 10.1038/s41467-020-16182-z

Ren, D., X. Wei, Y. Lin, F. Yuan, Y. Bi, Z. Guo, L. Liu, L. Ji, X. Yang, K. Han, and F. Yang. 2022. A novel heterozygous missense variant of the ARID4A gene identified in Han Chinese families with schizophrenia-diagnosed siblings that interferes with DNA-binding activity. Mol. Psychiatry 27(6), 2777 – 2786. DOI: 10.1038/s41380-022-01530-w

Ritchie, M. E., B. Phipson, D. I. Wu, Y. Hu, C. W. Law, W. Shi, and G. K. Smyth. 2015. limma powers differential expression analyses for RNA-sequencing and microarray studies. Nucleic Acids Res., 43(7), e47. DOI: doi.org/10.1093/nar/gkv007

Robertson, K. D. 2005. DNA methylation and human disease. Nat. Rev. Genet., 6(8), 597 – 610. DOI: 10.1038/nrg1655

Robinson, M. D., D. J. McCarthy, and G. K. Smyth. 2010. edgeR: a Bioconductor package for differential expression analysis of digital gene expression data. Bioinformatics, 26(1), 139 – 140. DOI: 10.1093/bioinformatics/btp616.

Rosen, B. D., D. M. Bickhart, R. D. Schnabel, S. Koren, C. G. Elsik, E. Tseng, T. N. Rowan, W. Y. Low, A. Zimin, C. Couldrey, and R. Hall. 2020. De novo assembly of the cattle reference genome with single-molecule sequencing. Gigascience, 9(3), giaa021. DOI: 10.1093/gigascience/giaa021

Schurch, N. J., P. Schofield, M. Gierliński, C. Cole, A. Sherstnev, V. Singh, N. Wrobel, K. Gharbi, G. G. Simpson, T. Owen-Hughes, and M. Blaxter. 2016. How many biological replicates are needed in an RNA-seq experiment and which differential expression tool should you use? RNA, 22(6), 839 – 851. DOI: 10.1261/rna.053959.115

Schommer, N. C., D. H. Hellhammer, and C. Kirschbaum. 2003. Dissociation between reactivity of the hypothalamus-pituitary-adrenal axis and the sympathetic-adrenal-medullary system to repeated psychosocial stress. Psychosom. Med., 65(3), 450 – 460. DOI: 10.1097/01.PSY.0000035721.12441.17

Seckl, J.R. 2007. Glucocorticoids, developmental ‘programming’and the risk of affective dysfunction. Prog. Brain Res., 167, 17 – 34. DOI: 10.1016/S0079-6123(07)67002-2

Shen, Y., S. Zhou, X. Zhao, H. Li, and J. Sun. 2020. Characterization of genome-wide DNA methylation and hydroxymethylation in mouse arcuate nucleus of hypothalamus during puberty process. Front. Genet., 11, 626536. DOI: 10.3389/fgene.2020.626536

Shutoh, Y., M. Takeda, R. Ohtsuka, A. Haishima, S. Yamaguchi, H. Fujie, Y. Komatsu, K. Maita, and T. Harada. 2009. Low dose effects of dichlorodiphenyltrichloroethane (DDT) on gene transcription and DNA methylation in the hypothalamus of young male rats: implication of hormesis-like effects. J. Toxicol. Sci., 34(5), 469 – 482. DOI: 10.2131/jts.34.469

Song, F., J. F. Smith, M. T. Kimura, A. D. Morrow, T. Matsuyama, H. Nagase, and W. A. Held. 2005. Association of tissue-specific differentially methylated regions (TDMs) with differential gene expression. PNAS, 102(9), 3336 – 3341. DOI: 10.1073/pnas.0408436102

Song, S., S. De, V. Nelson, S. Chopra, M. LaPan, K. Kampta, S. Sun, M. He, C. D. Thompson, D. Li, and T. Shih. 2020. Inhibition of IRF5 hyperactivation protects from lupus onset and severity. J. Clin. Investig., 130(12), 6700 – 6717. DOI: 10.1172/JCI120288

Sosnowski, D. W., C. Booth, T. P. York, A. B. Amstadter, and W. Kliewer. 2018. Maternal prenatal stress and infant DNA methylation: a systematic review. Dev. Psychobiol. 60(2), 127 – 139. DOI: 10.1002/dev.21604

Stewart, G. S., R. S. Maser, T. Stankovic, D. A. Bressan, M. I. Kaplan, N. G. Jaspers, A. Raams, P. J. Byrd, J. H. Petrini, and A. M. R. Taylor. 1999. The DNA double-strand break repair gene hMRE11 is mutated in individuals with an ataxia-telangiectasia-like disorder. Cell, 99(6), 577 – 587. DOI: 10.1016/S0092-8674(00)81547-0

Sun, Z., R. Vaisvila, L. M. Hussong, B. Yan, C. Baum, L. Saleh, M. Samaranayake, S. Guan, N. Dai, I. R. Corrêa, and S. Pradhan. 2021. Nondestructive enzymatic deamination enables single-molecule long-read amplicon sequencing for the determination of 5-methylcytosine and 5-hydroxymethylcytosine at single-base resolution. Genome Res. 31(2), 291 – 300. DOI: 10.1101/gr.265306.120

Svoboda, L.K., K. Neier, K. Wang, R. G. Cavalcante, C. A. Rygiel, Z. Tsai, T. R. Jones, S. Liu, J. M. Goodrich, C. Lalancette, and J. A. Colacino, M. A. Sartor, and D. C. Dolinoy. 2021. Tissue and sex-specific programming of DNA methylation by perinatal lead exposure: implications for environmental epigenetics studies. Epigenetics, 16(10), 1102 – 1122. DOI: 10.1080/15592294.2020.1841872

Tao, S., A. P. A. Monteiro, I. M. Thompson, M. J. Hayen, and G. E. Dahl. 2012. Effect of late-gestation maternal heat stress on growth and immune function of dairy calves. J. Dairy Sci., 95(12), 7128 – 7136. DOI: 10.3168/jds.2012-5697

Thompson, R. P., E. Nilsson, M. K. and Skinner. 2020. Environmental epigenetics and epigenetic inheritance in domestic farm animals. Anim. Reprod. Sci., 220, 106316. DOI: 10.1016/j.anireprosci.2020.106316Get

Tuchscherer, M., E. Kanitz, W. Otten, and A. Tuchscherer. 2002. Effects of prenatal stress on cellular and humoral immune responses in neonatal pigs. Vet. Immunol. Immunopathol., 86(3-4), 195 – 203. DOI: 10.1016/S0165-2427(02)00035-1

Vidal, A.C., S. E. B. Neelon, Y. Liu, A. M. Tuli, B. F. Fuemmeler, C. Hoyo, A. P. Murtha, Z. Huang, J. Schildkraut, F. Overcash, and J. Kurtzberg. 2014. Maternal stress, preterm birth, and DNA methylation at imprint regulatory sequences in humans. Genet. Epigenetics. 6, GEG-S18067. DOI: 10.4137/GEG.S18067

Walton, E., J. Hass, J. Liu, J. L. Roffman, F. Bernardoni, V. Roessner, M. Kirsch, G. Schackert, V. Calhoun, and S. Ehrlich. 2016. Correspondence of DNA methylation between blood and brain tissue and its application to schizophrenia research. Schizophr. Bull., 42(2), 406 – 414. DOI: 10.1093/schbul/sbv074

Wang, X., M. L. Richard, P. Li, B. Henry, S. Schutt, X. Z. Yu, H. Fan, W. Zhang, G. Gilkeson, and X. K. Zhang. 2021. Expression of GM-CSF is regulated by Fli-1 transcription factor, a potential drug target. J. Immunol., 206(1), 59 – 66. DOI: 10.4049/jimmunol.2000664

Wang, X., Zhu, H., Snieder, S. Su, D. Munn, G. Harshfield, B. L. Maria, Y. Dong, F. Treiber, B. Gutin, and H. Shi. 2010. Obesity related methylation changes in DNA of peripheral blood leukocytes. BMC Med., 8(1), 1 – 8. DOI: 10.1186/1741-7015-8-87

Weaver, I. C., M. Szyf, and M. J. Meaney. 2002. From maternal care to gene expression: DNA methylation and the maternal programming of stress responses. Endocr. Res. 28(4), 699. DOI: 10.1081/ERC-120016989

Wei, X., L. Zhang, and Y. Zeng. 2020. DNA methylation in Alzheimer's disease: In brain and peripheral blood. Mech. Ageing Dev., 191, 111319. DOI: 10.1016/j.mad.2020.111319

Wen, X., M. Liu, J. Du, and X. Wang. 2021. Meis homeobox 2 (MEIS2) inhibits the proliferation and promotes apoptosis of thyroid cancer cell and through the NF-κB signaling pathway. Bioengineered, 12(1), 1766 – 1772. DOI: 10.1080/21655979.2021.1923354

Wimmer, K., X. X. Zhu, J. M. Rouillard, P. F. Ambros, B. J. Lamb, R. Kuick, M. Eckart, A. Weinhäusl, C. Fonatsch, and S. M. Hanash. 2002. Combined restriction landmark genomic scanning and virtual genome scans identify a novel human homeobox gene, ALX3, that is hypermethylated in neuroblastoma. Genes Chromosom. Cancer, 33(3), 285-294. DOI: 10.1002/gcc.10030

Witzig, T. E., H. Tang, I. N. Micallef, S. M. Ansell, B. K. Link, D. J. Inwards, L. F. Porrata, P. B. Johnston, J. P. Colgan, S. N. Markovic, and G. S. Nowakowski. 2011. Multi-institutional phase 2 study of the farnesyltransferase inhibitor tipifarnib (R115777) in patients with relapsed and refractory lymphomas. Am. J. Hematol., 118(18), 4882 – 4889. DOI: 10.1182/blood-2011-02-334904

Woo, H. D., and J. Kim. 2012. Global DNA hypomethylation in peripheral blood leukocytes as a biomarker for cancer risk: a meta-analysis. PloS one, 7(4), e34615. DOI: 10.1371/journal.pone.0034615

Wu, M. Y., T. F. Tsai, and A. L. Beaudet. 2006. Deficiency of Rbbp1/Arid4a and Rbbp1l1/Arid4b alters epigenetic modifications and suppresses an imprinting defect in the PWS/AS domain. Genes Dev., 20(20), 2859 – 2870. DOI: 10.1101/gad.1452206

Wu, R. C., M. Jiang, A. L. Beaudet, and M. Y. Wu. 2013. ARID4A and ARID4B regulate male fertility, a functional link to the AR and RB pathways. Proc. Natl. Acad. Sci., 110(12), 4616 – 4621. DOI: 10.1073/pnas.1218318110

Wu, T. P., T. Wang, M. G. Seetin, Y. Lai, S. Zhu, K. Lin, Y. Liu, S. D. Byrum, S. G. Mackintosh, M. Zhong, A. Tackett, G. Wang, L. S. Hon, G. Fang, J. A. Swenberg, and A. Z. Xiao. 2016. DNA methylation on N6-adenine in mammalian embryonic stem cells. Nature, 532(7599), 329 – 333. DOI: 10.1038/nature17640

Zhang, J., Hou, S., You, Z., Li, G., Xu, S., Li, X., Zhang, X., Lei, B. and Pang, D., 2021. Expression and prognostic values of ARID family members in breast cancer. Aging (Albany NY), 13(4), 5621 – 5637. DOI: 10.18632/aging.202489

Zhang, L., M. Yao, M. Hisaoka, H. Sasano, and H. Gao. 2016. Primary Ewing sarcoma/primitive neuroectodermal tumor in the adrenal gland. Apmis, 124(7), 624 – 629. DOI: 10.1111/apm.12544

Zhang, S., L. Rattanatray, I. C. McMillen, C. M., Suter, and J. L. Morrison. 2011. Periconceptional nutrition and the early programming of a life of obesity or adversity. Progress in biophysics and molecular biology, 106(1), 307 – 314. DOI: 10.1016/j.pbiomolbio.2010.12.004

Zhang, Q., W. Wang, and Q. Gao. 2019. β-TRCP-mediated AEBP2 ubiquitination and destruction controls cisplatin resistance in ovarian cancer. Biochem. Biophys. Res. Commun., 523(1), 274 – 279. DOI: 10.1016/j.bbrc.2019.12.050

Zhou, Y., S. Liu, Y. Hu, L. Fang, Y. Gao, H. Xia, S. G. Schroeder, B. D. Rosen, E. E. Connor, C. J. Li, R. L. Baldwin, J. B. Cole, C. P. Van Tassell, L. Yang, L. Ma, and G. E. Liu. 2020. Comparative whole genome DNA methylation profiling across cattle tissues reveals global and tissue-specific methylation patterns. BMC Biol., 18(1), 1 – 17. DOI: 10.1186/s12915-020-00793-5